U.S. Fish & Wildlife Service

Adaptive Harvest Management

2021 Hunting Season

Adaptive Harvest Management

2021 Hunting Season

PREFACE

The process of setting waterfowl hunting regulations is conducted annually in the United States (U.S.; Blohm 1989) and involves a number of meetings where the status of waterfowl is reviewed by the agencies responsible for setting hunting regulations. In addition, the U.S. Fish and Wildlife Service (USFWS) publishes proposed regulations in the Federal Register to allow public comment. This document is part of a series of reports intended to support development of harvest regulations for the 2021 hunting season. Specifically, this report is intended to provide waterfowl managers and the public with information about the use of adaptive harvest management (AHM) for setting waterfowl hunting regulations in the U.S. This report provides the most current data, analyses, and decision-making protocols. However, adaptive management is a dynamic process and some information presented in this report will differ from that in previous reports.

Citation: U.S. Fish and Wildlife Service. 2020. Adaptive Harvest Management: 2021 Hunting Season. U.S. Department of Interior, Washington, D.C. 109 pp. Available online at http://www.fws.gov/birds/management/adaptive-harvest-management/publications-and-reports.php

ACKNOWLEDGMENTS

A Harvest Management Working Group (HMWG) comprised of representatives from the USFWS, the U.S. Geological Survey (USGS), the Canadian Wildlife Service (CWS), and the four Flyway Councils (Appendix A) was established in 1992 to review the scientific basis for managing waterfowl harvests. The working group, supported by technical experts from the waterfowl management and research communities, subsequently proposed a framework for adaptive harvest management, which was first implemented in 1995. The USFWS expresses its gratitude to the HMWG and to the many other individuals, organizations, and agencies that have contributed to the development and implementation of AHM.

We are grateful for the continuing technical support from our USGS colleagues: F. A. Johnson (*Retired*), M. C. Runge, and J. A. Royle. We are also grateful to K. Pardieck, J. Sauer, K. Brantley, J. Byun, N. Hanke, M. Lutmerding, D. Murry, and D. Ziolkowski of the USGS Patuxent Wildlife Research Center, and the thousands of USGS Breeding Bird Survey participants for providing wood duck data in a timely manner. We acknowledge that information provided by USGS in this report has not received the Director's approval and, as such, is provisional and subject to revision. In addition, we acknowledge that the use of trade, firm, or product names does not imply endorsement by these agencies.

This report was prepared by the USFWS Division of Migratory Bird Management. G. S. Boomer and G. S. Zimmerman were the principal authors. Individuals that provided essential information or otherwise assisted with report preparation included: J. Hostetler, P. Devers, N. Zimpfer, K. Fleming, and R. Raftovich (USFWS). Comments regarding this document should be sent to the Chief, Division of Migratory Bird Management, U.S. Fish & Wildlife Service Headquarters, MS: MB, 5275 Leesburg Pike, Falls Church, VA 22041-3803.

Cover art: The 2020–2021 Federal Duck Stamp featuring black-bellied whistling-ducks (*Dendrocygna autumnalis*) painted by Eddie LeRoy.

TABLE OF CONTENTS

LIST OF FIGURES

LIST OF TABLES

1 EXECUTIVE SUMMARY

In 1995 the U.S. Fish and Wildlife Service (USFWS) implemented the adaptive harvest management (AHM) program for setting duck hunting regulations in the United States (U.S.). The AHM approach provides a framework for making objective decisions in the face of incomplete knowledge concerning waterfowl population dynamics and regulatory impacts.

The coronavirus disease 2019 (COVID-19) pandemic prevented the USFWS and their partners from performing the Waterfowl Breeding Population and Habitat Survey (WBPHS) and estimating waterfowl breeding populations and habitat conditions in the spring of 2020. As a result, AHM protocols have been adjusted to inform duck hunting regulations based on model predictions of breeding populations and habitat conditions. In most cases, system models specific to each AHM decision framework have been used to predict breeding population sizes from the available information (e.g., 2019 observations). However, for some system state variables we have used updated time series models to forecast 2020 values based on the most recent information.

The AHM protocol is based on the population dynamics and status of two mallard (*Anas platyrhynchos*) stocks and a suite of waterfowl stocks in the Atlantic Flyway. Mid-continent mallards are defined as those breeding in the WBPHS strata 13–18, 20–50, and 75–77 plus mallards breeding in the states of Michigan, Minnesota, and Wisconsin (state surveys). The prescribed regulatory alternative for the Mississippi and Central Flyways depends exclusively on the status of these mallards. Western mallards are defined as those breeding in WBPHS strata 1–12 (hereafter Alaska) and in the states of California, Oregon, Washington, and the Canadian province of British Columbia (hereafter southern Pacific Flyway). The prescribed regulatory alternative for the Pacific Flyway depends exclusively on the status of these mallards. In 2018, the Atlantic Flyway and the USFWS adopted a multi-stock AHM protocol based on 4 populations of eastern waterfowl [American green-winged teal (*Anas crecca*), wood ducks (*Aix sponsa*), ring-necked ducks (*Aythya collaris*), and goldeneyes (both *Bucephala clangula* and *B. islandica* combined)]. The regulatory choice for the Atlantic Flyway depends exclusively on the status of these waterfowl populations.

Mallard population models are based on the best available information and account for uncertainty in population dynamics and the impact of harvest. Model-specific weights reflect the relative confidence in alternative hypotheses and are updated annually using comparisons of predicted to observed population sizes. For mid-continent mallards, current model weights favor the weakly density-dependent reproductive hypothesis (>99%) and the additive-mortality hypothesis (72%). Unlike mid-continent mallards, we consider a single functional form to predict western mallard and eastern waterfowl population dynamics but consider a wide range of parameter values each weighted relative to the support from the data.

For the 2021 hunting season, the USFWS is considering similar regulatory alternatives as 2020. The nature of the restrictive, moderate, and liberal alternatives has remained essentially unchanged since 1997, except that extended framework dates have been offered in the moderate and liberal alternatives since 2002. Harvest rates associated with each of the regulatory alternatives have been updated based on band-recovery data from pre-season banded birds. The expected harvest rates of adult males under liberal hunting seasons are 0.11, and 0.13 for mid-continent and western mallards, respectively. In the Atlantic Flyway, expected harvest rates under the liberal alternative are 0.12, 0.12, 0.13, and 0.03 for American green-winged teal, wood ducks, ring-necked ducks, and goldeneyes, respectively.

Optimal regulatory strategies for the 2021 hunting season were calculated using: (1) harvest-management objectives specific to each stock; (2) current regulatory alternatives; and (3) current population models and their relative weights. Based on liberal regulatory alternatives selected for the 2020 hunting season, a 2020 prediction of 9.07 million mid-continent mallards, 3.40 million ponds in Prairie Canada, 0.94 million western mallards predicted for Alaska (0.41 million) and the southern Pacific Flyway (0.53 million), and 0.35 million American green-winged teal, 0.94 million wood ducks, 0.70 million ring-necked ducks and 0.58 million goldeneyes predicted for the eastern survey area and Atlantic Flyway, the optimal choice for the 2021 hunting season in all four Flyways is the liberal regulatory alternative.

AHM concepts and tools have been successfully applied toward the development of formal adaptive harvest management protocols that inform American black duck (*Anas rubripes*), northern pintail (*Anas acuta*), and scaup (*Aythya affinis, A. marila* combined) harvest decisions.

For black ducks, the optimal country-specific regulatory strategies for the 2021 hunting season were calculated using: (1) an objective to achieve 98% of the maximum, long-term cumulative harvest; (2) current country-specific black duck regulatory alternatives; and (3) updated model parameters and weights. Based on a liberal regulatory alternative selected by Canada and a moderate regulatory alternative selected by the U.S. for the 2020 hunting season and the 2020 model prediction of 0.50 million breeding black ducks and 0.39 million breeding mallards predicted for the core survey area, the optimal regulatory choices for the 2021 hunting season are the liberal regulatory alternative in Canada and the moderate regulatory alternative in the United States.

For pintails, the optimal regulatory strategy for the 2021 hunting season was calculated using: (1) an objective of maximizing long-term cumulative harvest; (2) current pintail regulatory alternatives; and (3) current population models and their relative weights. Based on a liberal regulatory alternative with a 1-bird daily bag limit selected for the 2020 hunting season and the 2020 model prediction of 2.446 million pintails predicted to settle at a mean latitude of 55.16 degrees, the optimal regulatory choice for the 2021 hunting season for all four Flyways is the liberal regulatory alternative with a 1-bird daily bag limit.

For scaup, the optimal regulatory strategy for the 2021 hunting season was calculated using: (1) an objective to achieve 95% of the maximum, long-term cumulative harvest; (2) current scaup regulatory alternatives; and (3) updated model parameters and weights. Based on a restrictive regulatory alternative selected for the 2020 hunting season and a 2020 model prediction of 3.53 million scaup, the optimal regulatory choice for the 2021 hunting season for all four Flyways is the restrictive regulatory alternative.

2 BACKGROUND

The annual process of setting duck-hunting regulations in the U.S. is based on a system of resource monitoring, data analyses, and rule-making (Blohm 1989). Each year, monitoring activities such as aerial surveys, preseason banding, and hunter questionnaires provide information on population size, habitat conditions, and harvest levels. Data collected from these monitoring programs are analyzed each year, and proposals for duck-hunting regulations are developed by the Flyway Councils, States, and USFWS. After extensive public review, the USFWS announces regulatory guidelines within which States can set their hunting seasons.

In 1995, the USFWS adopted the concept of adaptive resource management (Walters 1986) for regulating duck harvests in the U.S. This approach explicitly recognizes that the consequences of hunting regulations cannot be predicted with certainty and provides a framework for making objective decisions in the face of that uncertainty (Williams and Johnson 1995). Inherent in the adaptive approach is an awareness that management performance can be maximized only if regulatory effects can be predicted reliably. Thus, adaptive management relies on an iterative cycle of monitoring, assessment, and decision-making to clarify the relationships among hunting regulations, harvests, and waterfowl abundance (Johnson et al. 2016).

In regulating waterfowl harvests, managers face four fundamental sources of uncertainty (Nichols et al. 1995*a*, Johnson et al. 1996, Williams et al. 1996):

(1) environmental variation – the temporal and spatial variation in weather conditions and other key features of waterfowl habitat; an example is the annual change in the number of ponds in the Prairie Pothole Region, where water conditions influence duck reproductive success;

(2) partial controllability – the ability of managers to control harvest only within limits; the harvest resulting from a particular set of hunting regulations cannot be predicted with certainty because of variation in weather conditions, timing of migration, hunter effort, and other factors;

(3) partial observability – the ability to estimate key population attributes (e.g., population size, reproductive rate, harvest) only within the precision afforded by extant monitoring programs; and

(4) structural uncertainty – an incomplete understanding of biological processes; a familiar example is the long-standing debate about whether harvest is additive to other sources of mortality or whether populations compensate for hunting losses through reduced natural mortality. Structural uncertainty increases contentiousness in the decision-making process and decreases the extent to which managers can meet long-term conservation goals.

AHM was developed as a systematic process for dealing objectively with these uncertainties. The key components of AHM include (Johnson et al. 1993, Williams and Johnson 1995):

(1) a limited number of regulatory alternatives, which describe Flyway-specific season lengths, bag limits, and framework dates;

(2) a set of population models describing various hypotheses about the effects of harvest and environmental factors on waterfowl abundance;

(3) a measure of reliability (probability or "weight") for each population model; and

(4) a mathematical description of the objective(s) of harvest management (i.e., an "objective function"), by which alternative regulatory strategies can be compared.

These components are used in a stochastic optimization procedure to derive a regulatory strategy. A regulatory strategy specifies the optimal regulatory choice, with respect to the stated management objectives, for each possible combination of breeding population size, environmental conditions, and model weights (Johnson et al. 1997). The setting of annual hunting regulations then involves an iterative process:

(1) each year, an optimal regulatory choice is identified based on resource and environmental conditions, and on current model weights;

(2) after the regulatory decision is made, model-specific predictions for subsequent breeding population size are determined;

(3) when monitoring data become available, model weights are increased to the extent that observations of population size agree with predictions, and decreased to the extent that they disagree; and

(4) the new model weights are used to start another iteration of the process.

By iteratively updating model weights and optimizing regulatory choices, the process should eventually identify which model is the best overall predictor of changes in population abundance. The process is optimal in the sense that it provides the regulatory choice each year necessary to maximize management performance. It is adaptive in the sense that the harvest strategy "evolves" to account for new knowledge generated by a comparison of predicted and observed population sizes.

3 ADJUSTMENTS TO THE 2020 REGULATORY PROCESS

Due to the coronavirus disease 2019 (COVID-19) pandemic, the USFWS and their partners were unable to perform the WBPHS and estimate waterfowl breeding populations as well as evaluate breeding habitat conditions in the spring of 2020. As a result, the information requirements, assessment methodologies, and decision protocols that typically define the annual regulatory process have required some modifications. The lack of an observable population size has immediate implications for learning through AHM. Model predictions for 2020 population responses cannot be compared to WBPHS estimates to update model weights. Because of this lack of updating, the USFWS and the Flyway councils have agreed to use optimal harvest policies calculated with model weights and model parameters based on the most recent information available to inform waterfowl harvest decisions for the 2020 regulations process. These policies represent optimal decisions based on our most recent observations and understanding of system dynamics. In the absence of 2020 breeding population information, the USFWS and Flyway councils have agreed to use predictions of breeding population sizes and habitat conditions to determine regulatory decisions for the 2021-22 hunting season. Current system models for which we have AHM decision frameworks were used to predict 2020 population sizes as a function of breeding population sizes, habitat conditions, harvest, and harvest rates observed during the 2019–20 hunting seasons. For some state variables (e.g., Canadian ponds) or 2019 unobservable information (e.g., Canadian harvest), we used formal time series analyses methods (Hyndman and Athanasopoulos 2018) to forecast these values. We provide the results of these forecasts in the body of this report and include the analytical details in the attached appendices.

4 WATERFOWL STOCKS AND FLYWAY MANAGEMENT

Since its inception AHM has focused on the population dynamics and harvest potential of mallards, especially those breeding in mid-continent North America. Mallards constitute a large portion of the total U.S. duck harvest, and traditionally have been a reliable indicator of the status of many other species. Geographic differences in the reproduction, mortality, and migrations of waterfowl stocks suggest that there may be corresponding differences in optimal levels of sport harvest. The ability to regulate harvests of mallards originating from various breeding areas is complicated, however, by the fact that a large degree of mixing occurs during the hunting season. The challenge for managers, then, is to vary hunting regulations among Flyways in a manner that recognizes each Flyway's unique breeding-ground derivation of waterfowl stocks. Of course, no Flyway receives waterfowl exclusively from one breeding area; therefore, Flyway-specific harvest strategies ideally should account for multiple breeding stocks that are exposed to a common harvest.

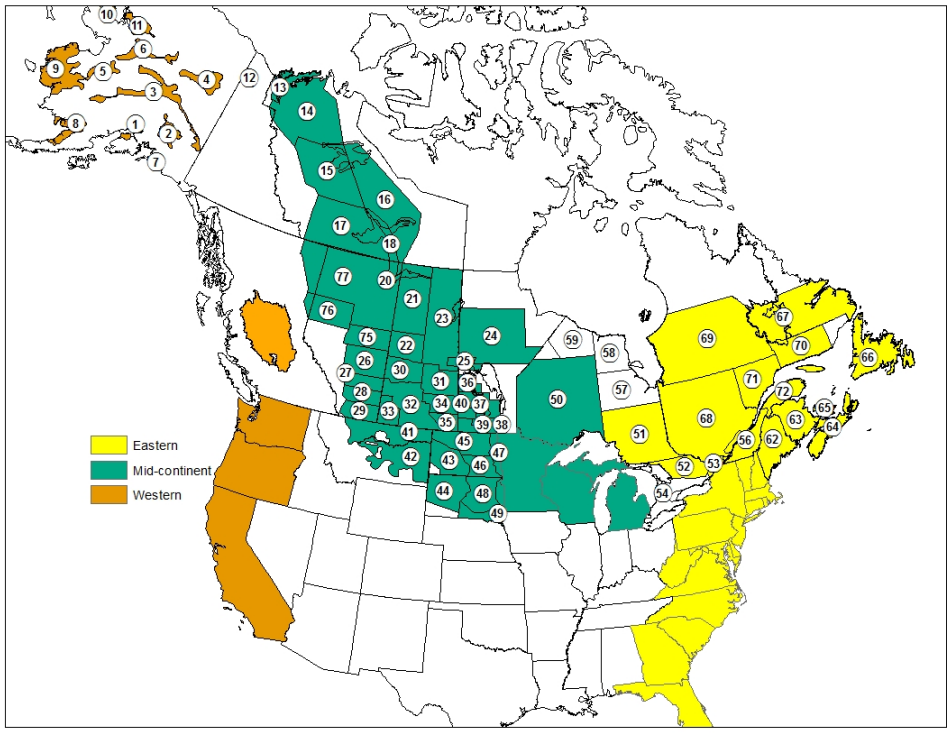

Figure 1 – Waterfowl Breeding Population and Habitat Survey (WBPHS) strata and state, provincial, and territorial survey areas currently assigned to the mid-continent and western stocks of mallards and eastern waterfowl stocks for the purposes of adaptive harvest management.

The optimization procedures used in AHM can account for breeding populations of waterfowl beyond the mid-continent region, and for the manner in which these ducks distribute themselves among the Flyways during the hunting season. An optimal approach would allow for Flyway-specific regulatory strategies, which represent an average of the optimal harvest strategies for each contributing breeding stock weighted by the relative size of each stock in the fall flight. This joint optimization of multiple stocks requires: (1) models of population dynamics for all recognized stocks; (2) an objective function that accounts for harvest-management goals for all stocks in the aggregate; and (3) decision rules allowing Flyway-specific regulatory choices. At present, however, a joint optimization of western, mid-continent, and eastern stocks is not feasible due to computational hurdles. However, our preliminary analyses suggest that the lack of a joint optimization does not result in a significant decrease in management performance.

Currently, two stocks of mallards (mid-continent and western) and stocks of four different species of eastern waterfowl populations (Atlantic Flyway multi-stock; hereafter 'multi-stock') are recognized for the purposes of AHM (Figure 1). We use a constrained approach to the optimization of these stocks' harvest, in which the regulatory strategy for the Mississippi and Central Flyways is based exclusively on the status of mid-continent mallards and the Pacific Flyway regulatory strategy is based exclusively on the status of western mallards. Historically, the Atlantic Flyway regulatory strategy was based exclusively on the status of eastern mallards. In 2018, the Atlantic Flyway and the USFWS adopted a multi-stock AHM framework. As a result, the Atlantic Flyway regulatory strategy is based exclusively on the status of American green-winged teal, wood ducks, ring-necked ducks, and goldeneyes breeding in the Atlantic Flyway states and eastern Canada.

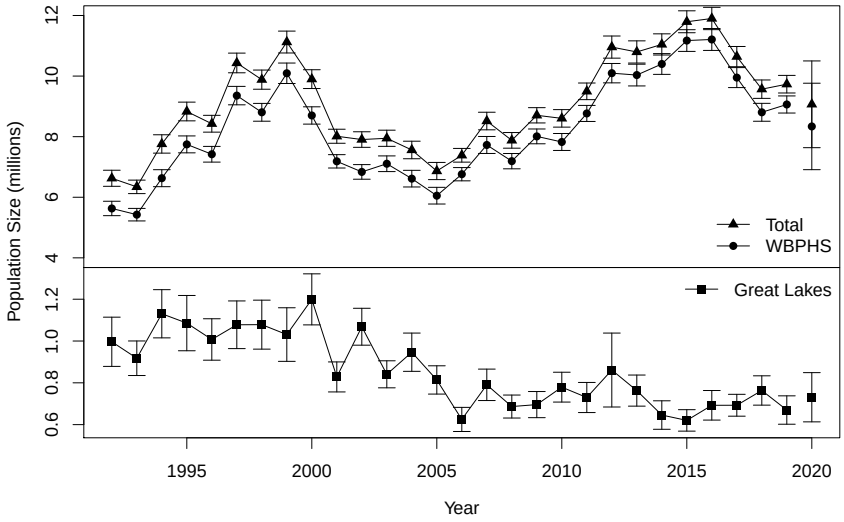

Figure 2 – Population estimates of mid-continent mallards observed in the WBPHS (strata: 13–18, 20–50, and 75–77) and the Great Lakes region (Michigan, Minnesota, and Wisconsin) from 1992 to 2019. Error bars represent one standard error. The 2020 values are based on model predictions.

5 WATERFOWL POPULATION DYNAMICS

5.1 Mid-Continent Mallard Stock

Mid-continent mallards are defined as those breeding in WBPHS strata 13–18, 20–50, and 75–77, and in the Great Lakes region (Michigan, Minnesota, and Wisconsin; see Figure 1). Estimates of this population have varied from 6.3 to 11.9 million since 1992 (Table H.1, Figure 2). For 2020, we used each model in the mid-continent mallard model set to predict the 2020 breeding population size and used the updated 2019 model weights to calculate a weighted average breeding population size of 8.34 million (SE = 1.43 million). In addition, we used a formal time series analysis to forecast a 2020 breeding population of Great Lakes region mallards equal to 0.73 million (SE = 0.12 million), see Appendix (D) for details. The total 2020 mid-continent mallard breeding population is predicted to be 9.07 million (SE = 1.43 million).

Details describing the set of population models for mid-continent mallards are provided in Appendix H. The set consists of four alternatives, formed by the combination of two survival hypotheses (additive vs. compensatory hunting mortality) and two reproductive hypotheses (strongly vs. weakly density dependent). Relative weights for the alternative models of mid-continent mallards changed little until all models under-predicted the change in population size from 1998 to 1999, perhaps indicating there is a significant factor affecting population dynamics that is absent from all four models (Figure 3). Updated model weights suggest greater evidence for the additive-mortality models (72%) over those describing hunting mortality as compensatory (28%). For most of the time frame, model weights have strongly favored the weakly density-dependent reproductive models over the strongly density-dependent ones, with current model weights greater than 99% and less than 1%, respectively. The reader is cautioned, however, that models can sometimes make reliable predictions of population size for reasons having little to do with the biological hypotheses expressed therein (Johnson et al. 2002).

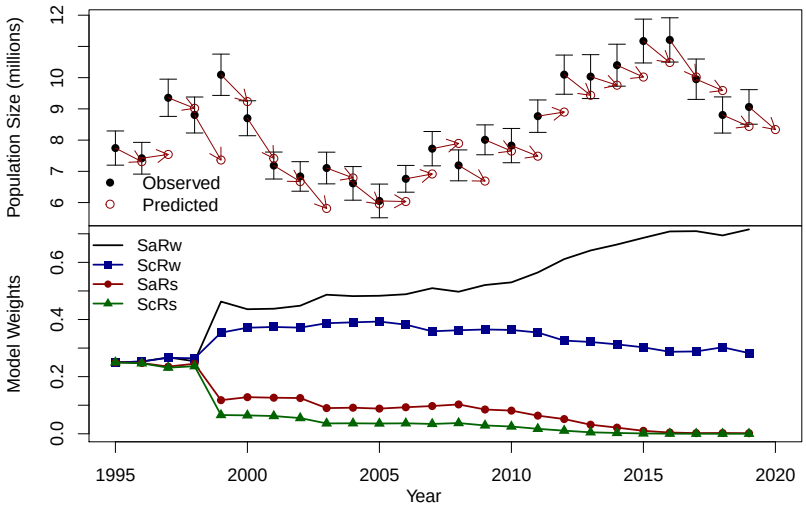

Figure 3 – Top panel: population estimates of mid-continent mallards observed in the WBPHS compared to mid-continent mallard model set predictions (weighted average based on 2019 model weight updates) from 1996 to 2019. Error bars represent 95% confidence intervals. Bottom panel: mid-continent mallard model weights (SaRw = additive mortality and weakly density-dependent reproduction, ScRw = compensatory mortality and weakly density-dependent reproduction, SaRs = additive mortality and strongly density-dependent reproduction, ScRs = compensatory mortality and strongly density-dependent reproduction). Model weights were assumed to be equal in 1995 and model weight updates were not calculated for 2020.

5.2 Western Mallard Stock

Western mallards consist of 2 substocks and are defined as those birds breeding in Alaska (WBPHS strata 1–12) and those birds breeding in the southern Pacific Flyway (California, Oregon, Washington, and British Columbia combined; see Figure 1). Estimates of these subpopulations have varied from 0.28 to 0.84 million in Alaska since 1990 and 0.43 to 0.64 million in the southern Pacific Flyway since 2010 (Table I.1, Figure 4). For 2020, we used the western mallard models and Bayesian estimation frameworks to predict a median breeding-population size of 0.94 million (SE = 0.09 million), including 0.41 million (SE = 0.07 million) from Alaska and 0.53 million (SE = 0.06 million) from the southern Pacific Flyway.

Details concerning the set of population models for western mallards are provided in Appendix I. To predict changes in abundance we used a discrete logistic model, which combines reproduction and natural mortality into a single parameter, r, the intrinsic rate of growth. This model assumes density-dependent growth, which is regulated by the ratio of population size, N, to the carrying capacity of the environment, K (i.e., equilibrium population size in the absence of harvest). In the traditional formulation of the logistic model, harvest mortality is completely additive and any compensation for hunting losses occurs as a result of density-dependent responses beginning in the subsequent breeding season. To increase the model's generality we included a scaling parameter for harvest that allows for the possibility of compensation prior to the breeding season. It is important to note, however, that this parameterization does not incorporate any hypothesized mechanism for harvest compensation and, therefore, must be interpreted cautiously. We modeled Alaska mallards independently of those in the southern Pacific Flyway because of differing population trajectories (see Figure 4) and substantial differences in the distribution of band recoveries.

We used Bayesian estimation methods in combination with a state-space model that accounts explicitly for both process and observation error in breeding population size (Meyer and Millar 1999). Breeding population estimates of mallards in Alaska are available since 1955, but we had to limit the time series to 1990–2019 because of changes in survey methodology and insufficient band-recovery data. The logistic model and

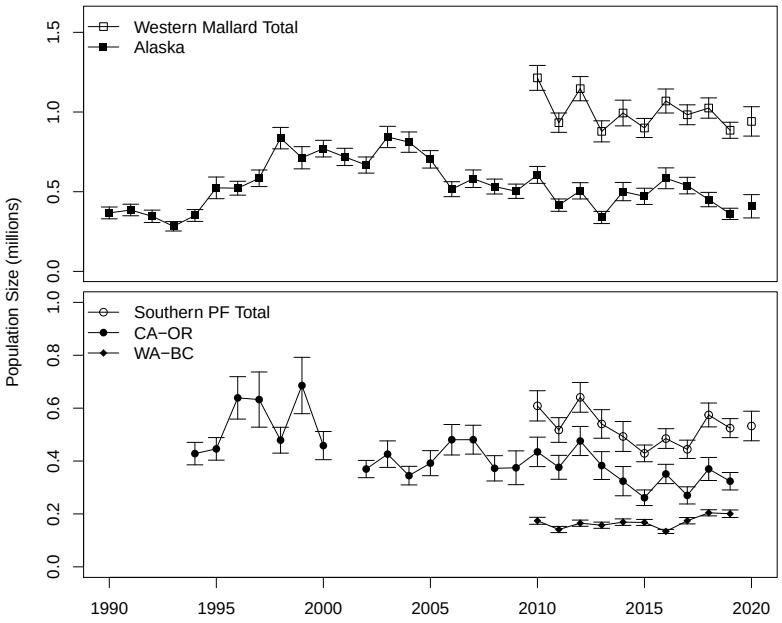

Figure 4 – Population estimates of western mallards observed in Alaska (WBPHS strata 1–12) and the southern Pacific Flyway (California, Oregon, Washington, and British Columbia combined) from 1990 to 2019. Error bars represent one standard error. The 2020 values are based on model predictions.

associated posterior parameter estimates provided a reasonable fit to the observed time series of Alaska population estimates. The estimated median carrying capacity was 1.02 million and the intrinsic rate of growth was 0.28. The posterior median estimate of the scaling parameter was 1.35. Breeding population and harvest-rate data were available for California-Oregon mallards for the period 1992–2019. Because the British Columbia survey did not begin until 2006 and the Washington survey was redesigned in 2010, we imputed data in a Markov chain Monte Carlo (MCMC) framework from the beginning of the British Columbia and Washington surveys back to 1992 (see details in Appendix I) to make the time series consistent for the southern Pacific Flyway. The logistic model also provided a reasonable fit to these data. The estimated median carrying capacity was 0.79 million, and the intrinsic rate of growth was 0.25. The posterior median estimate of the scaling parameter was 0.46.

The AHM protocol for western mallards is structured similarly to that used for mid-continent mallards, in which an optimal harvest strategy is based on the status of a single breeding stock (Alaska and southern Pacific Flyway substocks) and harvest regulations in a single Flyway. Although the contribution of mid-continent mallards to the Pacific Flyway harvest is significant, we believe an independent harvest strategy for western mallards poses little risk to the mid-continent stock. Further analyses will be needed to confirm this conclusion, and to better understand the potential effect of mid-continent mallard status on sustainable hunting opportunities in the Pacific Flyway.

5.3 Atlantic Flyway Multi-Stock

For the purposes of the Atlantic Flyway multi-stock AHM framework, eastern waterfowl stocks are defined as those breeding in eastern Canada and Maine (USFWS fixed-wing surveys in WBPHS strata 51-53, 56, and 62-70; CWS helicopter plot surveys in WBPHS strata 51-52, 63-64, 66-68, and 70-72) and Atlantic Flyway states from New Hampshire south to Virginia (AFBWS; Heusmann and Sauer 2000). These areas

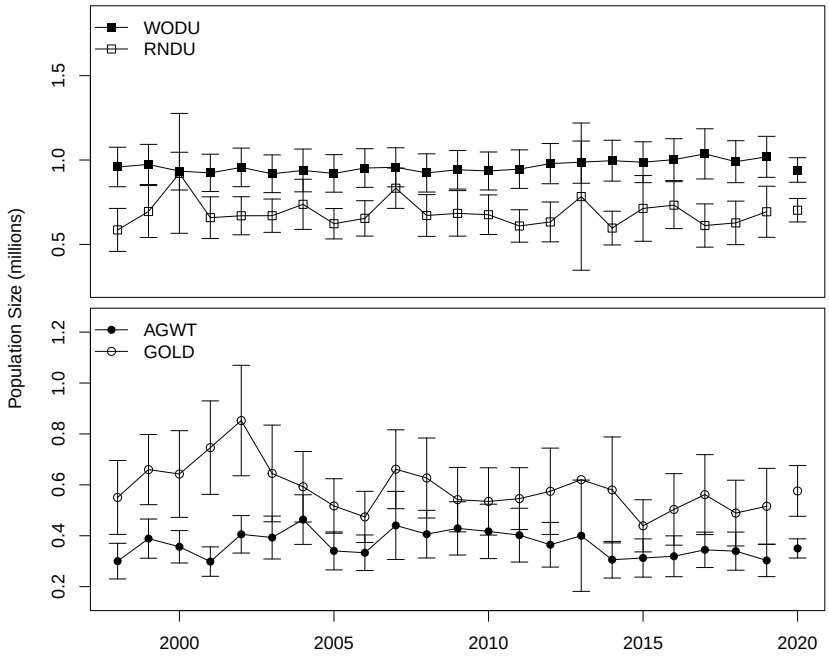

Figure 5 – Population estimates of American green-winged teal (AGWT), wood ducks (WODU), ring-necked ducks (RNDU), and goldeneyes (GOLD) observed in eastern Canada (WBPHS strata 51–53, 56, 62–72) and U.S. (Atlantic Flyway states) from 1998 to 2019. Error bars represent one standard error. The SE of the goldeneyes estimate for 2013 is not reported due to insufficient counts. The 2020 values are based on model predictions.

have been consistently surveyed since 1998. Breeding population size estimates for American green-winged teal, ring-necked ducks, and goldeneyes are derived annually by integrating USFWS and CWS survey data from eastern Canada and Maine (WBPHS strata 51-53, 56, and 62-72; (Zimmerman et al. 2012, U.S. Fish and Wildlife Service 2019*b*). Insufficient counts of American green-winged teal, ring-necked ducks, and goldeneyes in the AFBWS preclude the inclusion of those areas in the population estimates for those species. Breeding population size estimates for wood ducks in the Atlantic Flyway (Maine south to Florida) are estimated by integrating data from the AFBWS and the Breeding Bird Survey (BBS; Zimmerman et al. 2015). Insufficient counts of wood ducks from the USFWS and CWS surveys in Maine and Canada preclude incorporating those survey results into breeding population estimates. Estimates of the breeding population size for American green-winged teal have varied from 0.30 to 0.46 million, wood ducks varied from 0.92 to 1.04 million, ring-necked ducks varied from 0.59 to 0.92 million, and goldeneyes varied from 0.44 to 0.85 million since 1998 (Table J.1, Figure 5). For 2020, we used the multi-stock population models and Bayesian estimation frameworks to predict a median breeding population size of 0.35 million (SE = 0.04 million) for American green-winged teal, 0.94 million (SE = 0.07 million) for wood ducks, 0.70 million (SE = 0.07 million) for ring-necked ducks, and 0.58 million (SE = 0.10 million) for goldeneyes.

Details concerning the set of models used in Atlantic Flyway multi-stock AHM are provided in Appendix J. Similar to the methods used in western mallard AHM, we used a discrete logistic model to represent eastern waterfowl population and harvest dynamics and a state-space, Bayesian estimation framework to estimate the population parameters and process variation. We modeled each stock independently and found that the logistic model and associated posterior parameter estimates provided a reasonable fit to the observed time series of eastern waterfowl stocks. The estimated median carrying capacities were 0.53, 1.56, 0.87, and 0.71 for American green-winged teal, wood ducks, ring-necked ducks, and goldeneyes, respectively. The posterior median estimates of intrinsic rate of growth were 0.43, 0.39, 0.40, and 0.23 for American green-winged teal,

wood ducks, ring-necked ducks, and goldeneyes, respectively.

6 HARVEST-MANAGEMENT OBJECTIVES

The basic harvest-management objective for mid-continent mallards is to maximize cumulative harvest over the long term, which inherently requires perpetuation of a viable population. Moreover, this objective is constrained to avoid regulations that could be expected to result in a subsequent population size below the goal of the North American Waterfowl Management Plan (NAWMP). According to this constraint, the value of harvest decreases proportionally as the difference between the goal and expected population size increases. This balance of harvest and population objectives results in a regulatory strategy that is more conservative than that for maximizing long-term harvest, but more liberal than a strategy to attain the NAWMP goal (regardless of effects on hunting opportunity). The current objective for mid-continent mallards uses a population goal of 8.5 million birds, which consists of 7.9 million mallards from the WBPHS (strata 13–18, 20–50, and 75–77) corresponding to the mallard population goal in the 1998 update of the NAWMP (less the portion of the mallard goal comprised of birds breeding in Alaska) and a goal of 0.6 million for the combined states of Michigan, Minnesota, and Wisconsin.

The harvest management objectives for western mallards and eastern waterfowl stocks do not consider NAWMP goals or other established targets for desired population sizes. The management objective for western mallards is to maximize long-term cumulative (i.e., sustainable) harvest, and the objective for eastern waterfowl stocks is to attain 98% of the maximum, long-term cumulative harvest for the aggregate of the four species.

7 REGULATORY ALTERNATIVES

7.1 Evolution of Alternatives

When AHM was first implemented in 1995, three regulatory alternatives characterized as liberal, moderate, and restrictive were defined based on regulations used during 1979–1984, 1985–1987, and 1988–1993, respectively. These regulatory alternatives also were considered for the 1996 hunting season. In 1997, the regulatory alternatives were modified to include: (1) the addition of a very-restrictive alternative; (2) additional days and a higher duck bag limit in the moderate and liberal alternatives; and (3) an increase in the bag limit of hen mallards in the moderate and liberal alternatives. In 2002, the USFWS further modified the moderate and liberal alternatives to include extensions of approximately one week in both the opening and closing framework dates. During the 2019–2020 regulatory process, closing dates for all four Flyways were set to 31 January for all regulatory alternatives to comply with the John D. Dingell, Jr. Conservation, Management, and Recreation Act.

In 2003, the very-restrictive alternative was eliminated at the request of the Flyway Councils. Expected harvest rates under the very-restrictive alternative did not differ significantly from those under the restrictive alternative, and the very-restrictive alternative was expected to be prescribed for $<5\%$ of all hunting seasons. Also in 2003, at the request of the Flyway Councils the USFWS agreed to exclude closed duck-hunting seasons from the AHM protocol when the population size of mid-continent mallards (as defined in 2003: WBPHS strata 1–18, 20–50, and 75–77 plus the Great Lakes region) was $\geq$5.5 million. Based on our original assessment, closed hunting seasons did not appear to be necessary from the perspective of sustainable harvesting when the mid-continent mallard population exceeded this level. The impact of maintaining open seasons above this level also appeared negligible for other mid-continent duck species, as based on population models developed by Johnson (2003).

In 2008, the mid-continent mallard stock was redefined to exclude mallards breeding in Alaska, necessitating a re-scaling of the closed-season constraint. Initially, we attempted to adjust the original 5.5 million closure threshold by subtracting out the 1985 Alaska breeding population estimate, which was the year upon which the original closed season constraint was based. Our initial re-scaling resulted in a new threshold equal to 5.25 million. Simulations based on optimal policies using this revised closed season constraint suggested that the Mississippi and Central Flyways would experience a 70% increase in the frequency of closed seasons. At that time, we agreed to consider alternative re-scalings in order to minimize the effects on the mid-continent mallard strategy and account for the increase in mean breeding population sizes in Alaska over the past several decades. Based on this assessment, we recommended a revised closed season constraint of 4.75 million which resulted in a strategy performance equivalent to the performance expected prior to the re-definition of the mid-continent mallard stock. Because the performance of the revised strategy is essentially unchanged from the original strategy, we believe it will have no greater impact on other duck stocks in the Mississippi and Central Flyways. However, complete- or partial-season closures for particular species or populations could still be deemed necessary in some situations regardless of the status of mid-continent mallards.

For the development of the multi-stock AHM framework in the Atlantic Flyway, the USFWS and Atlantic Flyway decided to keep the same overall bag limits and season lengths that were used for eastern mallard AHM. Species-specific regulations are then based on harvest strategies informed by existing decision frameworks (e.g., black duck AHM).

At the time this report was prepared, the regulatory packages for the 2021-22 seasons had not been finalized by the U.S. Fish and Wildlife Service. However, we do not expect any changes from the 2020-21 packages. Therefore, optimal strategies were formulated using the 2020-21 packages and are referred to as "current" packages in subsequent text. Details of the regulatory alternatives for each Flyway are provided in Table 1.

7.2 Regulation-Specific Harvest Rates

Harvest rates of mallards associated with each of the open-season regulatory alternatives were initially predicted using harvest-rate estimates from 1979–1984, which were adjusted to reflect current hunter numbers and contemporary specifications of season lengths and bag limits. In the case of closed seasons in the United States, we assumed rates of harvest would be similar to those observed in Canada during 1988–1993, which was a period of restrictive regulations both in Canada and the United States. All harvest-rate predictions were based only in part on band-recovery data, and relied heavily on models of hunting effort and success derived from hunter surveys (Appendix C in U.S. Fish and Wildlife Service 2002). As such, these predictions had large sampling variances and their accuracy was uncertain.

In 2002, we began using Bayesian statistical methods for improving regulation-specific predictions of harvest rates, including predictions of the effects of framework-date extensions. Essentially, the idea is to use existing (prior) information to develop initial harvest-rate predictions (as above), to make regulatory decisions based on those predictions, and then to observe realized harvest rates. Those observed harvest rates, in turn, are treated as new sources of information for calculating updated (posterior) predictions. Bayesian methods are attractive because they provide a quantitative, formal, and an intuitive approach to adaptive management.

Annual harvest rate estimates for mid-continent and western mallards and eastern stocks of American green-winged teal and wood ducks are updated with band-recovery information from a cooperative banding program between the USFWS and CWS, along with state, provincial, and other participating partners. Recovery rate estimates from these data are adjusted with reporting rate probabilities resulting from recent reward band studies (Boomer et al. 2013, Garrettson et al. 2013). For mid-continent mallards, we have empirical estimates of harvest rate from the recent period of liberal hunting regulations (1998–2019). Bayesian methods allow us to combine these estimates with our prior predictions to provide updated estimates of harvest rates expected under the liberal regulatory alternative. Moreover, in the absence of experience (so far) with the restrictive and moderate regulatory alternatives, we reasoned that our initial predictions of harvest rates associated with those alternatives should be re-scaled based on a comparison of predicted and observed harvest rates under the liberal regulatory alternative. In other words, if observed harvest rates under the liberal alternative were

Table 1 – Current regulatory alternatives for the duck-hunting season.

Regulation	**Flyway**			
	Atlantic[a]	**Mississippi**	**Central**[b]	**Pacific**[c]
Shooting Hours	one-half hour before sunrise to sunset			
	Opening Date			
Restrictive	October 1	Saturday nearest October 1		
Moderate	Saturday nearest September 24			
Liberal				
	Closing Date			
Restrictive	January 31			
Moderate				
Liberal				
	Season Length (days)			
Restrictive	30	30	39	60
Moderate	45	45	60	86
Liberal	60	60	74	107
	Bag Limit (total / mallard[d] **/ hen mallard)**			
Restrictive	3 / - / -	3 / 2 / 1	3 / 3 / 1	4 / 3 / 1
Moderate	6 / - / -	6 / 4 / 1	6 / 5 / 1	7 / 5 / 2
Liberal	6 / - / -	6 / 4 / 2	6 / 5 / 2	7 / 7 / 2

[a] The states of Maine, Massachusetts, Connecticut, Pennsylvania, New Jersey, Maryland, Delaware, and North Carolina are permitted to exclude Sundays, which are closed to hunting, from their total allotment of season days.

[b] The High Plains Mallard Management Unit is allowed 12, 23, and 23 extra days in the restrictive, moderate, and liberal alternatives, respectively.

[c] The Columbia Basin Mallard Management Unit is allowed 7 extra days in the restrictive and moderate alternatives.

[d] For the Atlantic Flyway, the mallard bag limit is not prescribed by the regulatory alternative under the Multi-stock AHM protocol.

10% less than predicted, then we might also expect that the mean harvest rate under the moderate alternative would be 10% less than predicted. The appropriate scaling factors currently are based exclusively on prior beliefs about differences in mean harvest rate among regulatory alternatives, but they will be updated once we have experience with something other than the liberal alternative. A detailed description of the analytical framework for modeling mallard harvest rates is provided in Appendix K.

Our models of regulation-specific harvest rates also allow for the marginal effect of framework-date extensions in the moderate and liberal alternatives. A previous analysis by the U.S. Fish and Wildlife Service (2001) suggested that implementation of framework-date extensions might be expected to increase the harvest rate of mid-continent mallards by about 15%, or in absolute terms by about 0.02 (SD = 0.01). Based on the observed harvest rates during the 2002–2019 hunting seasons, the updated (posterior) estimate of the marginal change in harvest rate attributable to the framework-date extension is 0.004 (SD = 0.006). The estimated effect of the framework-date extension has been to increase harvest rate of mid-continent mallards by about 3% over what would otherwise be expected in the liberal alternative. However, the reader is strongly cautioned that reliable inference about the marginal effect of framework-date extensions ultimately depends on a rigorous experimental design (including controls and random application of treatments).

Current predictions of harvest rates of adult-male mid-continent mallards associated with each of the regulatory alternatives are provided in Table 2. Predictions of harvest rates for the other age and sex cohorts are based on the historical ratios of cohort-specific harvest rates to adult-male rates (Runge et al. 2002). These ratios are considered fixed at their long-term averages and are 1.5407, 0.7191, and 1.1175 for young males, adult females, and young females, respectively. We make the simplifying assumption that the harvest rates of mid-continent mallards depend solely on the regulatory choice in the Mississippi and Central Flyways.

Based on available estimates of harvest rates of mallards banded in California and Oregon during 1990–1995 and 2002–2007, there was no apparent relationship between harvest rate and regulatory changes in the Pacific Flyway. This is unusual given our ability to document such a relationship in other mallard stocks and in other species. We note, however, that the period 2002–2007 was comprised of both stable and liberal regulations and harvest rate estimates were based solely on reward bands. Regulations were relatively restrictive during most of the earlier period and harvest rates were estimated based on standard bands using reporting rates estimated from reward banding during 1987–1988. Additionally, 1993–1995 were transition years in which full-address and toll-free bands were being introduced and information to assess their reporting rates (and their effects on reporting rates of standard bands) is limited. Thus, the two periods in which we wish to compare harvest rates are characterized not only by changes in regulations, but also in estimation methods.

Consequently, we lack a sound empirical basis for predicting harvest rates of western mallards associated with current regulatory alternatives other than liberal in the Pacific Flyway. In 2009, we began using Bayesian statistical methods for improving regulation-specific predictions of harvest rates (see Appendix K). The methodology is analogous to that currently in use for mid-continent mallards except that the marginal effect of framework date extensions in moderate and liberal alternatives is inestimable because there are no data prior to implementation of extensions. In 2008, we specified prior regulation-specific harvest rates of 0.01, 0.06, 0.09, and 0.11 with associated standard deviations of 0.003, 0.02, 0.03, and 0.03 for the closed,

Table 2 – Predictions of harvest rates of adult male, mid-continent and western mallards expected with application of the current regulatory alternatives in the Mississippi, Central and Pacific Flyways.

	Mid-continent		Western	
Regulatory Alternative	Mean	SD	Mean	SD
Closed (U.S.)	0.009	0.002	0.009	0.018
Restrictive	0.054	0.013	0.069	0.017
Moderate	0.094	0.021	0.115	0.029
Liberal	0.111	0.017	0.135	0.027

restrictive, moderate, and liberal alternatives, respectively. The prior for the liberal regulation was then updated in 2011 with a harvest rate of 0.12 and standard deviation of 0.04. The harvest rates for the liberal alternative were based on empirical estimates realized under the current liberal alternative during 2002–2007 and determined from adult male mallards banded with reward and standard bands adjusted for band reporting rates in the southern Pacific Flyway. The development of priors was based on banding information from California and Oregon data only. Recently, we assessed the band-recovery data from Washington, Idaho, and British Columbia and found that the addition of these bands had a negligible influence on harvest rate estimates of western mallards. As a result, we have included Washington, Idaho, and British Columbia band-recovery information in our annual updates to western mallard harvest rate distributions. Harvest rates for the moderate and restrictive alternatives were based on the proportional (0.85 and 0.51) difference in harvest rates expected for mid-continent mallards under the respective alternatives. Finally, harvest rate for the closed alternative was based on what we might realize with a closed season in the United States (including Alaska) and a very restrictive season in Canada, similar to that for mid-continent mallards. A relatively large standard deviation (CV = 0.3) was chosen to reflect greater uncertainty about the means than that for mid-continent mallards (CV = 0.2). Current predictions of harvest rates of adult male western mallards associated with each regulatory alternative are provided in Table 2.

The harvest rates expected under the liberal season for the four populations associated with the Atlantic Flyway's multi-stock AHM were based on the average observed harvest rate from 1998–2014 for each species. The harvest rates for American green-winged teal and wood ducks were based on preseason banding and dead recovery data adjusted for reporting rates similar to mid-continent and western mallards. Because the discrete logistic model used for these species does not include age or sex structure, banding data for all cohorts were pooled to estimate an overall harvest rate. Insufficient banding data precluded the estimation of harvest rates for ring-necked ducks and goldeneyes in the Atlantic Flyway based on band recovery information, so harvest estimates from the Harvest Information Program were used to monitor harvest levels for these species in the multi-stock framework. Specifically, we estimated a fall population size from the discrete logistic model and calculated a harvest rate as the total harvest divided by the fall population size for ring-necked ducks and goldeneyes. The estimated harvest rates for each species under each regulation are listed in Table 3.

8 OPTIMAL REGULATORY STRATEGIES

The adoption of the preferred alternative specified in SEIS 2013 (U.S. Department of the Interior 2013) resulted in a new decision process based on a single regulatory meeting in the fall of year t to inform regulations for the next year's hunting season in year $t + 1$ (Appendix B). As a result, regulatory decisions are made in advance of observing the status of waterfowl breeding populations (BPOP) and habitat conditions during the spring prior to the upcoming hunting season. With the implementation of the SEIS, pre-survey regulatory decisions introduce a lag in the AHM process where model weight updating and state-dependent decision making are now governed by the previous year's monitoring information. Given that the original AHM protocols and decision frameworks were structured to inform decisions based on current monitoring information

Table 3 – Predictions of harvest rates of American green-winged teal (AGWT), wood ducks (WODU), ring-necked ducks (RNDU), and goldeneyes (GOLD) expected under closed, restrictive, moderate, and liberal regulations in the Atlantic Flyway.

Regulatory Alternative	AGWT	WODU	RNDU	GOLD
Closed (U.S.)	0.017	0.006	0.025	0.005
Restrictive	0.057	0.075	0.058	0.008
Moderate	0.089	0.091	0.097	0.015
Liberal	0.117	0.124	0.131	0.029

(i.e., post-survey), several technical adjustments and a new optimization framework were developed to support a pre-survey decision process. We revised the optimization procedures used to derive harvest policies by structuring the decision process based on the information that is available at the time of the decision, which includes the previous year's observation of the system, the previous year's regulation, and the latest update of model weights. Based on this new formulation, the prediction of future system states and harvest values now account for all possible outcomes from previous decisions, and as a result, the optimal policy is now conditional on the previous year's regulation. We modified the optimization code used for each AHM decision framework in order to continue to use stochastic dynamic programming (Williams et al. 2002) to derive optimal harvest policies while accounting for the pre-survey decision process (Johnson et al. 2016). Adjustments to these optimization procedures necessitated considerations of how closed season constraints and different objective functions were represented. Currently, we have implemented the closed season constraints and utility devaluation for mid-continent mallards conditional on the last observed state. With the cooperation of the Harvest Management Working Group, we are exploring alternative ways to implement these constraints that would be more consistent with the intent of the original specification (i.e., post-survey decision framework). A comparison of optimization and simulation results from pre- and post-survey AHM protocols suggested that the adjustments to the optimization procedures to account for changes in decision timing were not expected to result in major changes in expected management performance (Boomer et al. 2015). Updated optimization code was developed with the MDPSOLVE© (Fackler 2011) software tools implemented in MATLAB (2016).

Using stochastic dynamic programming (Williams et al. 2002) to evaluate a pre-survey decision process, we calculated the optimal regulatory strategy for the Mississippi and Central Flyways based on: (1) the dual objectives of maximizing long-term cumulative harvest and achieving a population goal of 8.5 million mid-continent mallards; (2) current regulatory alternatives and the closed-season constraint; and (3) current mid-continent mallard population models and associated weights. The resulting regulatory strategy includes options conditional on the regulatory alternative selected the previous hunting season (Figure 6). Note that prescriptions for closed seasons in this strategy represent resource conditions that are insufficient to support one of the current regulatory alternatives, given current harvest-management objectives and constraints. However, closed seasons under all of these conditions are not necessarily required for long-term resource protection, and simply reflect the NAWMP population goal and the nature of the current regulatory alternatives. Assuming that harvest management adhered to this strategy (and that current model weights accurately reflect population dynamics), breeding-population size would be expected to average 7.15 million (SD = 1.59 million). Based on a liberal regulatory alternative selected for the 2020 hunting season, the predicted 2020 breeding population size of 9.07 million mid-continent mallards and 3.40 million ponds predicted in Prairie Canada, the optimal choice for the 2021 hunting season in the Mississippi and Central Flyways is the liberal regulatory alternative (Table 4).

We calculated the optimal regulatory strategy for the Pacific Flyway based on: (1) an objective to maximize long-term cumulative harvest; (2) current regulatory alternatives; and (3) current population models and parameter estimates. The resulting regulatory strategy includes options conditional on the regulatory alternative selected the previous hunting season (Figure 7). We simulated the use of this regulatory strategy to determine expected performance characteristics. Assuming that harvest management adhered to this strategy (and that current model parameters accurately reflect population dynamics), breeding-population size would be expected to average 0.54 million (SD = 0.07 million) in Alaska and 0.57 million (SD = 0.05 million) in the southern Pacific Flyway. Based on a liberal regulatory alternative selected for the 2020 hunting season, a predicted 2020 breeding population size of 0.41 million mallards for Alaska, and 0.53 million for the southern Pacific Flyway, the optimal choice for the 2021 hunting season in the Pacific Flyway is the liberal regulatory alternative (Table 5).

We calculated the optimal regulatory strategy for the Atlantic Flyway based on: (1) an objective to achieve 98% of the maximum, long-term cumulative harvest for the aggregate of the four species; (2) current regulatory alternatives; and (3) current population models and parameter estimates. The resulting regulatory strategy includes options conditional on the regulatory alternative selected the previous hunting season (Figure 8). We simulated the use of this regulatory strategy to determine expected performance characteristics. Assuming that harvest management adhered to this strategy (and that the population models accurately

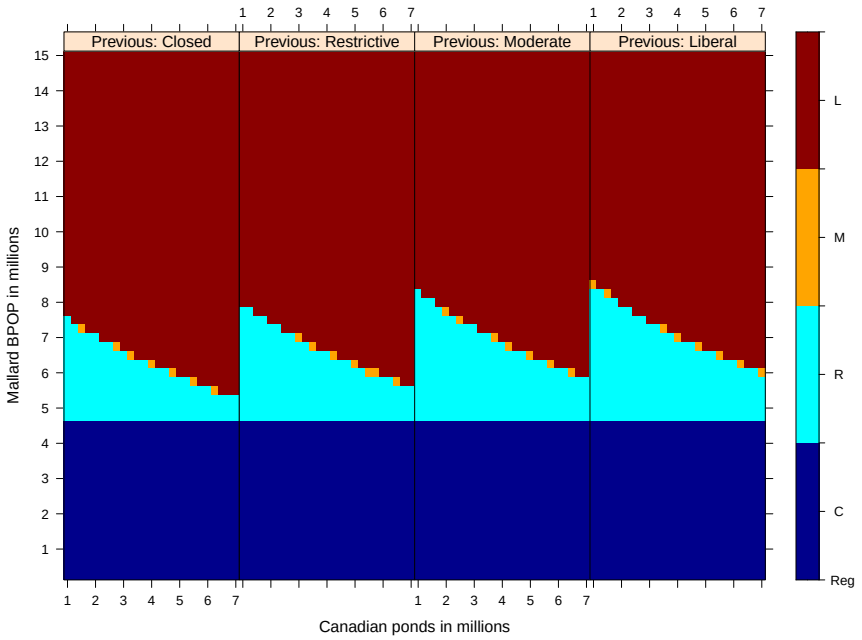

Figure 6 – Mid-continent mallard pre-survey harvest policies derived with updated optimization methods that account for changes in decision timing associated with adaptive harvest management protocols specified in the SEIS 2013. Harvest policies were calculated with current regulatory alternatives (including the closed-season constraint), mid-continent mallard models and weights, and the dual objectives of maximizing long-term cumulative harvest and achieving a population goal of 8.5 million mallards.

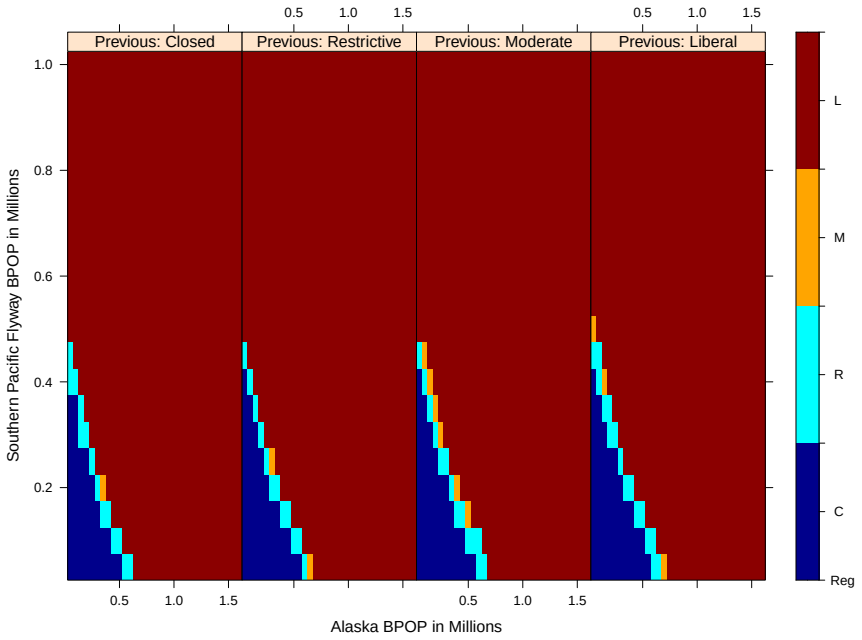

Figure 7 – Western mallard pre-survey harvest policies derived with updated optimization methods that account for changes in decision timing associated with adaptive harvest management protocols specified under the SEIS 2013. This strategy is based on current regulatory alternatives, updated (1990–2019) western mallard population models and parameter estimates, and an objective to maximize long-term cumulative harvest.

Table 4 – Optimal regulatory strategy[a] for the Mississippi and Central Flyways for the 2021 hunting season predicated on a liberal alternative selected the previous year (2020). This strategy is based on the current regulatory alternatives (including the closed-season constraint), mid-continent mallard models and weights, and the dual objectives of maximizing long-term cumulative harvest and achieving a population goal of 8.5 million mallards. The shaded cell indicates the regulatory prescription for the 2021 hunting season.

	Ponds[c]																		
BPOP[b]	1.50	1.75	2.00	2.25	2.50	2.75	3.00	3.25	3.50	3.75	4.00	4.25	4.50	4.75	5.00	5.25	5.50	5.75	6.00
≤4.50	C	C	C	C	C	C	C	C	C	C	C	C	C	C	C	C	C	C	C
4.75	R	R	R	R	R	R	R	R	R	R	R	R	R	R	R	R	R	R	R
5.00	R	R	R	R	R	R	R	R	R	R	R	R	R	R	R	R	R	R	R
5.25	R	R	R	R	R	R	R	R	R	R	R	R	R	R	R	R	R	R	R
5.50	R	R	R	R	R	R	R	R	R	R	R	R	R	R	R	R	R	R	R
5.75	R	R	R	R	R	R	R	R	R	R	R	R	R	R	R	R	R	R	R
6.00	R	R	R	R	R	R	R	R	R	R	R	R	R	R	R	R	R	R	R
6.25	R	R	R	R	R	R	R	R	R	R	R	R	R	R	R	R	R	R	R
6.50	R	R	R	R	R	R	R	R	R	R	R	R	R	R	R	R	M	L	L
6.75	R	R	R	R	R	R	R	R	R	R	R	R	R	M	L	L	L	L	L
7.00	R	R	R	R	R	R	R	R	R	R	M	L	L	L	L	L	L	L	L
7.25	R	R	R	R	R	R	R	R	M	L	L	L	L	L	L	L	L	L	L
7.50	R	R	R	R	R	R	L	L	L	L	L	L	L	L	L	L	L	L	L
7.75	R	R	R	R	L	L	L	L	L	L	L	L	L	L	L	L	L	L	L
8.00	R	R	L	L	L	L	L	L	L	L	L	L	L	L	L	L	L	L	L
8.25	M	L	L	L	L	L	L	L	L	L	L	L	L	L	L	L	L	L	L
≥8.50	L	L	L	L	L	L	L	L	L	L	L	L	L	L	L	L	L	L	L

[a] C = closed season, R = restrictive, M = moderate, L = liberal.

[b] Mallard breeding population size (in millions) observed in the WBPHS (strata 13–18, 20–50, 75–77) and Michigan, Minnesota, and Wisconsin.

[c] Ponds (in millions) observed in Prairie Canada in May.

Table 5 – Optimal regulatory strategy[a] for the Pacific Flyway for the 2021 hunting season predicated on a liberal alternative selected the previous year (2020). This strategy is based on current regulatory alternatives, updated (1990–2019) western mallard population models and parameter estimates, and an objective to maximize long-term cumulative harvest. The shaded cell indicates the regulatory prescription for 2021.

Southern Pacific Flyway BPOP[c]	Alaska BPOP[b]														
	0.05	0.10	0.15	0.20	0.25	0.30	0.35	0.40	0.45	0.50	0.55	0.60	0.65	0.70	≥0.75
0.05	C	C	C	C	C	C	C	C	C	C	C	R	R	M	L
0.10	C	C	C	C	C	C	C	C	C	C	R	R	L	L	L
0.15	C	C	C	C	C	C	C	C	R	R	L	L	L	L	L
0.20	C	C	C	C	C	C	R	R	L	L	L	L	L	L	L
0.25	C	C	C	C	C	R	L	L	L	L	L	L	L	L	L
0.30	C	C	C	R	R	L	L	L	L	L	L	L	L	L	L
0.35	C	C	R	R	L	L	L	L	L	L	L	L	L	L	L
0.40	C	R	M	L	L	L	L	L	L	L	L	L	L	L	L
0.45	R	R	L	L	L	L	L	L	L	L	L	L	L	L	L
0.50	M	L	L	L	L	L	L	L	L	L	L	L	L	L	L
0.55	L	L	L	L	L	L	L	L	L	L	L	L	L	L	L
0.60	L	L	L	L	L	L	L	L	L	L	L	L	L	L	L
0.65	L	L	L	L	L	L	L	L	L	L	L	L	L	L	L
0.70	L	L	L	L	L	L	L	L	L	L	L	L	L	L	L
≥0.75	L	L	L	L	L	L	L	L	L	L	L	L	L	L	L

[a] C = closed season, R = restrictive, M = moderate, L = liberal.

[b] Estimated number of mallards (in millions) observed in Alaska (WBPHS strata 1–12).

[c] Estimated number of mallards (in millions) observed in the southern Pacific Flyway (California, Oregon, Washington, and British Columbia combined).

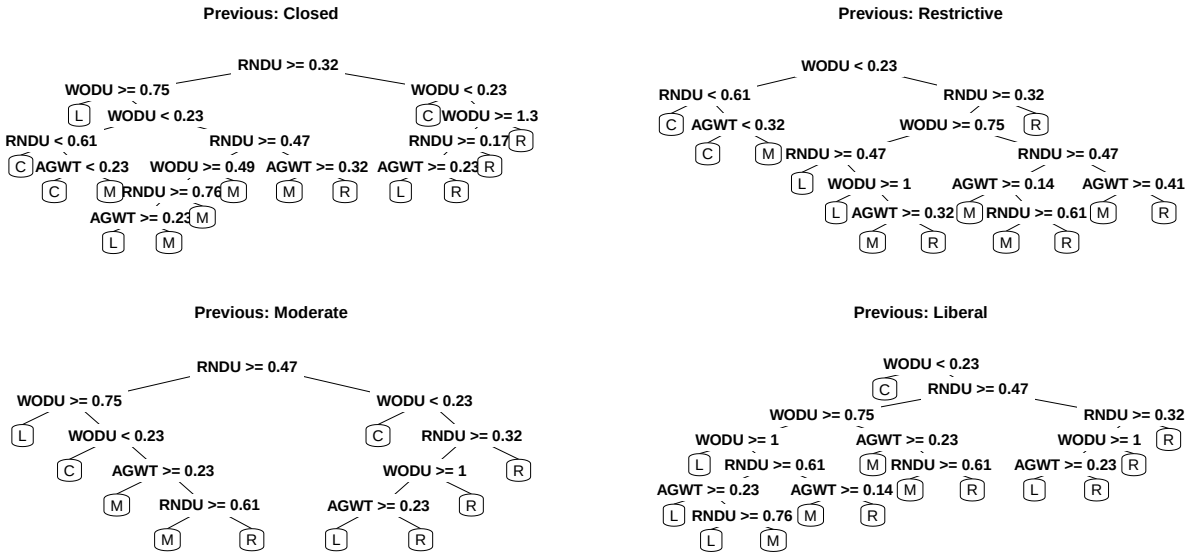

Figure 8 – A graphical representation of the Atlantic Flyway multi-stock pre-survey harvest policies derived with updated optimization methods that account for changes in decision timing associated with adaptive harvest management protocols specified under the SEIS 2013. This strategy is based on current regulatory alternatives, updated (1998–2019) population models and parameter estimates, and an objective to achieve 98% of the maximum, long-term cumulative harvest of the aggregate stocks. The classification trees are a statistical representation of the policies and do not depict all possible combinations of breeding population states and regulatory alternatives.

reflect population dynamics), breeding-population sizes would be expected to average 0.37 (SD = 0.03), 1.02 (SD = 0.07), 0.56 (SD = 0.04), and 0.62 (SD = 0.10) million for American green-winged teal, wood ducks, ring-necked ducks, and goldeneyes, respectively. Based on a liberal regulatory alternative selected for the 2020 hunting season and predicted 2020 breeding population sizes of 0.35 million American green-winged teal, 0.94 million wood ducks, 0.70 million ring-necked ducks, and 0.58 million goldeneyes, the optimal choice for 2021 hunting season in the Atlantic Flyway is the liberal regulatory alternative (see Table 6).

9 APPLICATION OF ADAPTIVE HARVEST MANAGEMENT CONCEPTS TO OTHER STOCKS

The USFWS is working to apply the principles and tools of AHM to improve decision-making for several other stocks of waterfowl. Below, we provide AHM updates for the 2021 hunting season that are currently informing American black duck, northern pintail, and scaup harvest management decisions.

9.1 American Black Duck

Federal, state, and provincial agencies in the U.S. and Canada agreed that an international harvest strategy for black ducks is needed because the resource is valued by both countries and both countries have the ability to influence the resource through harvest. The partners also agreed a harvest strategy should be developed with an AHM approach based on the integrated breeding-ground survey data (Zimmerman et al.

Table 6 – Optimal regulatory strategy[a] for the Atlantic Flyway for the 2021 hunting season. This strategy is based on current regulatory alternatives, species-specific population models and parameter estimates, and an objective to achieve 98% of the maximum, long-term cumulative harvest of the aggregate stocks. Predicated on a liberal alternative selected the previous year (2020), the shaded cells indicate current breeding population sizes and the regulatory prescription for 2021.

Species[b] Population (in millions)				
AGWT	WODU	RNDU	GOLD	Regulation
0.364	0.622	0.684	0.69	M
0.364	0.622	0.83	0.454	M
0.364	0.622	0.83	0.572	M
0.364	0.622	0.83	0.69	M
0.364	0.883	0.538	0.454	M
0.364	0.883	0.538	0.572	M
0.364	0.883	0.538	0.69	L
0.364	0.883	0.684	0.454	L
0.364	0.883	0.684	0.572	L
0.364	0.883	0.684	0.69	L
0.364	0.883	0.83	0.454	L
0.364	0.883	0.83	0.572	L
0.364	0.883	0.83	0.69	L
0.364	1.144	0.538	0.454	L
0.364	1.144	0.538	0.572	L
0.364	1.144	0.538	0.69	L
0.364	1.144	0.684	0.454	L

[a] C = closed season, M = moderate, R = restrictive, L = liberal.

[b] AGWT = American green-winged teal, WODU = wood duck, RNDU = ring-necked duck, GOLD = goldeneyes.

2012, U.S. Fish and Wildlife Service 2019*b*). Finally, the strategy should also provide a formal approach to determining appropriate harvest levels and fair allocation of the harvest between countries (Conroy 2010).

The overall goals of the Black Duck International Harvest strategy include:

(1) maintain a black duck population that meets legal mandates and provides consumptive and non-consumptive use commensurate with habitat carrying capacity;

(2) maintain societal values associated with the hunting tradition; and

(3) maintain equitable access to the black duck resource in Canada and the U.S.

The objectives of the harvest strategy are to achieve 98% of the long-term cumulative harvest and to share the allocated harvest (i.e., parity) equitably between countries. Historically, the realized allocation of harvest between Canada and the U.S. has ranged from 40% to 60% in either country. Recognizing the historical allocation and acknowledging incomplete control over harvest, parity is achieved through a constraint which discounts combinations of country-specific harvest rates that are expected to result in allocation of harvest that is >50% in one country. The constraint applies a mild penalty on country-specific harvest options that result in one country receiving >50% but <60% of the harvest allocation and a stronger discount on combinations resulting in one country receiving >60% of the harvest allocation (Figure 9). The goals and objectives of the black duck AHM framework were developed through a formal consultation process with representatives from the CWS, USFWS, Atlantic Flyway Council and Mississippi Flyway Council.

Country-specific harvest opportunities were determined from a set of expected harvest rate distributions defined as regulatory alternatives. Canada has developed 4 regulatory alternatives (liberal, moderate, restrictive and closed); and the U.S. has developed 3 (moderate, restrictive, closed; Figure 10). Expected harvest rates under each regulatory alternative are updated annually using Bayesian methods and modeling the mean harvest rate and variance using a beta-binomial distribution. The beta-binomial distribution is updated annually conditional on the country specific regulatory alternative implemented the previous year.

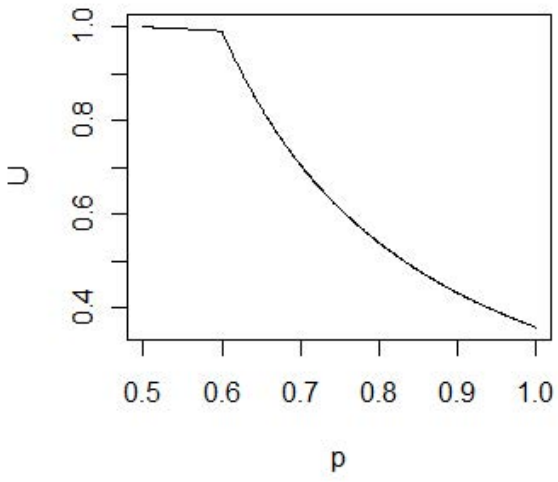

Figure 9 – Functional form of the harvest parity constraint designed to allocate allowable black duck harvest equally between the U.S. and Canada. The value of p is the proportion of harvest allocated to one country, and U is the utility of a specific combination of country-specific harvest options in achieving the objective of black duck adaptive harvest management.

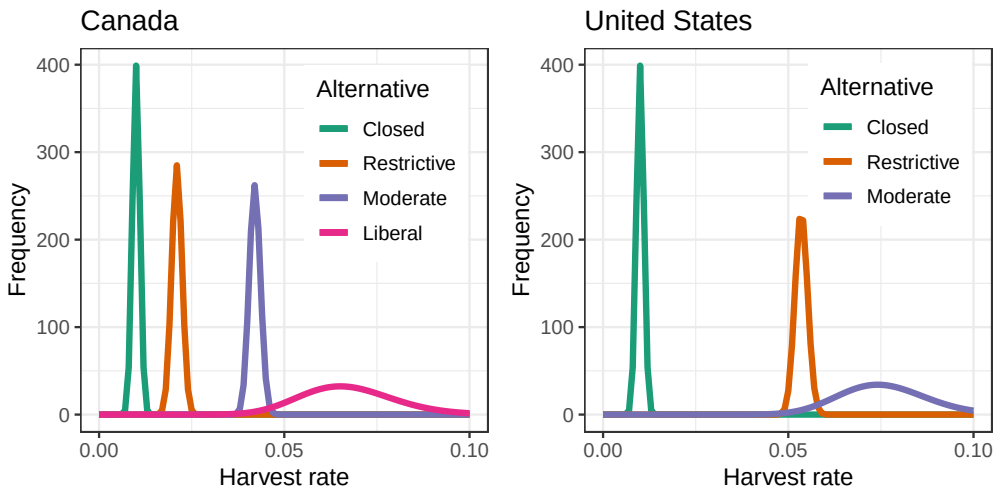

Figure 10 – Predictive harvest rate distributions for adult male black ducks expected under the application of the current regulatory alternatives in Canada (left) and the U.S. (right).

Since the implementation of black duck AHM, neither the closed alternative (in either country) or the restrictive alternative in Canada have been implemented. Therefore, we assume a prior distribution with mean harvest rate of 0.01 (±0.001 SE) and 0.021 (±0.0014 SE) for the closed and Canadian restrictive alternatives, respectively. The closed alternative requires either country to prohibit black duck harvest. The expected harvest rates (and associated variances) for the 2021 Canadian liberal and U.S. moderate alternatives are based on prior distributions and banding data resulting in broad, posterior harvest rate distributions (see Figure 10). Canada and the U.S. will determine, independently, appropriate regulations designed to achieve their prescribed harvest targets as identified under the regulatory alternatives. Regulations will vary independently between countries based on the status of the population and optimal strategy as determined through the AHM protocol.

The AHM model is based on spring breeding-ground abundance as estimated by the integrated Eastern Waterfowl Survey from the core survey area. The core survey area is comprised of USFWS survey strata 51, 52, 63, 64, 66, 67, 68, 70, 71, and 72. The American black duck population measure is based on "indicated pairs", defined as 1 individual observed equals 1 indicated pair whereas a group of 2 is assumed to represent 1.5 indicated pairs. Fall age ratios are estimated using harvest age ratios derived from the USFWS and CWS parts collection surveys, adjusted for differential vulnerability. Age- and sex-specific harvest rates are based on direct recoveries of black ducks banded in Canada, 1990–2019, adjusted by country- and band inscription-specific reporting rates. Direct and indirect band recoveries of adult and juvenile male and female black ducks banded in Canada, 1990–2019, were used to estimate age- and sex-specific annual survival rates.

The black duck AHM framework is based on two hypotheses regarding black duck population ecology. The first hypothesis states that black duck population growth is limited by competition with mallards during the breeding season. As the effect of mallard competition ($c2$) increases, black duck productivity decreases which then limits black duck population growth. The second hypothesis states that black duck population growth is limited by harvest because hunting mortality is additive to natural mortality. As the effect of harvest mortality, or additivity ($a1$) increases, annual survival decreases and limits black duck population growth. The current AHM framework incorporates each of these hypotheses into a single parametric (i.e., regression) model. Estimates of each parameter (i.e., mallard competition and additive hunting mortality) are updated with current year's monitoring data (Figure 11) and are used to establish annual harvest regulations. For 2020, we used the black duck integrated population model with the most recent information to predict a breeding population of 0.50 million. We then forecasted the 2020 eastern mallard population with recent data (see Appendix E) which resulted in a predicted value equal to 0.39 million.

Optimal country-specific regulatory strategies for the 2021 hunting season were calculated using: (1) the

black duck harvest objective (98% of long-term cumulative harvest); (2) current, country-specific regulatory alternatives (see Figure 10); (3) current parameter estimates for mallard competition and additive mortality (see Figure 11); (4) 2020 median predictions of 0.50 million breeding black ducks and 0.39 million breeding mallards in the core survey area; and (5) the country-specific 2020 regulations (liberal in Canada and moderate in the U.S). The optimal regulatory choices are the liberal alternative in Canada and moderate alternative in the U.S. (Table 7).

9.2 Northern Pintails

In 2010, the Flyway Councils and the USFWS established an adaptive management framework to inform northern pintail harvest decisions. The current protocol is based on: (1) an explicit harvest management objective; (2) regulatory alternatives that do not permit partial seasons (i.e., shorter pintail season within the general duck season) or 3-bird daily bag limits; (3) a formal optimization process using stochastic dynamic programming (Williams et al. 2002); (4) harvest allocation on a national rather than Flyway-by-Flyway basis, with no explicit attempt to achieve a particular allocation of harvest among Flyways; and (5) current system models. Details describing the historical development of the technical and policy elements of the northern pintail adaptive management framework can be found in the northern pintail harvest strategy document (U.S. Fish and Wildlife Service 2010).

The harvest-management objective for the northern pintail population is to maximize long-term cumulative harvest, which inherently requires perpetuation of a viable population. This objective is specified under a constraint that provides for an open hunting season when the observed breeding population is $\geq$1.75 million birds (based on the lowest observed breeding population size since 1985 of 1.79 million birds in 2002). The single objective and constraint, in conjunction with the regulatory alternatives were determined after an intensive consultation process with the waterfowl management community. The resulting management objective serves to integrate and balance multiple competing objectives for pintail harvest management, including minimizing closed seasons, eliminating partial seasons, maximizing seasons with liberal season length and greater than 1-bird daily bag limit, and minimizing large changes in regulations.

The adaptive management protocol considers a range of regulatory alternatives for pintail harvest management that includes a closed season, 1-bird daily bag limit, or 2-bird daily bag limit. The maximum pintail season length depends on the general duck season framework (characterized as liberal, moderate, or restrictive and varying by Flyway) specified by mallard or multi-stock AHM. An optimal pintail regulation is calculated under the assumption of a liberal mallard or multi-stock season length in all Flyways. However, if the season

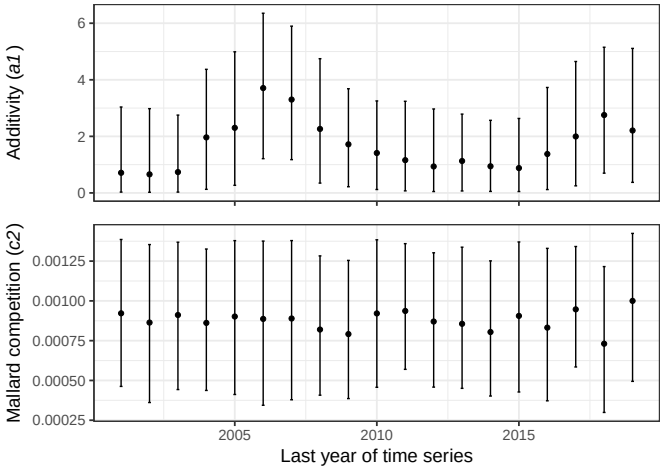

Figure 11 – Updated median estimates of black duck harvest additivity (*a1*; top panel) and mallard competition (*c2*; bottom panel) parameters over time. Error bars represent 95% credibility intervals.

Table 7 – Black duck optimal regulatory strategies[a] for Canada and the United States for the 2021 hunting season predicated on a liberal alternative selected by Canada and a moderate alternative selected by the United States the previous year (2020). This strategy is based on current regulatory alternatives, black duck model, and the objective of achieving 98% of the maximum, long-term cumulative harvest and to share the allocated harvest (i.e., parity) equitably between countries. The shaded cell indicates the regulatory prescription for each country in 2021.

Canada	MALL[b]																	
ABDU[b]	0.05	0.10	0.15	0.20	0.25	0.30	0.35	0.40	0.45	0.50	0.55	0.60	0.65	0.70	0.75	0.80	0.85	0.90
0.05	C	C	C	C	C	C	C	C	C	C	C	C	C	C	C	C	C	C
0.10	M	M	C	C	C	C	C	C	C	C	C	C	C	C	C	C	C	C
0.15	L	M	M	M	M	M	M	M	M	M	M	M	M	M	M	M	M	M
0.20	L	L	L	L	L	L	L	M	M	M	M	M	M	M	M	M	M	M
0.25	L	L	L	L	L	L	L	L	L	L	L	L	L	L	L	L	L	L
0.30	L	L	L	L	L	L	L	L	L	L	L	L	L	L	L	L	L	L
0.35	L	L	L	L	L	L	L	L	L	L	L	L	L	L	L	L	L	L
0.40	L	L	L	L	L	L	L	L	L	L	L	L	L	L	L	L	L	L
0.45	L	L	L	L	L	L	L	L	L	L	L	L	L	L	L	L	L	L
0.50	L	L	L	L	L	L	L	L	L	L	L	L	L	L	L	L	L	L
0.55	L	L	L	L	L	L	L	L	L	L	L	L	L	L	L	L	L	L
0.60	L	L	L	L	L	L	L	L	L	L	L	L	L	L	L	L	L	L
0.65	L	L	L	L	L	L	L	L	L	L	L	L	L	L	L	L	L	L
0.70	L	L	L	L	L	L	L	L	L	L	L	L	L	L	L	L	L	L
0.75	L	L	L	L	L	L	L	L	L	L	L	L	L	L	L	L	L	L
0.80	L	L	L	L	L	L	L	L	L	L	L	L	L	L	L	L	L	L

United States	MALL[b]																	
ABDU[b]	0.05	0.10	0.15	0.20	0.25	0.30	0.35	0.40	0.45	0.50	0.55	0.60	0.65	0.70	0.75	0.80	0.85	0.90
0.05	C	C	C	C	C	C	C	C	C	C	C	C	C	C	C	C	C	C
0.10	R	R	C	C	C	C	C	C	C	C	C	C	C	C	C	C	C	C
0.15	R	R	R	R	R	R	R	R	R	R	R	R	R	R	R	R	R	R
0.20	M	M	M	M	R	R	R	R	R	R	R	R	R	R	R	R	R	R
0.25	M	M	M	M	M	M	M	M	M	M	M	M	R	R	R	R	R	M
0.30	M	M	M	M	M	M	M	M	M	M	M	M	M	M	M	M	M	M
0.35	M	M	M	M	M	M	M	M	M	M	M	M	M	M	M	M	M	M
0.40	M	M	M	M	M	M	M	M	M	M	M	M	M	M	M	M	M	M
0.45	M	M	M	M	M	M	M	M	M	M	M	M	M	M	M	M	M	M
0.50	M	M	M	M	M	M	M	M	M	M	M	M	M	M	M	M	M	M
0.55	M	M	M	M	M	M	M	M	M	M	M	M	M	M	M	M	M	M
0.60	M	M	M	M	M	M	M	M	M	M	M	M	M	M	M	M	M	M
0.65	M	M	M	M	M	M	M	M	M	M	M	M	M	M	M	M	M	M
0.70	M	M	M	M	M	M	M	M	M	M	M	M	M	M	M	M	M	M
0.75	M	M	M	M	M	M	M	M	M	M	M	M	M	M	M	M	M	M
0.80	M	M	M	M	M	M	M	M	M	M	M	M	M	M	M	M	M	M

[a] C = closed season, R = restrictive, M = moderate, L = liberal.

[b] Mallard and black duck breeding population sizes (in millions).

Table 8 – Substitution rules in the Central and Mississippi Flyways for joint implementation of northern pintail and mallard harvest strategies. The mid-continent mallard AHM strategy stipulates the maximum season length for pintails in the Central and Mississippi Flyways. The substitutions are used when the mid-continent mallard season length is less than liberal. For example, if the pintail strategy calls for a liberal season length with a 2-bird daily bag limit, but the mid-continent mallard strategy calls for a restrictive season length, the recommended pintail regulation for the Central and Mississippi Flyways would be restrictive in length with a 3-bird daily bag limit.

Pintail	Mid-continent mallard adaptive harvest management season length			
Regulation	Closed	Restrictive	Moderate	Liberal
Closed	Closed	Closed	Closed	Closed
Liberal 1	Closed	Restrictive 3	Moderate 3	Liberal 1
Liberal 2	Closed	Restrictive 3	Moderate 3	Liberal 2

length of the general duck season determined by mallard or multi-stock AHM is less than liberal in any of the Flyways, then an appropriate pintail daily bag limit would be substituted for that Flyway. Thus, a shorter season length dictated by mallard or multi-stock AHM would result in an equivalent season length for pintails, but with increased bag limit if the expected harvest remained within allowable limits.

Regulatory substitution rules have been developed for the Central and Mississippi Flyways, where the general duck season length is driven by the mid-continent mallard AHM protocol (Table 8). These substitutions were determined by finding a pintail daily bag limit whose expected harvest was less than or equal to that called for under the national recommendation. Thus, if the national pintail harvest strategy called for a liberal 2-bird bag limit, but the mid-continent mallard season length was moderate, the recommended pintail regulation for the Central and Mississippi Flyways would be moderate in length with a 3-bird bag limit. Because season lengths more restrictive than liberal are expected infrequently in the Atlantic and Pacific Flyways under current eastern multi-stock and western mallard AHM strategies, substitution rules have not yet been developed for these Flyways. If shorter season lengths were called for in the Pacific or Atlantic Flyway, then similar rules would be specified for these Flyways and used to identify the appropriate substitution. In all cases, a substitution produces a lower expected harvest than the harvest allowed under the pintail strategy.

The current AHM protocol for pintails considers two population models. Each model represents an alternative hypothesis about the effect of harvest on population dynamics: one in which harvest is additive to natural mortality, and another in which harvest is compensatory to natural mortality. The compensatory model assumes that the mechanism for compensation is density-dependent post-harvest (winter) survival. The models differ only in how they incorporate the winter survival rate. In the additive model, winter survival rate is a constant, whereas winter survival is density-dependent in the compensatory model. A complete description of the model set used to predict pintail population change can be found in Appendix L. Model weights for the pintail model set have been updated annually since 2007 by comparing model predictions with observed survey results. As of 2019, model weights favor the hypothesis that harvest mortality is additive (57%). For 2020, we used the pintail model set to calculate a weighted average of 2.446 million (SE = 0.489 million) on the observed scale. We updated the latitude model with recent data (see Appendix F) to forecast the 2020 pintail breeding distribution (latitude) which resulted in a predicted value equal to 55.16 (SE = 1.73) degrees.

An optimal regulatory strategy for the 2021 hunting season was calculated for northern pintails using: (1) an objective to maximize long-term cumulative harvest; (2) current regulatory alternatives and the closed-season constraint; and (3) current population models and model weights. The resulting regulatory strategy includes options conditional on the regulatory alternative selected the previous hunting season (Figure 12). Based on a liberal, 1-bird daily bag limit, regulatory alternative selected for the 2020 hunting season and a predicted 2020 breeding population size of 2.446 million pintails observed at a mean latitude of 55.16 degrees, the optimal regulatory choice for the 2021 hunting season for all four Flyways is the liberal regulatory alternative with a 1-bird daily bag limit (Table 9).

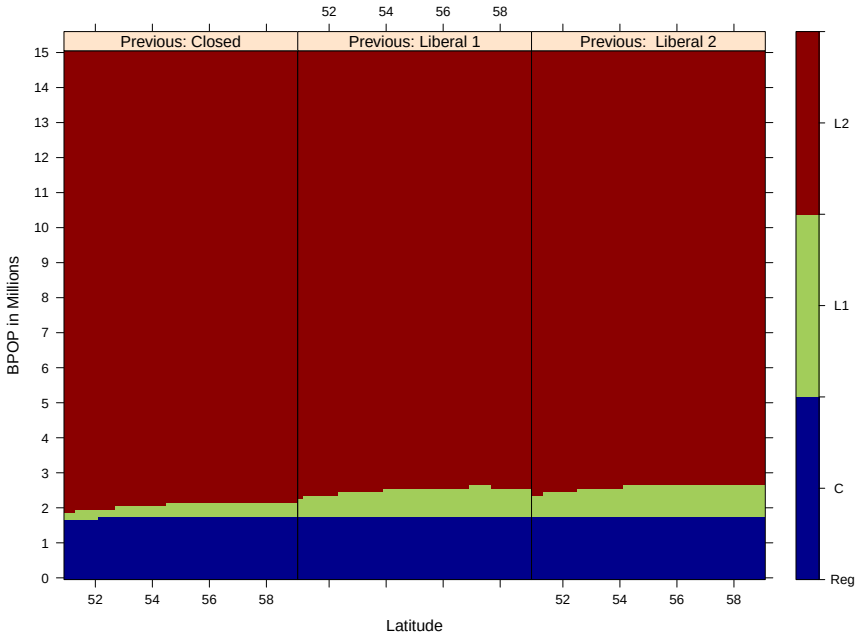

Figure 12 – Northern pintail pre-survey harvest policies derived with updated optimization methods that account for changes in decision timing associated with adaptive harvest management protocols specified in the SEIS 2013. This strategy is based on current regulatory alternatives, current population models and their weights, and an objective to maximize long-term cumulative harvest.

Table 9 – Northern pintail optimal regulatory strategy[a] for the 2021 hunting season predicated on a liberal season and a 1-bird daily bag limit selected the previous year (2020). This strategy is based on current regulatory alternatives, northern pintail models and weights, and the objective of maximizing long-term cumulative harvest constrained to provide for an open hunting season when the observed breeding population is ≥1.75 million birds. The shaded cell indicates the regulatory prescription for 2021.

	Mean latitude[c]																				
BPOP[b]	53	53.2	53.4	53.6	53.8	54	54.2	54.4	54.6	54.8	55	55.2	55.4	55.6	55.8	56	56.2	56.4	56.6	56.8	57
≤ 1.7	C	C	C	C	C	C	C	C	C	C	C	C	C	C	C	C	C	C	C	C	C
1.8	L1	L1	L1	L1	L1	L1	L1	L1	L1	L1	L1	L1	L1	L1	L1	L1	L1	L1	L1	L1	L1
1.9	L1	L1	L1	L1	L1	L1	L1	L1	L1	L1	L1	L1	L1	L1	L1	L1	L1	L1	L1	L1	L1
2	L1	L1	L1	L1	L1	L1	L1	L1	L1	L1	L1	L1	L1	L1	L1	L1	L1	L1	L1	L1	L1
2.1	L1	L1	L1	L1	L1	L1	L1	L1	L1	L1	L1	L1	L1	L1	L1	L1	L1	L1	L1	L1	L1
2.2	L1	L1	L1	L1	L1	L1	L1	L1	L1	L1	L1	L1	L1	L1	L1	L1	L1	L1	L1	L1	L1
2.3	L1	L1	L1	L1	L1	L1	L1	L1	L1	L1	L1	L1	L1	L1	L1	L1	L1	L1	L1	L1	L1
2.4	L1	L1	L1	L1	L1	L1	L1	L1	L1	L1	L1	L1	L1	L1	L1	L1	L1	L1	L1	L1	L1
2.5	L2	L2	L2	L2	L2	L1	L1	L1	L1	L1	L1	L1	L1	L1	L1	L1	L1	L1	L1	L1	L1
2.6	L2	L2	L2	L2	L2	L2	L2	L2	L2	L2	L2	L2	L2	L2	L2	L2	L2	L2	L2	L2	L1
2.7	L2	L2	L2	L2	L2	L2	L2	L2	L2	L2	L2	L2	L2	L2	L2	L2	L2	L2	L2	L2	L2
2.8	L2	L2	L2	L2	L2	L2	L2	L2	L2	L2	L2	L2	L2	L2	L2	L2	L2	L2	L2	L2	L2
2.9	L2	L2	L2	L2	L2	L2	L2	L2	L2	L2	L2	L2	L2	L2	L2	L2	L2	L2	L2	L2	L2
≥3	L2	L2	L2	L2	L2	L2	L2	L2	L2	L2	L2	L2	L2	L2	L2	L2	L2	L2	L2	L2	L2

[a] C = closed season, L1 = liberal season with 1-bird daily bag limit, L2 = liberal season with 2-bird daily bag limit.

[b] Observed northern pintail breeding population size (in millions) from the WBPHS (strata 1–18, 20–50, 75–77).

[c] Mean latitude (in degrees) is the average latitude of the WBPHS strata weighted by population size.

Table 10 – Regulatory alternatives[a] and total expected harvest levels corresponding to the closed, restrictive, moderate, and liberal packages considered in the scaup adaptive harvest management decision framework.

Package	Atlantic	Mississippi	Central	Pacific	Expected Harvest[c]
Closed					0.04
Restrictive	20(2)/40(1)[b]	45(2)/15(1)[b]	39(2)/35(1)[b]	86(2)	0.20
Moderate	60(2)	60(3)	74(3)	86(3)	0.35
Liberal	60(4)	60(4)	74(6)	107(7)	0.60

[a] Season length in days (daily bag limit); these alternatives assume an overall liberal adaptive harvest management framework as determined by the status of mallards or multiple stocks in the Atlantic Flyway.

[b] Multiple day and daily bag limit combinations refer to hybrid seasons which allow for different daily bag limits over a continuous season length.

[c] Total harvest in millions (Canada and United States combined).

9.3 Scaup

The USFWS implemented an AHM decision-making framework to inform scaup harvest regulations in 2008 (Boomer and Johnson 2007). Prior to the implementation of the SEIS 2013, the scaup AHM protocol first derived optimal harvest levels which were then used to determine the recommended regulatory package. Each year, an optimization was performed to identify the optimal harvest level based on updated scaup population parameters. The harvest regulation was then determined by comparing the optimal harvest level to the harvest thresholds corresponding to restrictive, moderate, and liberal packages (see Boomer et al. 2007). Due to the changes in decision timing associated with the SEIS, these procedures are not possible because decision makers would have to condition their regulatory decision on the harvest levels observed during the previous hunting season and this information would not be available. As a result, the decision variable (harvest) in the scaup optimization was changed from harvest levels to a set of packages with associated expected harvest levels in the updated optimization methods. We used the thresholds identified in Boomer et al. (2007) to specify expected harvest levels for each package (Table 10). To account for partial controllability of the scaup harvest, we assumed that the harvest under each package could be represented with a normal distribution with the mean set to the expected harvest level, assuming a coefficient of variation equal to 20%.

Initial scaup regulatory alternatives associated with restrictive, moderate, and liberal packages were developed based on a simulation of an optimal policy derived under an objective to achieve 95% of the maximum, long-term cumulative harvest (Boomer et al. 2007). This objective resulted in a strategy less sensitive to small changes in population size compared to a strategy derived under an objective to achieve 100% of the maximum, long-term cumulative harvest and allowed for some harvest opportunity at relatively low population sizes. The USFWS worked with the Flyways to specify Flyway-specific regulatory alternatives to achieve the allowable harvest thresholds corresponding to each package. At this time, the USFWS also agreed to consider "hybrid season" options that would be available to all Flyways for the restrictive and moderate packages. Hybrid seasons allow daily bag limits to vary for certain continuous portions of the scaup season length. In 2008, restrictive, moderate, and liberal scaup regulatory alternatives were defined and implemented in all four Flyways. Subsequent feedback from the Flyways led the USFWS to further clarify criteria associated with the establishment of "hybrid seasons" and to allow additional modifications of the alternatives for each Flyway resulting in updated regulatory alternatives that were adopted in 2009. Because of the considerable uncertainty involved with predicting scaup harvest, the USFWS and the Flyways agreed to keep these packages in place for at least 3 years. In 2013, the moderate packages for the Mississippi and Central Flyways were modified to include a 3-bird daily bag limit.

The lack of scaup demographic information over a sufficient time frame and at a continental scale precludes the use of a traditional balance equation to represent scaup population and harvest dynamics. As a result, we used a discrete-time, stochastic, logistic-growth population model to represent changes in scaup abundance, while explicitly accounting for scaling issues associated with the monitoring data. Details describing the modeling and assessment framework that has been developed for scaup can be found in Appendix M and in

Boomer and Johnson (2007).

We updated the scaup assessment based on the current model formulation and data extending from 1974 through 2019 and predicted the 2020 breeding population size equal to a median 3.53 million (SE = 0.37). As in past analyses, the state-space formulation and Bayesian analysis framework provided reasonable fits to the observed breeding population and total harvest estimates with realistic measures of variation. The posterior mean estimate of the intrinsic rate of increase (r) is 0.13 while the posterior mean estimate of the carrying capacity (K) is 8.76 million birds. The posterior mean estimate of the scaling parameter (q) is 0.76, ranging between 0.68 and 0.84 with 95% probability.

An optimal regulatory strategy for the 2021 hunting season was calculated for scaup using: (1) an objective to achieve 95% of the maximum, long-term cumulative harvest; (2) current regulatory alternatives; and (3) the current population model and updated parameter estimates. The resulting regulatory strategy includes options conditional on the regulatory alternative selected the previous hunting season (Table 11). We simulated the use of this regulatory strategy to determine expected performance characteristics. Assuming that harvest management adhered to this strategy (and that current model parameters accurately reflect population dynamics), breeding-population size would be expected to average 4.95 million (SD = 0.87 million). Based on a restrictive regulatory alternative selected for the 2020 hunting season and a predicted 2020 breeding population size of 3.53 million scaup, the optimal regulatory choice for the 2021 hunting season for all four Flyways is the restrictive regulatory alternative (see Table 11).

10 EMERGING ISSUES IN ADAPTIVE HARVEST MANAGEMENT

Learning occurs passively with current AHM protocols as annual comparisons of model predictions to observations from monitoring programs are used to update model weights and relative beliefs about system responses to management (Johnson et al. 2002) or as model parameters are updated based on an assessment of the most recent monitoring data (Boomer and Johnson 2007, Johnson et al. 2007). However, learning can also occur as decision-making frameworks are evaluated to determine if objectives are being achieved, have changed, or if other aspects of the decision problem are adequately being addressed. Often the feedback resulting from this process results in a form of "double-loop" learning (Lee 1993) that offers the opportunity to adapt decision-making frameworks in response to a shifting decision context, novel or emerging management alternatives, or a need to revise assumptions and models that may perform poorly or need to account for new information. Adaptive management depends on this iterative process to ensure that decision-making protocols remain relevant in evolving biological and social systems. Throughout the waterfowl harvest management community, substantial progress has been made to outline the important issues that must be considered in the revision of each AHM protocol (Johnson et al. 2015). In response to these large-scale issues, the HMWG has been focusing efforts on the evolving needs of AHM and the role of the working group in planning for and executing the double-loop learning phase of AHM in relation to various decision-making frameworks.

In addition, the HMWG has been discussing the technical challenges involved with dealing with large-scale habitat and environmental change on the decision-making frameworks used to inform waterfowl harvest management. We anticipate that large-scale system change will exacerbate most forms of uncertainty that affect waterfowl AHM, but we believe that the elements of the current AHM framework provide the necessary structure for coping with these changing systems (Nichols et al. 2011).

The 2019 HMWG meeting focused on the evaluation of the Central Flyway's proposal for a two-tier regulations system along with revisions to northern pintail AHM (U.S. Fish and Wildlife Service 2019*a*). The HMWG proposed changes to the timing of how HMWG priorities are evaluated and established, by including a mid-summer conference call among working group members to discuss progress and current HMWG priorities. After this year's July conference call, the HMWG proposed an updated set of fiscal year (FY2021) priorities for 2021 (Appendix C).

Table 11 – Scaup optimal regulatory strategy[a] for the 2021 hunting season. This strategy is based on the current scaup population model and an objective to achieve 95% of the maximum, long-term cumulative harvest. Predicated on a restrictive regulatory alternative selected the previous year (2020), the shaded cell indicates the regulatory prescription for the 2021 hunting season.

	Previous Regulation			
BPOP[b]	Closed	Restrictive	Moderate	Liberal
≤2.7	C	C	C	C
2.8	C	C	C	C
2.9	R	C	C	C
3.0	R	R	C	C
3.1	R	R	R	C
3.2	R	R	R	C
3.3	R	R	R	R
3.4	R	R	R	R
3.5	R	R	R	R
3.6	R	R	R	R
3.7	R	R	R	R
3.8	R	R	R	R
3.9	R	R	R	R
4.0	R	R	R	R
4.1	M	R	R	R
4.2	M	R	R	R
4.3	M	M	R	R
4.4	M	M	M	R
4.5	M	M	M	R
4.6	M	M	M	M
4.7	M	M	M	M
4.8	M	M	M	M
4.9	M	M	M	M
5.0	M	M	M	M
5.1	M	M	M	M
5.2	M	M	M	M
5.3	M	M	M	M
5.4	M	M	M	M
5.5	L	M	M	M
5.6	L	M	M	M
5.7	L	L	M	M
5.8	L	L	L	M
5.9	L	L	L	M
≥6	L	L	L	L

[a] C = closed season, R = restrictive, M = moderate, L = liberal.

[b] Estimated scaup breeding population (in millions) observed in the WBPHS (strata 1–18, 20–50, 75–77).

LITERATURE CITED

Anderson, D. R., and K. P. Burnham. 1976. Population ecology of the mallard. VI. The effect of exploitation on survival. U.S. Fish and Wildlife Service Resource Publication. 128. 66pp.

Balkcom, G. D., P. R. Garrettson, and P. I. Padding. 2010. Predicting wood duck harvest rates in Eastern North America. Journal of Wildlife Management 74:1575–1579.

Blohm, R. J. 1989. Introduction to harvest – understanding surveys and season setting. Proceedings of the International Waterfowl Symposium 6:118–133.

Blohm, R. J., R. E. Reynolds, J. P. Bladen, J. D. Nichols, J. E. Hines, K. P. Pollock, and R. T. Eberhardt. 1987. Mallard mortality rates on key breeding and wintering areas. Transactions of the North American Wildilfe and Resources Conference 52:246–263.

Boomer, G. S., and F. A. Johnson. 2007. A proposed assessment and decision-making framework to inform scaup harvest management. Unpublished Report. U.S. Fish and Wildlife Service, Laurel, MD. 26pp. URL http://www.fws.gov/migratorybirds/NewReportsPublications/SpecialTopics/BySpecies/SCAUP2007Report.pdf.

Boomer, G. S., F. A. Johnson, M. D. Koneff, T. A. Sanders, and R. E. Trost. 2007. A process to determine scaup regulatory alternatives. Unpublished Scoping Document. U.S. Fish and Wildlife Service, Laurel, MD. 20pp. URL http://www.fws.gov/migratorybirds/NewReportsPublications/SpecialTopics/BySpecies/scaup_regs_scoping_draftVI.pdf.

Boomer, G. S., F. A. Johnson, and G. S. Zimmerman. 2015. Adaptive harvest management: adjustments for SEIS 2013. U. S. Department of Interior, Washington, D. C. 21pp. URL http://www.fws.gov/migratorybirds/pdf/management/AHM/SEIS&AHMReportFinal.pdf.

Boomer, G. S., G. S. Zimmerman, P. R. Garrettson, M. D. Koneff, T. A. Sanders, K. D. Magruder, and J. A. Royle. 2013. Band reporting probabilities for mallards recovered in the United States and Canada. Journal of Wildlife Management 77:1059–1066.

Brooks, S. P., and A. Gelman. 1998. Alternative methods for monitoring convergence of iterative simulations. Journal of Computational and Graphical Statistics 7:434–455.

Burnham, K. P., G. C. White, and D. R. Anderson. 1984. Estimating the effect of hunting on annual survival rates of adult mallards. Journal of Wildlife Management 48:350–361.

Conroy, M. J. 2010. Technical support for adaptive harvest management for American black ducks. Unpublished Final Report. Cooperative Fish and Wildlife Research Unit, U.S. Geological Survey, Warnell School of Forestry and Natural Resources, University of Georgia, Athens, GA.

Fackler, P. 2011. User's Guide, MDPSOLVE: A MATLAB Toolbox for Solving Markov Decision Problems with Dynamic Programming.

Garrettson, P. R., R. V. Raftovich, J. E. Hines, and G. S. Zimmerman. 2013. Band reporting probabilities of mallards, American black ducks, and wood ducks in eastern North America. Journal of Wildlife Management 78:50–57.

Henny, C. J., and K. P. Burnham. 1976. A reward band study of mallards to estimate reporting rates. Journal of Wildlife Management 40:1–14.

Heusmann, H. W., and J. R. Sauer. 2000. The northeastern states' waterfowl breeding population survey. Wildlife Society Bulletin 28:355–364.

Hodges, J. L., J. G. King, B. Conant, and H. A. Hanson. 1996. Aerial surveys of waterbirds in Alaska 1975–94: population trends and observer variability. National Biological Service, U.S. Department of the Interior Information and Technology Report 4, Washington, D.C.

Hyndman, R. J., and G. Athanasopoulos. 2018. Forecasting: principles and practice, 2nd edition. OTexts: Melbourne, Australia, OTexts.com/fpp2. Accessed on 14 July 2020.

Johnson, F. A. 2003. Population dynamics of ducks other than mallards in mid-continent North America. Draft. U.S. Fish and Wildlife Service, U.S. Department of the Interior, Washington, D.C. 15pp.

Johnson, F. A., G. S. Boomer, and T. A. Sanders. 2007. A proposed protocol for the adaptive harvest management of mallards breeding in Western North America. Unpublished Report. U.S. Fish and Wildlife Service, Laurel, MD. 33pp.

Johnson, F. A., G. S. Boomer, B. K. Williams, J. D. Nichols, and D. J. Case. 2015. Multilevel Learning in the Adaptive Management of Waterfowl Harvests: 20 Years and Counting. Wildlife Society Bulletin 39:9–19. URL http://dx.doi.org/10.1002/wsb.518.

Johnson, F. A., P. L. Fackler, G. S. Boomer, G. S. Zimmerman, B. K. Williams, J. D. Nichols, and R. M. Dorazio. 2016. State-dependent resource harvesting with lagged information about system states. PLoS ONE 11:1–21. URL http://dx.doi.org/10.1371%2Fjournal.pone.0157373.

Johnson, F. A., W. L. Kendall, and J. A. Dubovsky. 2002. Conditions and limitations on learning in the adaptive management of mallard harvests. Wildlife Society Bulletin 30:176–185.

Johnson, F. A., C. T. Moore, W. L. Kendall, J. A. Dubovsky, D. F. Caithamer, J. Kelley, J. R., and B. K. Williams. 1997. Uncertainty and the management of mallard harvests. Journal of Wildlife Management 61:202–216.

Johnson, F. A., M. A. Walters, and G. S. Boomer. 2012. Allowable levels of take for the trade in Nearctic songbirds. Ecological Applications 22:1114–1130. URL https://esajournals.onlinelibrary.wiley.com/doi/abs/10.1890/11-1164.1.

Johnson, F. A., B. K. Williams, J. D. Nichols, J. E. Hines, W. L. Kendall, G. W. Smith, and D. F. Caithamer. 1993. Developing an adaptive management strategy for harvesting waterfowl in North America. Transactions of the North American Wildlife and Natural Resources Conference 58:565–583.

Johnson, F. A., B. K. Williams, and P. R. Schmidt. 1996. Adaptive decision-making in waterfowl harvest and habitat management. Proceedings of the International Waterfowl Symposium 7:26–33.

Lee, K. N. 1993. Compass and Gyroscope: Integrating Science and Politics for the Environment. Island Press, Washington, D.C.

Martin, E. M., and S. M. Carney. 1977. Population ecology of the mallard. IV. A review of duck hunting regulations, activity, and success, with special reference to the mallard. U.S. Fish and Wildlife Service, Washington D.C.

MATLAB. 2016. Version 9.0.0.341360 (R2016a). The MathWorks Inc., Natick, Massachusetts.

Meyer, R., and R. B. Millar. 1999. BUGS in Bayesian stock assessments. Canadian Journal of Fisheries and Aquatic Sciences 56:10078–1086.

Millar, R. B., and R. Meyer. 2000. Non-linear state space modeling of fisheries biomass dynamics by using Metropolis-Hastings within Gibbs sampling. Applied Statistics 49:327–342.

Nichols, J. D., F. A. Johnson, and B. K. Williams. 1995*a*. Managing North American waterfowl in the face of uncertainty. Annual Review of Ecology and Systematics 26:177–199.

Nichols, J. D., M. D. Koneff, P. J. Heglund, M. G. Knutson, M. E. Seamans, J. E. Lyons, J. M. Morton, M. T. Jones, G. S. Boomer, and B. K. Williams. 2011. Climate change, uncertainty, and natural resource management. Journal of Wildlife Management 75:6–18.

Nichols, J. D., R. E. Reynolds, R. J. Blohm, R. E. Trost, J. E. Hines, and J. P. Bladen. 1995*b*. Geographic variation in band reporting rates for mallards based on reward banding. Journal of Wildlife Management 59:697–708.

Niel, C., and J.-D. Lebreton. 2005. Using demographic invariants to detect overharvested bird populations from incomplete data. Conservation Biology 19:826–835. URL http://www.jstor.org/stable/3591072.

Padding, P. I., G. S. Zimmerman, M. T. Huang, G. D. Balkcom, and P. K. Devers. 2018. A multi-stock adaptive harvest management protocol for informing annual harvest regulations in the Atlantic Flyway. Unpublished Final Report. U.S. Fish and Wildlife Service Division of Migratory Bird Management and the Atlantic Flyway.

Plummer, M., 2003. JAGS: A program for analysis of Bayesian graphical models using Gibbs sampling. Pages 1–10 *in* K. Hornik, F. Leisch, and A. Zeileis, editors. Proceedings of the 3rd international workshop on distributed statistical computing (DSC 2003). Vienna, Austria.

Runge, M. C. 2007. Northern pintail harvest strategy: development of a compensatory model. Unpublished Report. U.S. Geological Survey, Patuxent Wildlife Research Center, Laurel, MD.

Runge, M. C., and G. S. Boomer. 2005. Population dynamics and harvest management of the continental northern pintail population. Unpublished Report. U.S. Geological Survey, Patuxent Wildlife Research Center, Laurel, MD. 42pp.

Runge, M. C., F. A. Johnson, J. A. Dubovsky, W. L. Kendall, J. Lawrence, and J. Gammonley. 2002. A revised protocol for the adaptive harvest management of mid-continent mallards. U.S. Fish and Wildlife Service, U.S. Department of the Interior Technical report, Washington, D.C. URL http://www.fws.gov/migratorybirds/NewReportsPublications/AHM/Year2002/MCMrevise2002.pdf.

Runge, M. C., W. L. Kendall, and J. D. Nichols, 2004. Exploitation. *in* W. J. Sutherland and R. Green, editors. Bird Ecology and Conservation: A Handbook of Techniques. Oxford University Press, Inc., Oxford, UK.

Schaefer, M. B. 1954. Some aspects of the dynamics of populations important to the management of commercial marine fisheries. Bulletin of the Inter-American Tropical Tuna Commission 1:25–56.

Smith, G. W. 1995. A critical review of the aerial and ground surveys of breeding waterfowl in North America. National Biological Service, U.S. Department of the Interior Biological Science Report 5, Washington, D.C.

Spiegelhalter, D. J., A. Thomas, N. Best, and D. Lunn. 2003. WinBUGS 1.4 User manual. MRC Biostatistics Unit, Institues of Public Health, Cambridge, UK.

U.S. Department of the Interior. 2013. Final Supplemental Environmental Impact Statement: Issuance of Annual Regulations Permitting the Hunting of Migratory Birds. U.S. Fish and Wildlife Service, Washington, D.C. 418pp. URL http://www.fws.gov/migratorybirds/pdfs/FSEIS%20Issuance%20of%20Annual%20Regulations%20Permitting%20the%20Hunting%20of%20Migratory%20Birds.pdf.

U.S. Fish and Wildlife Service. 2000. Adaptive harvest management: 2000 duck hunting season. U.S. Department of Interior, Washington, D.C. 43pp. URL http://www.fws.gov/migratorybirds/NewReportsPublications/AHM/Year2000/ahm2000.pdf.

U.S. Fish and Wildlife Service. 2001. Framework-date extensions for duck hunting in the United States: projected impacts & coping with uncertainty. U.S. Department of Interior, Washington, D.C. 8pp. URL http://www.fws.gov/migratorybirds/NewReportsPublications/AHM/Year2001/fwassess.PDF.

U.S. Fish and Wildlife Service. 2002. Adaptive harvest management: 2002 duck hunting season. U.S. Department of Interior, Washington, D.C. 34pp. URL http://www.fws.gov/migratorybirds/NewReportsPublications/AHM/Year2002/2002-AHM-report.pdf.

U.S. Fish and Wildlife Service. 2010. Northern Pintail Harvest Strategy. U.S. Department of Interior, Washington, D.C. 20pp. URL http://www.fws.gov/migratorybirds/NewReportsPublications/SpecialTopics/BySpecies/Nopi%20Harvest%20Strategy%202010%20Final.pdf.

U.S. Fish and Wildlife Service. 2017. Adaptive harvest management: 2018 hunting season. U.S. Department of Interior, Washington, D.C. 58pp. URL https://www.fws.gov/migratorybirds/pdf/management/AHM/AHMReport2018.pdf.

U.S. Fish and Wildlife Service. 2019*a*. Harvest Management Working Group: 2019 Annual Meeting Report. U.S. Department of Interior, Washington, D.C. 41pp. URL https://www.fws.gov/migratorybirds/pdf/management/AHM/HMWGReport2019.pdf.

U.S. Fish and Wildlife Service. 2019*b*. Waterfowl population status, 2019. U.S. Department of Interior, Washington, D.C. URL https://www.fws.gov/migratorybirds/pdf/surveys-and-data/Population-status/Waterfowl/WaterfowlPopulationStatusReport19.pdf.

Walters, C. 1986. Adaptive Management of Renewable Resources. Macmillian, New York.

Williams, B. K., and F. A. Johnson. 1995. Adaptive management and the regulation of waterfowl harvests. Wildlife Society Bulletin 23:430–436.

Williams, B. K., F. A. Johnson, and K. Wilkins. 1996. Uncertainty and the adaptive management of waterfowl harvests. Journal of Wildlife Management 60:223–232.

Williams, B. K., J. D. Nichols, and M. J. Conroy. 2002. Analysis and Management of Animal Populations. Academic Press, San Diego, CA.

Zimmerman, G. S., J. R. Sauer, K. Fleming, W. A. Link, and P. R. Garrettson. 2015. Combining waterfowl and breeding bird survey data to estimate wood duck breeding population size in the Atlantic Flyway. Journal of Wildlife Management 79:1051–1061.

Zimmerman, G. S., J. R. Sauer, W. A. Link, and M. Otto. 2012. Composite analysis of black duck breeding population surveys in eastern North America. Journal of Wildlife Management 76:1165–1176.

Appendix A Harvest Management Working Group Members

This list includes only permanent members of the Harvest Management Working Group. Not listed here are numerous persons from federal and state agencies that assist the Working Group on an ad-hoc basis.

Coordinator:

Scott Boomer
U.S. Fish & Wildlife Service
11510 American Holly Drive
Laurel, Maryland 20708-4017
phone: 301-497-5684; fax: 301-497-5871
e-mail: scott_boomer@fws.gov

USFWS Representatives:

Nanette Seto (Region 1)
U.S. Fish & Wildlife Service
911 NE 11TH Avenue
Portland, OR 97232-4181
phone: 503 231-6159
fax: 503 231-2019
e-mail: nanette_seto@fws.gov

Scott Carleton (Region 2)
U.S. Fish & Wildlife Service
500 Gold SW - 8th Floor
Albuquerque, NM 87103
phone: 505-248-6639
fax: 505-248-7885
e-mail: scott_carleton@fws.gov

Tom Cooper (Region 3)
U.S. Fish & Wildlife Service
5600 American Blvd West
Bloomington, MN 55437-1458
phone: 612-713-5101
fax: 612-713-5393
e-mail: tom_cooper@fws.gov

Bill Uihlein (Region 4)
U.S. Fish & Wildlife Service
1875 Century Blvd.
Atlanta, GA 30345
phone: 404-679-7288
fax: 404 679-4180
e-mail:bill_uihlein@fws.gov

Pam Toschik (Region 5)
U.S. Fish & Wildlife Service
300 Westgate Center Drive
Hadley, MA 01035-9589
phone: 413-253-8610
fax: 413-253-8293
e-mail:pamela_toschik@fws.gov

Brian Smith (Region 6)
U.S. Fish & Wildlife Service
P.O. Box 25486-DFC
Denver, CO 80225-0486
phone: 303-236-4403
fax: 303-236-8680
e-mail:brian_w_smith@fws.gov

Eric Taylor (Region 7)
U.S. Fish & Wildlife Service
1011 East Tudor Road
Anchorage, AK 99503-6119
phone: 907-786-3446

Amedee Brickey (Region 8)
U.S. Fish & Wildlife Service
2800 Cottage Way, W-2606
Sacramento, CA 95825
phone: 916-414-6480

fax: 907-786-3641
e-mail: eric_taylor@fws.gov

Kathy Fleming (Headquarters)
Chief, Branch of Monitoring and Data Management
U.S. Fish & Wildlife Service
11510 American Holly Drive
Laurel, Maryland 20708-4017
phone:
fax: 301-497-5871
e-mail: kathy_fleming@fws.gov

Atlantic Flyway Representative (Headquarters)
U.S. Fish & Wildlife Service
Vacant

Jim Dubovsky (Headquarters)
Central Flyway Representative
U.S. Fish & Wildlife Service
134 Union Blvd., Suite 540
Lakewood, CO 80228
phone: 303-275-2386
fax: 303-275-2384
e-mail: james_dubovsky@fws.gov

fax: 916-414-6486
e-mail: amedee_brickey@fws.gov

Pat Devers (Headquarters)
Chief, Branch of Assessment and Decision Support
U.S. Fish & Wildlife Service
11510 American Holly Drive
Laurel, Maryland 20708-4017
phone:
fax: 301-497-5871
e-mail: pat_devers@fws.gov

Mississippi Flyway Representative (Headquarters)
U.S. Fish & Wildlife Service
Vacant

Todd Sanders (Headquarters)
Pacific Flyway Representative
U.S. Fish & Wildlife Service
1211 SE Cardinal Court, Suite 100
Vancouver, WA 98683
phone: 360-604-2562
fax: 360-604-2505
e-mail: todd_sanders@fws.gov

Canadian Wildlife Service Representatives:

Christian Roy
Canadian Wildlife Service
351 Saint-Joseph Blvd,
Gatineau, Que, K1A 0H3
phone: 819-938-5418
fax:
e-mail:christian.roy3@canada.ca

Vacant
Canadian Wildlife Service
Suite 150, 123 Main Street
Winnipeg, MB R3C 4W2
phone:
fax:
e-mail:

Flyway Council Representatives:

Min Huang (Atlantic Flyway)
CT Dept. of Environmental Protection
Franklin Wildlife Mgmt. Area
391 Route 32 North Franklin, CT 06254
phone: 860-642-6528
fax: 860-642-7964
e-mail: min.huang@po.state.ct.us

Greg Balkcom (Atlantic Flyway)
GA Dept. of Natural Resources
1014 Martin Luther King Blvd.
Fort Valley, GA 31030
phone: 478-825-6354
fax: 478-825-6421
e-mail:greg.balkcom@dnr.state.ga.us

John Brunjes (Mississippi Flyway)
Kentucky Dept. Of Fish and Wildlife Resources
1 Sportsman's Lane
Frankfort, KY 40601
phone: 502-892-4500
fax:
e-mail: john.brunjes@ky.gov

Adam Phelps (Mississippi Flyway)
Indiana Division of Fish and Wildlife
5596 E State Road 46
Bloomington, IN 47401
phone: 812-334-1137
fax: 812-339-4807
e-mail: APhelps@dnr.IN.gov

Mike Szymanski (Central Flyway)
North Dakota Game and Fish Department
100 North Bismarck Expressway
Bismarck, ND 58501-5095
phone: 701-328-6360
fax: 701-328-6352
e-mail: mszymanski@state.nd.us

Kevin Kraai (Central Flyway)
Texas Parks and Wildlife Department
P.O. Box 659
Canyon, TX 79015
phone: 806-651-3011
fax:
email: kevin.kraai@tpwd.texas.gov

Brandon Reishus (Pacific Flyway)
Oregon Dept of Fish and Wildlife
4034 Fairview Industrial Dr. SE
Salem, OR 97302
phone: 503-947-6324
fax: 503-947-6330
e-mail: brandon.s.reishus@state.or.us

Jason Schamber (Pacific Flyway)
Alaska Dept. Fish & Game
525 W. 67th Ave
Anchorage, AK 99518
phone: 907-267-2206
fax: 907-267-2859
e-mail: jason.schamber@alaska.gov

USGS Scientist:

Mike Runge (USGS)
Patuxent Wildlife Research Center
U.S. Geological Survey
12100 Beech Forest Rd. Laurel, MD 20708
phone: 301-497-5748
fax: 301-497-5545
e-mail: mrunge@usgs.gov

Appendix B 2021-2022 Regulatory Schedule

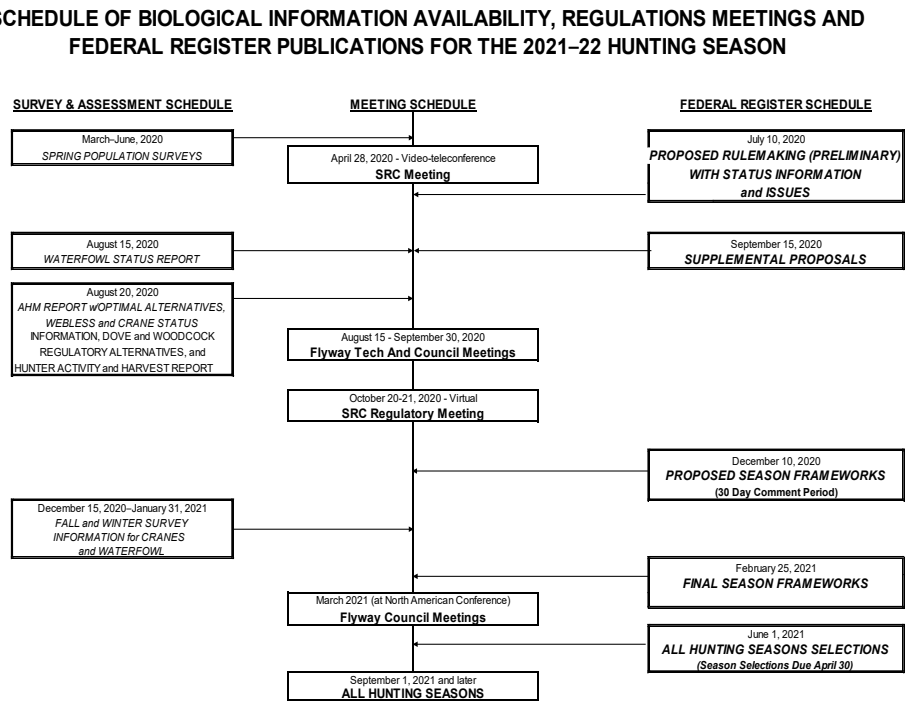

Figure B.1 – Schedule of biological information availability, regulation meetings, and Federal Register publications for the 2021–2022 hunting season.

Appendix C

Proposed FY2021 Harvest Management Working Group Priorities

Table C.1 – Priority rankings and project leads identified for the technical work proposed at the 2019 Harvest Management Working Group meeting and updated during the summer of 2020.

Priority Level	Status	Participants
Highest Priorities (Urgent and Important)		
Evaluation of Experimental two-tier license system	On-going	Central Flyway, DMBM
Northern Pintail AHM revision	On-going	DMBM, Flyway Councils, USGS
Reconsideration of North American Duck Harvest Management	On-going	DMBM, Flyway Councils
Development of an Eastern mallard harvest strategy	On-going	Atlantic Flyway Council, DMBM
Re-invigorating institutional support for AHM	On-going	DMBM, HMWG communications team
Long-range Priorities (Non-urgent, but Very Important)		
Time-dependent optimal solutions to address system change (e.g., habitat change; hunter dynamics; climate change).	On-going	USGS, BADS
Western mallard AHM revision	On-going	Pacific Flyway, BADS
Additional Priorities		
Waterfowl Banding Needs Assessment	On-going	BADS, USGS, Flyway Councils
Waterfowl harvest potential assessment methods case study development	On-going	Atlantic Flyway Office, DMBM

Forecasting Canadian Ponds: Spring 2020

G. Scott Boomer

Branch of Assessment and Decision Support
Division of Migratory Bird Management
U.S. Fish and Wildlife Service
scott_boomer@fws.gov

20 August 2020

Abstract

Due to the COVID-19 pandemic, waterfowl habitat conditions (ponds) were not directly observed in the spring of 2020. As a result, waterfowl harvest regulations will have to be informed with information based on predictions of breeding population sizes and habitat conditions. We developed an estimation and forecasting framework to predict the number of Canadian ponds in the spring of 2020 based on information that is available to decision makers during the 2020–2021 regulations process. We summarized annual, total precipitation for prairie Canada and used this variable as a predictor in an autoregressive integrated moving average (ARIMA) estimation framework to develop a model to forecast the number of Canadian ponds in 2020. The top ranked model that was best supported by the data included a 1st order moving average term [ARIMA (0,0,1)]. Based on our selected model, the 2020 forecast of the number of Canadian ponds is 3.40 million (95% PI = 1.75 – 5.06).

Contents

List of Tables

List of Figures

Background

Due to the COVID-19 pandemic, the United States Fish and Wildlife Service (USFWS) and its partners were unable to participate in the Waterfowl Breeding Population and Habitat Survey (WBPHS) to estimate the 2020 waterfowl breeding populations as well as evaluate breeding habitat conditions. As a result, the promulgation of waterfowl harvest regulations in 2020 will require some modifications to the adaptive harvest management (AHM) decision protocols that typically govern the regulatory process. For example, observed breeding population estimates are used to determine optimal levels of harvest. In the absence of this information, the USFWS proposes to base 2020 regulatory decisions on predictions of breeding population sizes and habitat conditions. Current system models for which we have AHM decision frameworks will be used to predict 2020 population sizes based on the breeding population sizes, habitat conditions, harvest, and harvest rates observed in 2019. Under the mid-continent mallard AHM decision framework, we use a 1st order autoregressive time series model to predict the number of Canadian ponds as a function of the number of ponds observed the previous year. However, this model is based on data from 1961 – 2001 and there is interest in updating the original pond model that was developed for mid-continent mallard AHM with the available information, including an additional predictor (total precipitation) that is available at the time decision makers will be considering regulatory decisions. As a result, we developed an estimation framework that will predict the number of Canadian ponds as a function of the number of ponds observed in 2019 and the total annual precipitation observed since the last WBPHS.

Data

We are interested in predicting the number of Canadian ponds for the 2020 breeding season from the available information for ponds observed in 2019 and the total amount of recorded precipitation from prairie weather stations from 1 June 2019 through 31 May 2020. Based on earlier work (Pospahala et al. 1974, Johnson et al. 1997), we selected weather stations from the Canadian prairies with continual observations of daily precipitation totals from 1961–2020 (Table 1). We then summarized the number of Canadian ponds observed in the traditional survey area of the Waterfowl Breeding Population and Habitat Survey (U.S. Fish and Wildlife Service 2019). We then summed the total precipitation recorded at the prairie weather stations from the 365 day period extending from 1 June to 31 May on the year of the WBPHS (i.e., the 2019 total precipitation value would be the sum of daily precipitation values observed from 1 June 2018 through 31 May 2019).

From 1961–2020, total precipitation in the Canadian prairies varied from a low of 271 mm in 2018 and a high of 563 mm in 1974 (Figure 1). The observed precipitation in 2020 was 394 mm.

Table 1: Weather stations used to summarize total annual precipitation observed in prairie Canada from 1961–2020

Province	Station_Name	Station_ID	Start_year	End_year
Alberta	EDMONTON INT'L A	1865	1959	2012
Alberta	EDMONTON INT'L A	50149	2012	2020
Alberta	MEDICINE HAT A	2273	1883	2008
Alberta	MEDICINE HAT RCS	30347	2000	2020
Manitoba	BRANDON A	3471	1941	2012
Manitoba	BRANDON RCS	49909	2012	2020
Manitoba	WINNIPEG RICHARDSON INT'L A	3698	1938	2008
Manitoba	WINNIPEG A CS	27174	1996	2020
Saskatchewan	REGINA INT'L A	3002	1959	2013
Saskatchewan	REGINA RCS	28011	2012	2020
Saskatchewan	SASKATOON DIEFENBAKER INT'L A	3328	1883	2012
Saskatchewan	SASKATOON RCS	47707	2000	2020

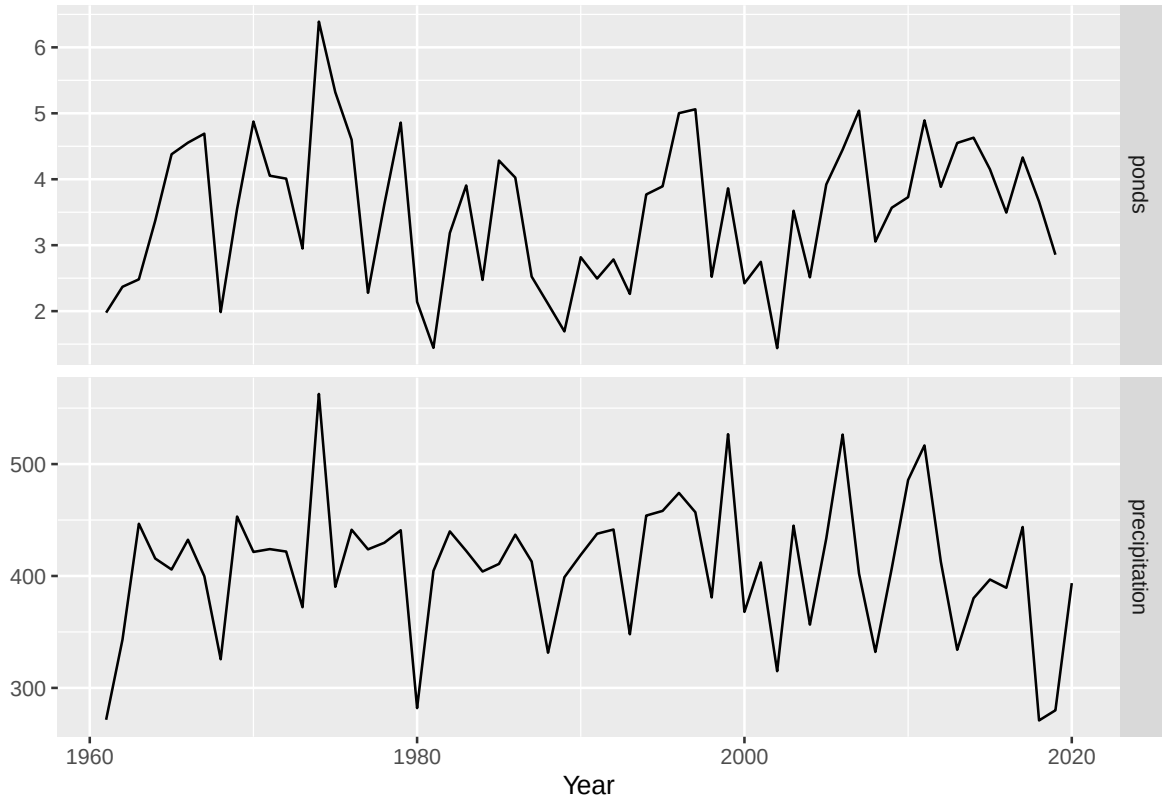

Figure 1: The number of ponds (millions) and total annual precipitation (mm) observed in prairie Canada from 1961–2020.

We first examined autocorrelation plots to evaluate the information in the Canadian pond time series (Figure 2) and used an augmented Dickey-Fuller test from the tseries R package (Trapletti and Hornik 2019) to analyze the time series for stationarity. The results from this test suggest there is evidence to reject the null hypothesis so we conclude that the data are stationary.

```
ggtsdisplay(window(cp_ts,end=2019)[,"ponds"],ylab="Canadian ponds")
```

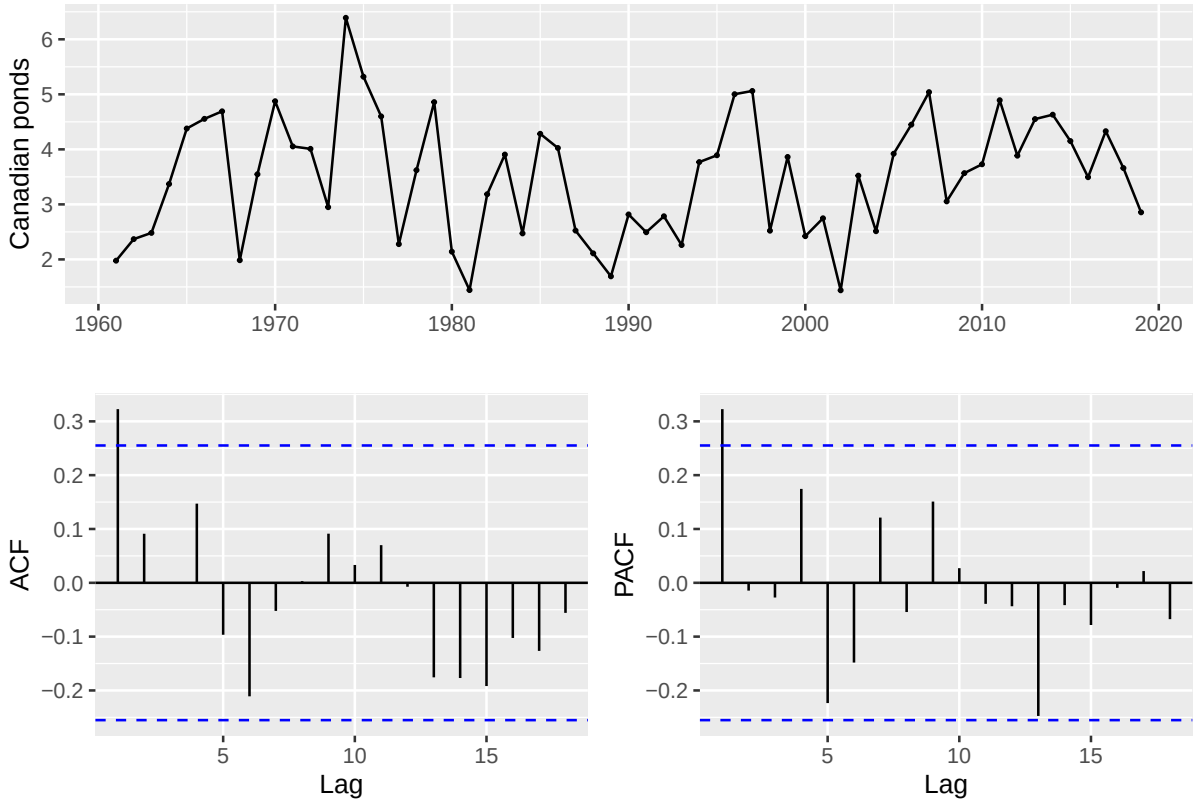

Figure 2: Autocorrelation plots of Canadian ponds (millions) observed in prairie Canada from 1961–2019.

```
#ggPacf(bwt_ts)

adf.test(window(cp_ts,end=2019)[,"ponds"],alternative="stationary",k=0)
```

```
## Warning in adf.test(window(cp_ts, end = 2019)[, "ponds"], alternative =
## "stationary", : p-value smaller than printed p-value

##
##  Augmented Dickey-Fuller Test
##
## data:  window(cp_ts, end = 2019)[, "ponds"]
## Dickey-Fuller = -5.3609, Lag order = 0, p-value = 0.01
## alternative hypothesis: stationary
```

To confirm this result, we used a KPSS test that can account for a trend.

```
kpss.test(window(cp_ts,end=2019)[,"ponds"],null="Trend")
```

```
## Warning in kpss.test(window(cp_ts, end = 2019)[, "ponds"], null = "Trend"): p-
## value greater than printed p-value
```

```
##
##  KPSS Test for Trend Stationarity
##
## data:  window(cp_ts, end = 2019)[, "ponds"]
## KPSS Trend = 0.10376, Truncation lag parameter = 3, p-value = 0.1
```

For the KPSS test, the null hypothesis is that the time series is stationary. Our test results provides little evidence to reject the null hypothesis that the pond time series is stationary, suggesting that we will not have to consider differencing in our analysis.

Time Series Analysis

We are interested in predicting the number of Canadian ponds for the 2020 breeding season as a function of the number of ponds observed in 2019 and the total amount of recorded precipitation from prairie weather stations from 1 June 2019 through 31 May 2020. We revisited the original formulation of the Canadian pond model developed for the mid-continent mallard AHM program (Johnson et al. 1997). The predictive equation used to project the number of Canadian ponds (P) included

$$P_t = \beta_0 + \alpha P_{t-1} + \beta_1 Precip_t + \epsilon_t$$

where, β_0 is the intercept, α is the autoregressive term, β_1 is the slope term for the precipitation covariate and error term ϵ is the assumed to be white noise.

We analyzed the updated information with an autoregressive integrated moving average (ARIMA) estimation framework, using the R function auto.arima from the forecast R package (Hyndman et al. 2020, Hyndman and Khandakar 2008) to determine the appropriate number of lags and levels of differencing (Hyndman and Athanasopoulos 2018) for the final specification of our ARIMA regression model.

```
fit<-auto.arima(window(cp_ts,end=2019)[,"ponds"],
                xreg=window(cp_ts,end=2019)[,"precipitation"],
                stepwise=FALSE,
                approximation=FALSE,
                seasonal=FALSE,
                trace=TRUE)
```

```
##
##  ARIMA(0,0,0) with zero mean     : 161.5068
##  ARIMA(0,0,0) with non-zero mean : 163.3993
##  ARIMA(0,0,1) with zero mean     : 152.119
##  ARIMA(0,0,1) with non-zero mean : 153.6019
##  ARIMA(0,0,2) with zero mean     : 153.751
##  ARIMA(0,0,2) with non-zero mean : 155.6254
##  ARIMA(0,0,3) with zero mean     : 155.8635
##  ARIMA(0,0,3) with non-zero mean : 157.9997
##  ARIMA(0,0,4) with zero mean     : 157.1322
##  ARIMA(0,0,4) with non-zero mean : 159.6507
##  ARIMA(0,0,5) with zero mean     : 159.1683
##  ARIMA(0,0,5) with non-zero mean : 161.6738
##  ARIMA(1,0,0) with zero mean     : 152.4232
##  ARIMA(1,0,0) with non-zero mean : 154.4094
```

```
##  ARIMA(1,0,1) with zero mean     : 153.8641
##  ARIMA(1,0,1) with non-zero mean : 155.6688
##  ARIMA(1,0,2) with zero mean     : 155.8828
##  ARIMA(1,0,2) with non-zero mean : 157.6111
##  ARIMA(1,0,3) with zero mean     : 158.0459
##  ARIMA(1,0,3) with non-zero mean : 160.3997
##  ARIMA(1,0,4) with zero mean     : 159.407
##  ARIMA(1,0,4) with non-zero mean : 161.965
##  ARIMA(2,0,0) with zero mean     : 154.0319
##  ARIMA(2,0,0) with non-zero mean : 155.9521
##  ARIMA(2,0,1) with zero mean     : 156.247
##  ARIMA(2,0,1) with non-zero mean : 158.1479
##  ARIMA(2,0,2) with zero mean     : 158.3529
##  ARIMA(2,0,2) with non-zero mean : 160.1859
##  ARIMA(2,0,3) with zero mean     : 160.304
##  ARIMA(2,0,3) with non-zero mean : Inf
##  ARIMA(3,0,0) with zero mean     : 155.6994
##  ARIMA(3,0,0) with non-zero mean : 157.4428
##  ARIMA(3,0,1) with zero mean     : 157.6636
##  ARIMA(3,0,1) with non-zero mean : 159.3361
##  ARIMA(3,0,2) with zero mean     : 158.8419
##  ARIMA(3,0,2) with non-zero mean : Inf
##  ARIMA(4,0,0) with zero mean     : 156.8177
##  ARIMA(4,0,0) with non-zero mean : 158.8691
##  ARIMA(4,0,1) with zero mean     : 159.152
##  ARIMA(4,0,1) with non-zero mean : 161.5277
##  ARIMA(5,0,0) with zero mean     : 159.0008
##  ARIMA(5,0,0) with non-zero mean : 161.4971
##
##
##
##  Best model: Regression with ARIMA(0,0,1) errors
```

```
print(fit)
```

```
## Series: window(cp_ts, end = 2019)[, "ponds"]
## Regression with ARIMA(0,0,1) errors
##
## Coefficients:
##          ma1    xreg
##       0.4205  0.0087
## s.e.  0.1038  0.0004
##
## sigma^2 estimated as 0.7136:  log likelihood=-72.84
## AIC=151.68   AICc=152.12   BIC=157.92
```

The results from the testing in the auto.arima function suggest that the ARIMA estimation does not require differencing or the consideration of lags in predictors (i.e., autoregressive terms). In contrast to the previous autoregressive model developed for mid-continent mallard AHM, we can now use a 1st order moving average model [ARIMA (0,0,1)] to forecast changes in the number of

Canadian ponds as function of observed total precipitation. The residuals from the selected model suggest that the ARIMA errors do not deviate from white noise (Figure 3) and (Figure 4).

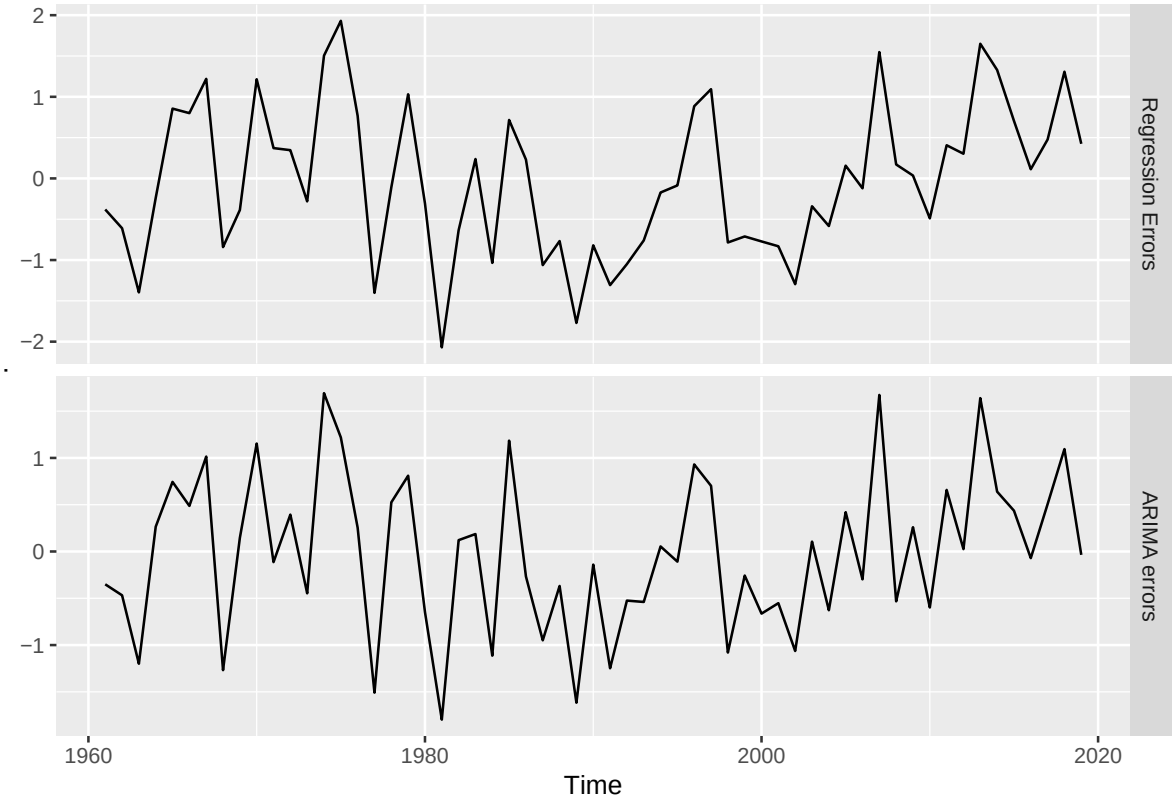

Figure 3: Regression and ARIMA residuals from the selected model [ARIMA(0,0,1)].

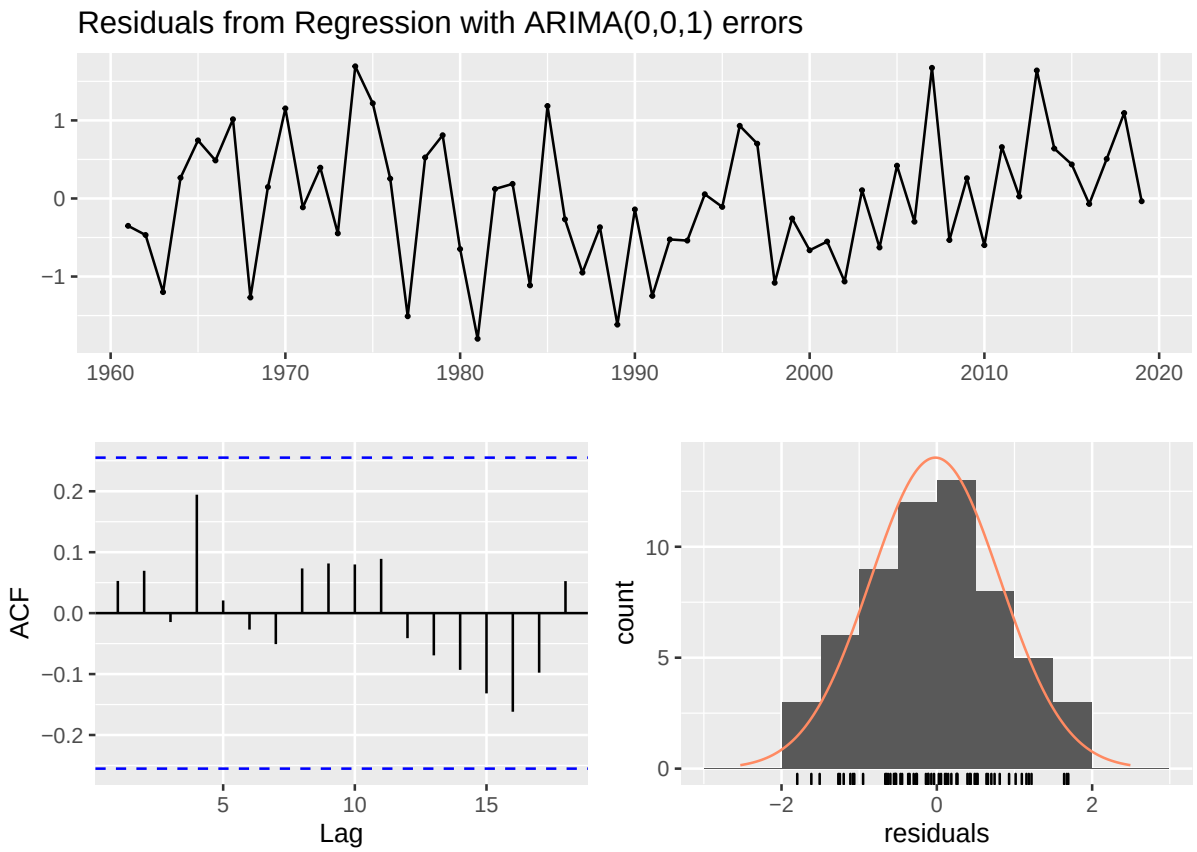

Figure 4: Residual diagnostics from the selected model [ARIMA(0,0,1)].

```
##
##  Ljung-Box test
##
## data:  Residuals from Regression with ARIMA(0,0,1) errors
## Q* = 4.5471, df = 8, p-value = 0.8047
##
## Model df: 2.   Total lags used: 10
```

2020 Forecast

The selected regression model predicts ponds in the next time step as a function of the observed precipitation and residuals from previous predictions based on a 1st order moving average model [ARIMA (0,0,1)] (Hyndman and Athanasopoulos 2018). We can use this model to forecast the number of Canadian ponds with the available precipitation information for 2020 (1 June 2019–May 2020) which is currently 394 millimeters of precipitation.

```
cp_2020 <- forecast(fit, xreg=window(cp_ts,start=2020)[,"precipitation"],h=1)
summary(cp_2020)
```

```
##
## Forecast method: Regression with ARIMA(0,0,1) errors
##
## Model Information:
```

```
## Series: window(cp_ts, end = 2019)[, "ponds"]
## Regression with ARIMA(0,0,1) errors
##
## Coefficients:
##          ma1    xreg
##       0.4205  0.0087
## s.e.  0.1038  0.0004
##
## sigma^2 estimated as 0.7136:  log likelihood=-72.84
## AIC=151.68   AICc=152.12   BIC=157.92
##
## Error measures:
##                       ME      RMSE       MAE       MPE     MAPE      MASE
## Training set -0.01886045 0.8302826 0.6745656 -8.634856 22.91599 0.6661257
##                     ACF1
## Training set 0.05283315
##
## Forecasts:
##      Point Forecast   Lo 80    Hi 80    Lo 95    Hi 95
## 2020       3.402836 2.32028 4.485393 1.747209 5.058464
```

```
autoplot(cp_2020) + xlab("Year") +  ylab("Canadian Ponds") +ggtitle("")
```

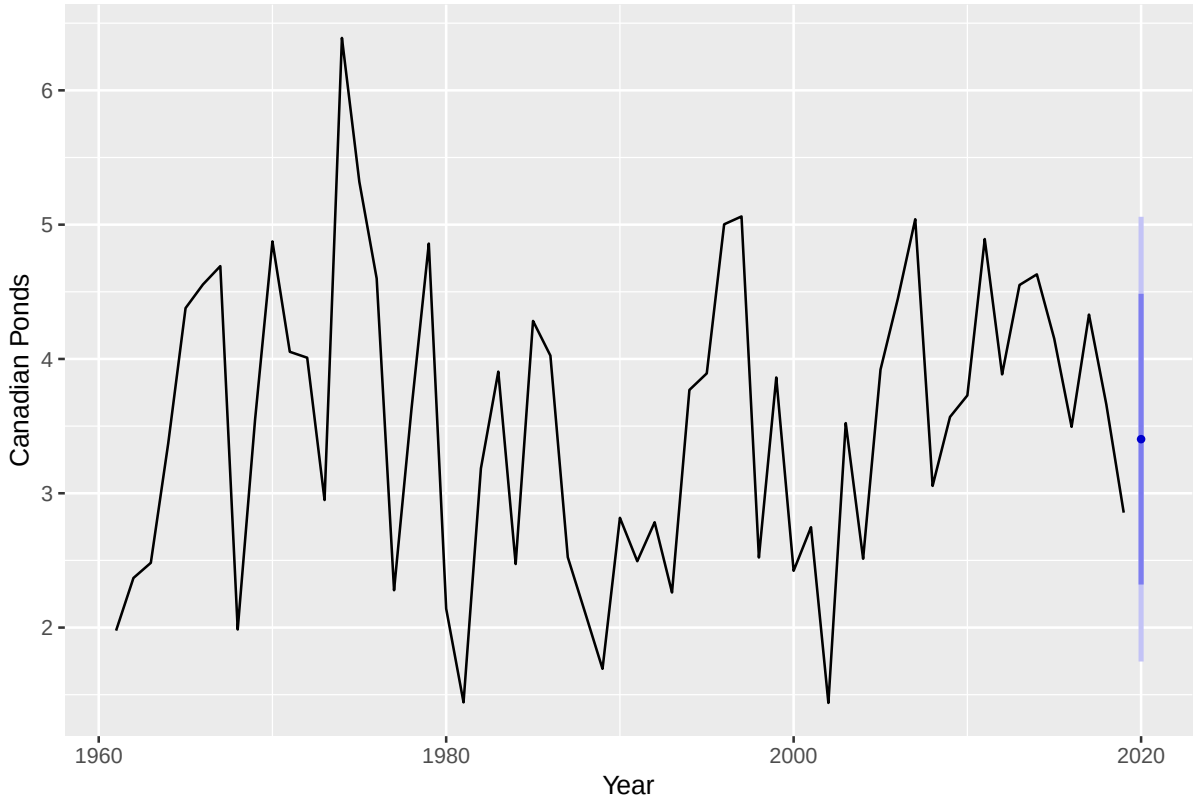

Figure 5: The 2020 forecast of Canadian ponds from an ARIMA(0,0,1) regression model.

```
mean_abs <- format(round(as.numeric(cp_2020$mean),2),nsmall=2)
upper_abs<-round(cp_2020$upper[2],2)
lower_abs<-round(cp_2020$lower[2],2)
#print(mean_abs)
```

Based on these numbers, the forecast for the number of Canadian ponds in the spring of 2020 is 3.40 million with a 95% prediction interval ranging from 1.75 to 5.06 million (Figure 5).

References

Hyndman, R., G. Athanasopoulos, C. Bergmeir, G. Caceres, L. Chhay, M. O'Hara-Wild, F. Petropoulos, S. Razbash, E. Wang, and F. Yasmeen. 2020. forecast: Forecasting functions for time series and linear models. R package version 8.12. URL http://pkg.robjhyndman.com/forecast.

Hyndman, R. J., and G. Athanasopoulos. 2018. Forecasting: principles and practice, 2nd edition. OTexts: Melbourne, Australia, OTexts.com/fpp2. Accessed on 14 July 2020.

Hyndman, R. J., and Y. Khandakar. 2008. Automatic time series forecasting: the forecast package for R. Journal of Statistical Software 26:1–22. URL http://www.jstatsoft.org/article/view/v027i03.

Johnson, F. A., C. T. Moore, W. L. Kendall, J. A. Dubovsky, D. F. Caithamer, J. Kelley, J. R., and B. K. Williams. 1997. Uncertainty and the management of mallard harvests. Journal of Wildlife Management 61:202–216.

Pospahala, R. S., D. R. Anderson, and C. J. Henny, 1974. Population ecology of the mallard. II. Breeding habitat conditions, size of breeding populations, and production indices. U.S. Fish and Wildlife Service Resource Publication. 115. 73pp.

Trapletti, A., and K. Hornik. 2019. tseries: Time Series Analysis and Computational Finance. R package version 0.10-47. URL https://CRAN.R-project.org/package=tseries.

U.S. Fish and Wildlife Service, 2019. Waterfowl population status, 2019. U.S. Department of Interior, Washington, D.C., URL https://www.fws.gov/migratorybirds/pdf/surveys-and-data/Population-status/Waterfowl/WaterfowlPopulationStatusReport19.pdf.

Great Lakes mallard population forecast: Spring 2020

G. Scott Boomer

Branch of Assessment and Decision Support
Division of Migratory Bird Management
U.S. Fish and Wildlife Service
scott_boomer@fws.gov

20 August 2020

Abstract

Due to the COVID-19 pandemic, waterfowl breeding populations were not directly observed in the spring of 2020. As a result, waterfowl harvest regulations will have to be informed with information based on predictions of breeding population sizes and habitat conditions. We developed an estimation and forecasting framework to predict the 2020 Great Lakes region (Minnesota, Michigan, and Wisconsin combined) mallard (*Anas platyrhnchous*) breeding population based on historical breeding population estimates from 1991–2019. We used an autoregressive integrated moving average (ARIMA) estimation framework to develop a model to forecast the abundance of Great Lakes region mallards in 2020. The top ranked model that was best supported by the data included a 1st order autoregressive term with 1st order differencing of the data [ARIMA (1,1,0)]. Based on our selected model, the 2020 forecast of the number of Great Lakes mallards is 0.73 million (95% PI = 0.50 – 0.96).

Contents

List of Tables

List of Figures

Background

Due to the COVID-19 pandemic, the United States Fish and Wildlife Service (USFWS) and its partners were unable to participate in the Waterfowl Breeding Population and Habitat Survey (WBPHS) to estimate the 2020 waterfowl breeding populations as well as evaluate breeding habitat conditions. As a result, the promulgation of waterfowl harvest regulations in 2020 will require some modifications to the decision protocols that typically govern the regulatory process. For example, observed breeding population estimates are used to determine waterfowl harvest regulations. In the absence of this information, the USFWS proposes to base 2020 regulatory decisions on predictions of breeding population sizes and habitat conditions. Current system models for which we have AHM decision frameworks will be used to predict 2020 population sizes based on the breeding population sizes, habitat conditions, harvest, and harvest rates observed in 2019. However, several populations of interest do not have predictive modeling frameworks that can be used to develop population estimates for the 2020 breeding population. As a result, we developed an estimation framework to predict the 2020 breeding population of Great Lakes (GL) region mallards as a function of historical data.

Data

We summarized historical breeding population information for GL mallards from 1991–2019 and used this information as the basis of our time series analysis.

```
getwd()
```

```
## [1] "C:/workspace/2020/MCMallard20/lake_states/code"
```

```
mall_dat <- read.csv(
  "C:/workspace/2020/MCMallard20/lake_states/data/lakestatesmallardbpop.csv",
  header=TRUE)
# bind data into a time series object for convenience
mall_ts<-ts(mall_dat[,5],frequency=1,start=1991,end=2019)
```

We are interested in predicting the 2020 GL mallard population from the historical time series of breeding population estimates from 1991–2019. The population appears to undergo a shift in dynamics from relatively high population levels throughout the 1990's to a consistent declining trend since 2000 (Figure 1).

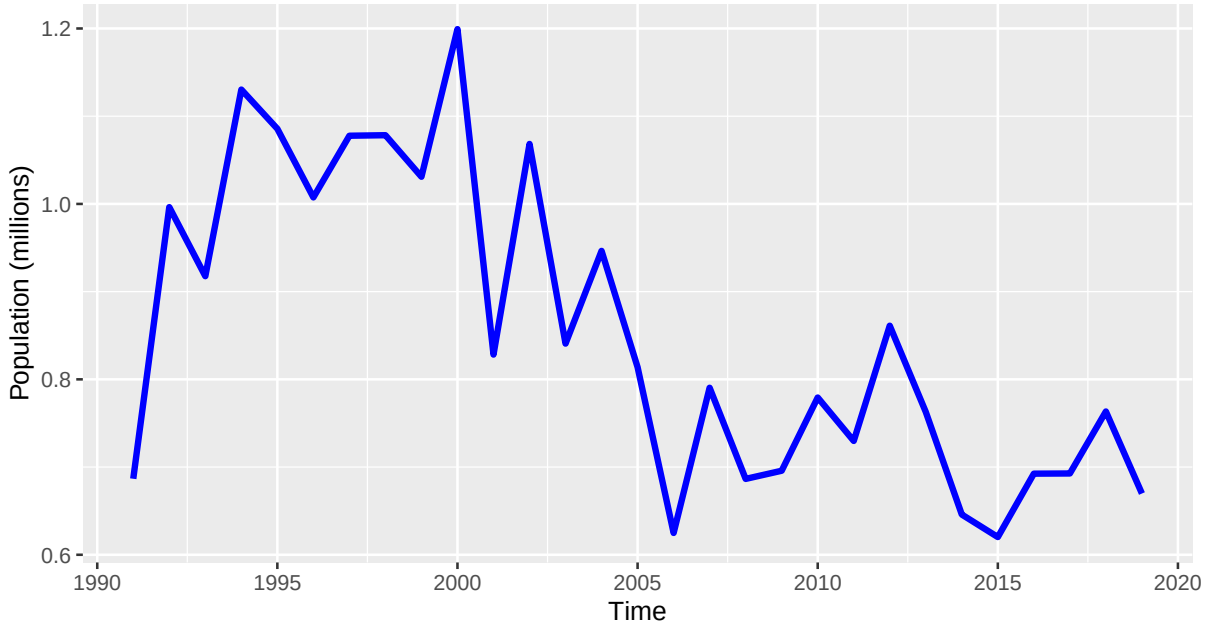

Figure 1: Great Lakes region mallard population estimates (millions) from 1991–2019.

We first examined autocorrelation plots to evaluate the information in the GL mallard time series (Figure 2). We then tested for non-stationary patterns in the data with an augmented Dicky-Fuller test from the tseries R package (Trapletti and Hornik 2019).

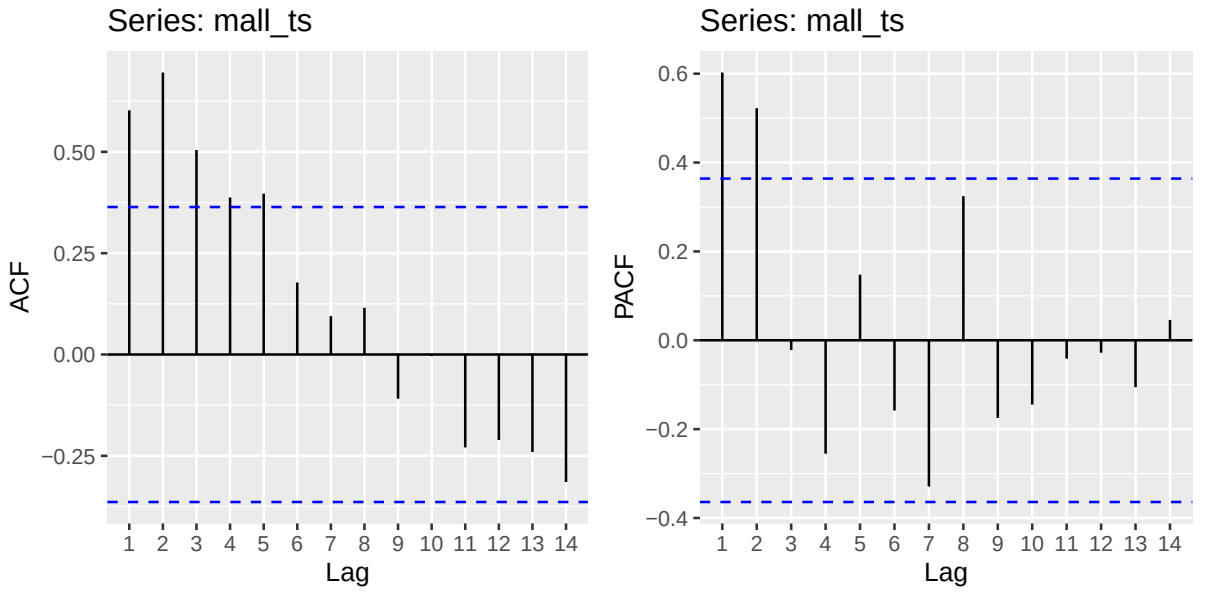

Figure 2: Autocorrelation plots of Great Lakes region mallard population estimates.

```
## Warning in adf.test(mall_ts, alternative = "stationary", k = 0): p-value smaller
## than printed p-value

##
##  Augmented Dickey-Fuller Test
```

```
##
## data:  mall_ts
## Dickey-Fuller = -5.3795, Lag order = 0, p-value = 0.01
## alternative hypothesis: stationary
```

The results from this test suggest there is evidence to reject the null hypothesis so we conclude that the data are stationary, but because there is a suggestion of a trend, we can further test for stationarity around the trend with a KPSS test. The null hypothesis for the KPSS test is that the time series is stationary around a trend. Our test results provides little evidence to reject the null hypothesis that the GL mallard time series is stationary, suggesting that we will not have to consider differencing in our analysis. However, when performing the KPSS test assuming no trend, we do find some evidence to reject the null hypothesis that the data are not level stationary (assuming no trend).

```
kpss.test(mall_ts,null="Trend")
```

```
## Warning in kpss.test(mall_ts, null = "Trend"): p-value greater than printed p-
## value

##
##  KPSS Test for Trend Stationarity
##
## data:  mall_ts
## KPSS Trend = 0.10891, Truncation lag parameter = 2, p-value = 0.1
```

```
kpss.test(mall_ts,null="Level")
```

```
##
##  KPSS Test for Level Stationarity
##
## data:  mall_ts
## KPSS Level = 0.73533, Truncation lag parameter = 2, p-value = 0.01033
```

Time Series Analysis

We are interested in forecasting the change in GL mallard population from 2019 to 2020. We analysed the GL mallard information with an autoregressive integrated moving average (ARIMA) estimation framework, using the R function auto.arima from the Forecast R package (Hyndman et al. 2020, Hyndman and Khandakar 2008) to determine the appropriate number of lags and levels of differencing (Hyndman and Athanasopoulos 2018) for the final specification of our ARIMA model. All of the top models from the auto.arima procedure suggest that a 1st order differencing should be used when fitting this time series information. Model selection results suggest that a 1st order autoregressive model with a 1st order difference is best supported by the data.

```
fit<-auto.arima(mall_ts,
                seasonal=FALSE,
                approximation=FALSE,
                trace=TRUE)
```

```
##
##  ARIMA(2,1,2) with drift         : -33.23978
##  ARIMA(0,1,0) with drift         : -23.16837
##  ARIMA(1,1,0) with drift         : -33.86648
##  ARIMA(0,1,1) with drift         : -29.62652
##  ARIMA(0,1,0)                    : -25.49406
##  ARIMA(2,1,0) with drift         : -31.13157
##  ARIMA(1,1,1) with drift         : -31.12988
##  ARIMA(2,1,1) with drift         : -28.17964
##  ARIMA(1,1,0)                    : -36.30742
##  ARIMA(2,1,0)                    : -33.7882
##  ARIMA(1,1,1)                    : -33.78788
##  ARIMA(0,1,1)                    : -31.89385
##  ARIMA(2,1,1)                    : -31.12815
##
##  Best model: ARIMA(1,1,0)
```

```
print(fit)
```

```
## Series: mall_ts
## ARIMA(1,1,0)
##
## Coefficients:
##           ar1
##       -0.6538
## s.e.   0.1542
##
## sigma^2 estimated as 0.01387:  log likelihood=20.39
## AIC=-36.79   AICc=-36.31   BIC=-34.12
```

Diagnostics of the selected model provide strong evidence that the residuals are well behaved (low autocorrelation) and little evidence to suggest that they are not consistent with white noise.

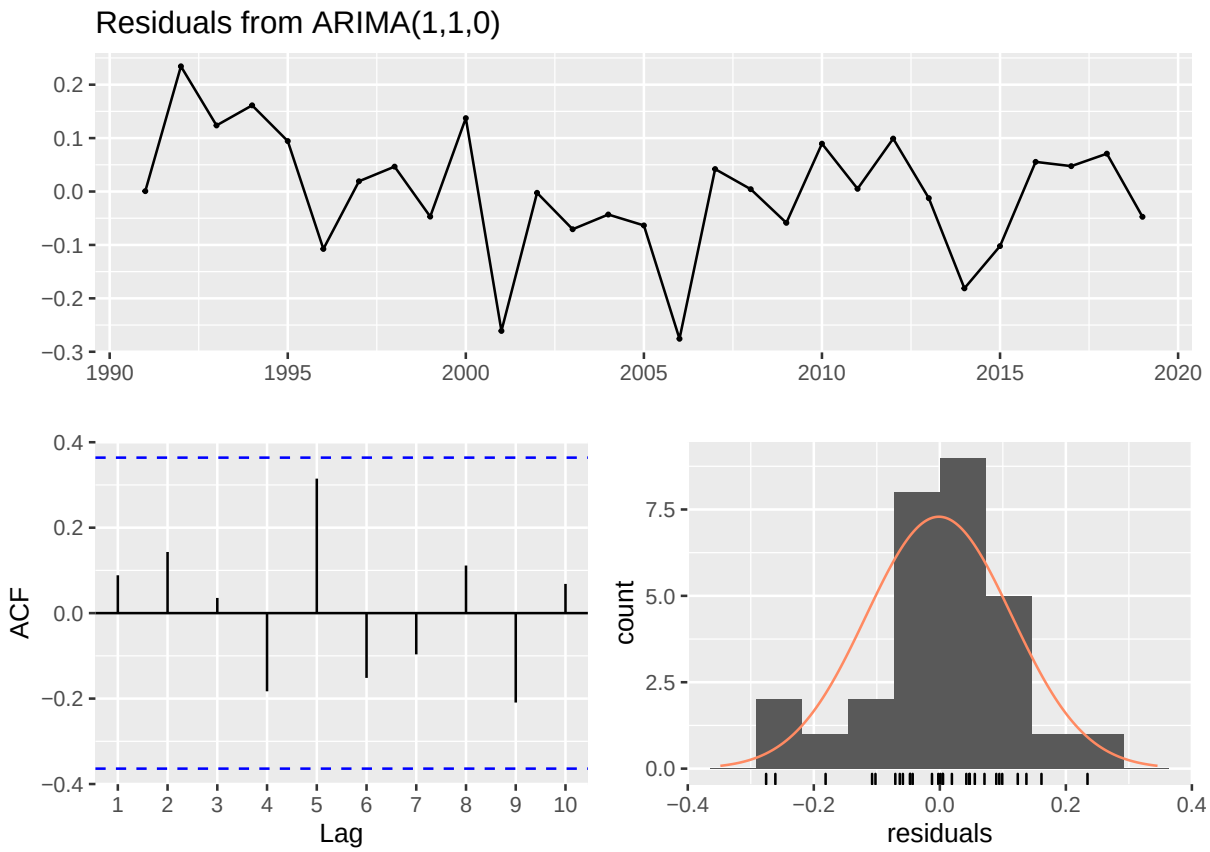

Figure 3: Residual diagnostics from the selected model [ARIMA (1,1,0)].

```
##
##  Ljung-Box test
##
## data:  Residuals from ARIMA(1,1,0)
## Q* = 6.7928, df = 5, p-value = 0.2365
##
## Model df: 1.   Total lags used: 6
```

2020 Forecast

The selected model is equivalent to a 1st order autoregressive model of the differenced (1 year) data (Hyndman and Athanasopoulos 2018). Under this specification, we can use this parameterization to forecast the Great Lakes mallard population for 2020.

```
mall_2020 <- forecast(fit,h=1)
autoplot(mall_2020) + xlab("Year") +
  ylab("Great Lakes mallard population (millions)") +
  ggtitle("")
```

Figure 4: The forecast of the Great Lakes mallard population for 2020.

```
summary(mall_2020)
```

```
##
## Forecast method: ARIMA(1,1,0)
##
## Model Information:
## Series: mall_ts
## ARIMA(1,1,0)
##
## Coefficients:
##           ar1
##       -0.6538
## s.e.   0.1542
##
## sigma^2 estimated as 0.01387:  log likelihood=20.39
## AIC=-36.79   AICc=-36.31   BIC=-34.12
##
## Error measures:
##                        ME      RMSE        MAE       MPE     MAPE      MASE
## Training set -0.001426459 0.1136323 0.08634756 -1.452362 10.51424 0.7330502
##                     ACF1
## Training set 0.08860074
##
```

```
## Forecasts:
##      Point Forecast     Lo 80     Hi 80     Lo 95     Hi 95
## 2020      0.7309913 0.5800685 0.8819141 0.5001748 0.9618078
```

```
  mall_2020_sd<-(mall_2020$upper[,1] - mall_2020$lower[,1]) /
    (2 * qnorm(.5 + mall_2020$level[1] / 200))
  print(paste("SD = ",round(mall_2020_sd,3),sep=""))
```

```
## [1] "SD = 0.118"
```

```
  mean_abs <- format(round(as.numeric(mall_2020$mean),2),nsmall=2)
  upper_abs<- format(round(mall_2020$upper[2],2),nsmall=2)
  lower_abs<- format(round(mall_2020$lower[2],2),nsmall=2)
```

Based on these results, the forecast for the GL mallard population in the spring of 2020 is a mean estimate of 0.73 with a 95% prediction interval ranging from 0.50 to 0.96 (Figure 4).

References

Hyndman, R., G. Athanasopoulos, C. Bergmeir, G. Caceres, L. Chhay, M. O'Hara-Wild, F. Petropoulos, S. Razbash, E. Wang, and F. Yasmeen. 2020. forecast: Forecasting functions for time series and linear models. R package version 8.12. URL http://pkg.robjhyndman.com/forecast.

Hyndman, R. J., and G. Athanasopoulos. 2018. Forecasting: principles and practice, 2nd edition. OTexts: Melbourne, Australia, OTexts.com/fpp2. Accessed on 14 July 2020.

Hyndman, R. J., and Y. Khandakar. 2008. Automatic time series forecasting: the forecast package for R. Journal of Statistical Software 26:1–22. URL http://www.jstatsoft.org/article/view/v027i03.

Trapletti, A., and K. Hornik. 2019. tseries: Time Series Analysis and Computational Finance. R package version 0.10-47. URL https://CRAN.R-project.org/package=tseries.

EMALL Forcasting for ABDU AHM

Guthrie Zimmerman and Patrick Devers

7/23/2020

Abstract

The American black duck (ABDU) Adaptive Harvest Management framework uses ABDU population size and eastern mallard (EMALL) population size as state variables. EMALL were hypothesized to compete with breeding ABDU and reduce recruitment. Due to the Covid-19 epidemic, spring breeding population surveys for waterfowl were not conducted during the spring of 2020. We do not have a population model that can be used to predict EMALL breeding population size in 2020, so we used a formal time series analysis to predict the 2020 breeding population size for EMALL to inform ABDU AHM. Our time series analysis indicated that a single difference and first-order moving average model fit the time series best. The predicted breeding population size for 2020 from this model was 387,269 (95% PI = 331,265 - 443,273).

Contents

1 Introduction

American black duck (ABDU) AHM is currently informed by two states: ABDU breeeding population size (BPOP) and eastern mallard (EMALL) BPOP in eastern Canada. Although the management community is moving towards defining the ABDU population as all black ducks breeding in eastern Canada and the eastern U.S., the current definition is ABDU breeding in the core breeding range of eastern Canada (WBPHS strata 51, 52, 63, 64, 66, 67, 68, 70, 71, and 72). The EMALL population used in ABDU AHM is comprised of those breeding in the same strata as the current ABDU population definition. All WBPHS were cancelled for the spring 2020 due to the Covid-19 epidemic, so we do not have an estimate of the current state for either ABDU and EMALL. We used the ABDU integrated population model with last year's population size, 2019 pre-season banding data, and predicted 2019 recruitment based on the 2019 ABDU BPOP (density-dependent term), 2019 EMALL BPOP (competition hypothesis), and a long-term trend. However, we do not have a current population model to predict the EMALL population size for 2020. The population model used to support the former eastern mallard AHM strategy was based on a different population of mallards (i.e., those breeding in WBPHS strata 51, 52, 53, and 56; and in the states of VA north to NH), so we could not use that model to predict EMALL BPOP for ABDU AHM. Therefore, we used an Auto Regressive

Integrated Moving Average (ARIMA) approach to predict a 2020 BPOP for EMALL based on the historic time series.

We used the 'forecast' package with the ARIMA function in program R as recommended by Hyndman and Athanasopoulos (2018) to identify the best approach for forecasting the 2020 EMALL population:

1. Inspect the raw data for stationarity - a stationary population is one with random fluctuations where a count is not influenced by the time at which its observed (i.e., no trends or seasonality).
2. Use model selection (AICc) and a stepwise selection to identify the best autoregressive, differencing, or moving average (and order for each) is best for forecasting the time series based on the nature of the historic data.
3. Present fit tests to assess how well the selected model fits.

2 Raw Data

We explored the raw data for stationarity using:

1. Plot pf the raw data through time and simple regression of year and time to see if there is evidence of a trend
2. Produced an Autocorrelation plot of the coefficients of correlation between a time series and lags of that time series. Stationary data have autocorrelation go to zero rapidly within very few time lags.
3. Conducted a Box-Ljung test, which assess the overall randomness of the data rather than autocorrelation at specific time lags. The null hypothesis for this test is that the data represent randomness or white noise
4. Conducted a KPSS unit root test to assess whether differencing (i.e., use the difference between subsequent observations in the analysis) is likely needed to achieve stationarity. The null hypothesis is that the data are random, so rejecting the null suggests that differencing is needed. As implemented in ARIMA, the test statistic is compared to the critical values at different levels in the output.

```
raw.dat <- read.csv(paste(root,'integrated.csv',sep=''))
  mall <- raw.dat[,c('Year','mall_med','mall_se','mall_LCI95','mall_UCI95')]
  # Assess stationarity
    # Visualize data and run simple regression to look for trends and extreme observations
      plot(mall$Year,mall$mall_med/100,type='l',lwd=3,xlab = 'Year',ylab = 'EMALL BPOP (in 100,000s)',y
        lines(mall$Year,mall$mall_LCI95/100000,lty=3,lwd=3)
        lines(mall$Year,mall$mall_UCI95/100000,lty=3,lwd=3)
```

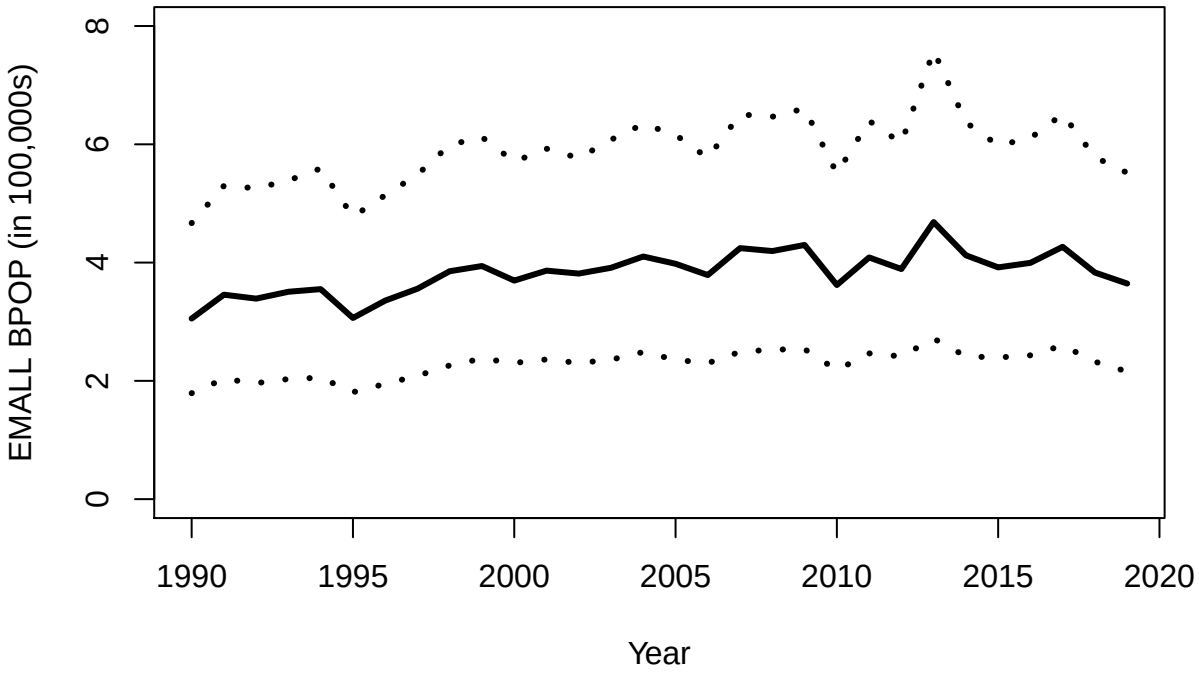


```
glm.trend <- glm(mall_med ~ Year, data = mall)
summary(glm.trend)
```

```
##
## Call:
## glm(formula = mall_med ~ Year, data = mall)
##
## Deviance Residuals:
##     Min       1Q   Median       3Q      Max
## -58.017  -14.518    1.383   14.159   62.640
##
## Coefficients:
##               Estimate Std. Error t value  Pr(>|t|)
## (Intercept) -5180.5994  1164.2915  -4.450  0.000125 ***
## Year            2.7752     0.5808   4.778 0.0000509 ***
## ---
## Signif. codes:  0 '***' 0.001 '**' 0.01 '*' 0.05 '.' 0.1 ' ' 1
##
## (Dispersion parameter for gaussian family taken to be 758.2334)
##
##     Null deviance: 38540  on 29  degrees of freedom
## Residual deviance: 21231  on 28  degrees of freedom
## AIC: 288
##
## Number of Fisher Scoring iterations: 2
```

```r
# Autocorrelation plot
  acf(mall$mall_med, main="")
```

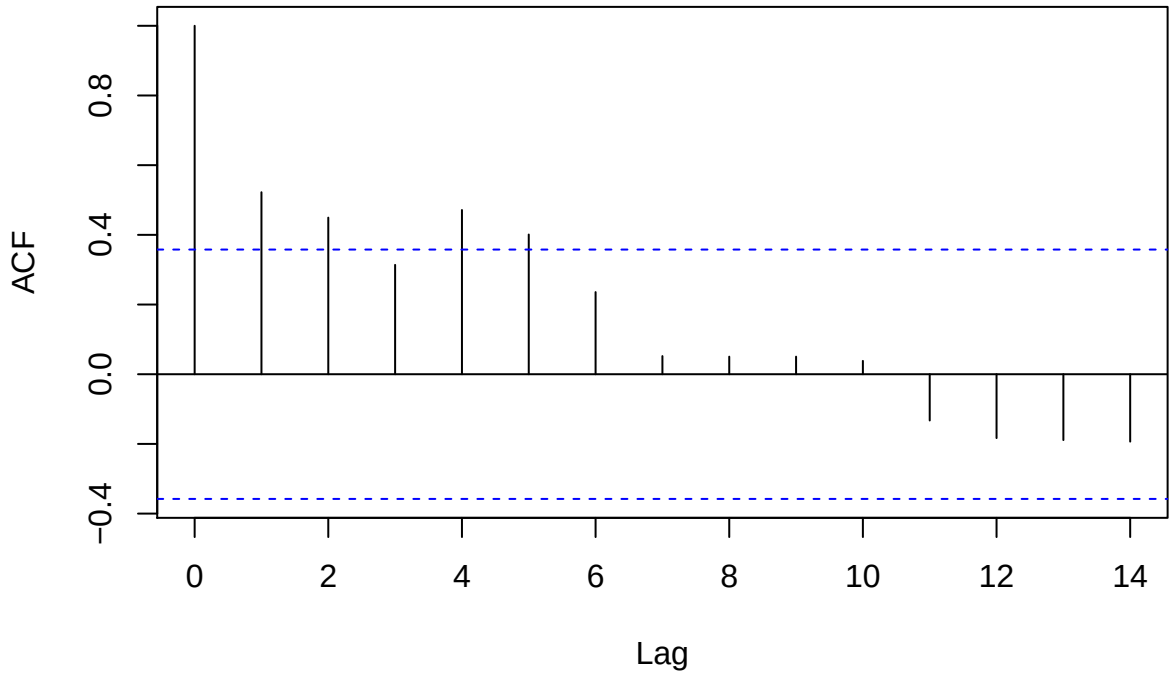


```r
# Box-Ljung test
  Box.test(mall$mall_med, lag=10, type="Ljung-Box")
```

```
##
##  Box-Ljung test
##
## data:  mall$mall_med
## X-squared = 36.479, df = 10, p-value = 0.00006963
```

```r
# KPSS Unit Root Test
  mall$mall_med %>%
    ur.kpss() %>%
    summary()
```

```
##
## ########################
## # KPSS Unit Root Test #
## ########################
##
## Test is of type: mu with 2 lags.
##
```

```
## Value of test-statistic is: 0.7761
##
## Critical value for a significance level of:
##                 10pct  5pct 2.5pct  1pct
## critical values 0.347 0.463  0.574 0.739
```

Inspection of the raw data indicated that the EMALL time series is not stationary, and that differencing is likely needed and a basic autocorrelation or random walk model might not be appropriate. The 4 checks indicated:

1. The raw data plot indicated an increasing trend over time and the simple linear regression indicated a significant positive slope
2. The autocorrelation did not approach zero until several lags; and even went slightly negative towards the longest lags
3. The Box-Ljung test had a small p-value, which rejects the null hypothesis of randomness in the data
4. The unit root test test-statistic was slightly greater than the significance level at 1 percent (i.e., out in the tail), so it rejects the hypothesis of overall stationarity in the data.

3 Analysis

We used the auto.arima function to estimate the best approach and ordering for forecasting EMALL BPOP based on the historic time series. The auto.arima function returns a vector with three elements to summarize the results of model selection (i.e., ARIMA(x,y,z)):

1. Element x represents autoregressive models (0 = autoregressive model not appropriate, >0 = order for autoregressive model AR(1), AR(2), etc)
2. Element y represents differencing (0 = differencing not needed, >0 = order for differencing)
3. Element z represents whether a moving average model is appropriate (0 = moving average model not needed, >0 = order for moving average model)

3.1 Results Summary and 2020 Prediction

Model selection indicated ARIMA(0,1,1) indicating that differencing of 1 time step and MA(1) fit the data best. The regression was conducted on differences among years (N=29) rather than the actual annual estimates (N=30) and the values were the current and single time lag regression errors rather than the population sizes. The resulting regression equation is: $y_t = \varepsilon_t - 0.6110\varepsilon_{t-1}$. The ε_t terms in this model are not directly observed, so this is not a standard regression and the values in the model are estimated from recursive estimation. The population sizes are considered weighted moving averages of the past year's forecast error. This model was selected at best due to the inherent trend in the time series.

```
## Series: dat
## ARIMA(0,1,1)
##
## Coefficients:
##           ma1
##       -0.6110
## s.e.   0.1402
##
## sigma^2 estimated as 816.5:  log likelihood=-138.1
## AIC=280.19   AICc=280.65   BIC=282.93
```

Table 1: Predicted BPOP for EMALL (and prediction intervals) for 2020

	Point Forecast	Lo 80	Hi 80	Lo 95	Hi 95
2020	387.2688	350.6497	423.8879	331.2647	443.2729

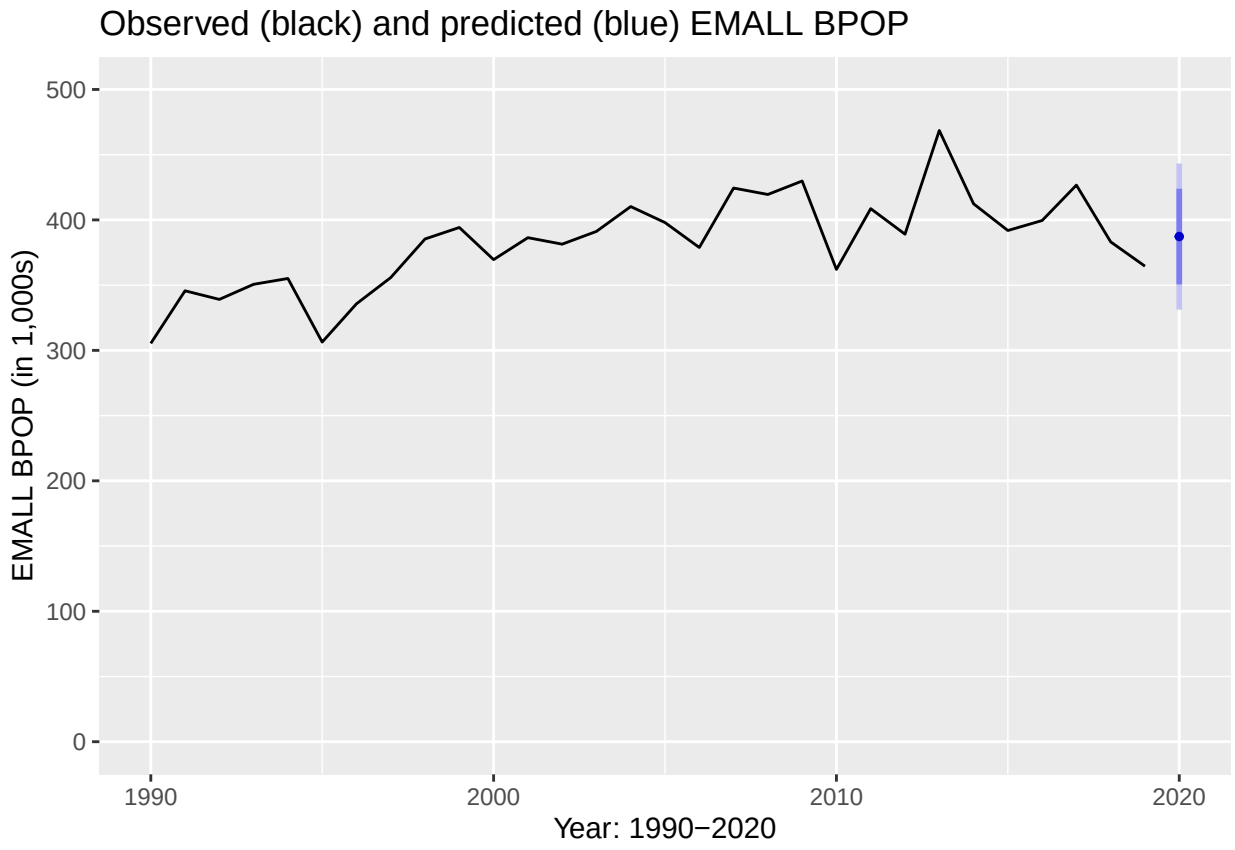

3.2 Assess Model Fit

Inspection of model fit indicated that ARIMA(0,1,1) model adequately fit the time series. The Ljung-Box test had a p-value of 0.328, so we do not reject the null hypothesis of random variation and the autocorrelation plot centered around zero within acceptable limits (dotted blue lines in the ACF plot below). Although overall, the model appeared to fit well, the residual plots indicated some lack of fit. The time series of residual plot indicated a slight declining trend and the residual histogram was slightly left-skewed. The mean of the residuals should ideally be zero (equally under and over fit), but the mean of the residuals was about 6. This pattern indicated that early in the time series the model slightly over-predicted, whereas later in the time series, the model slightly under-predicted. This is likely due to the trend in the raw data where the population was increasing until a certain point where it appears to stabilize or slightly decrease.

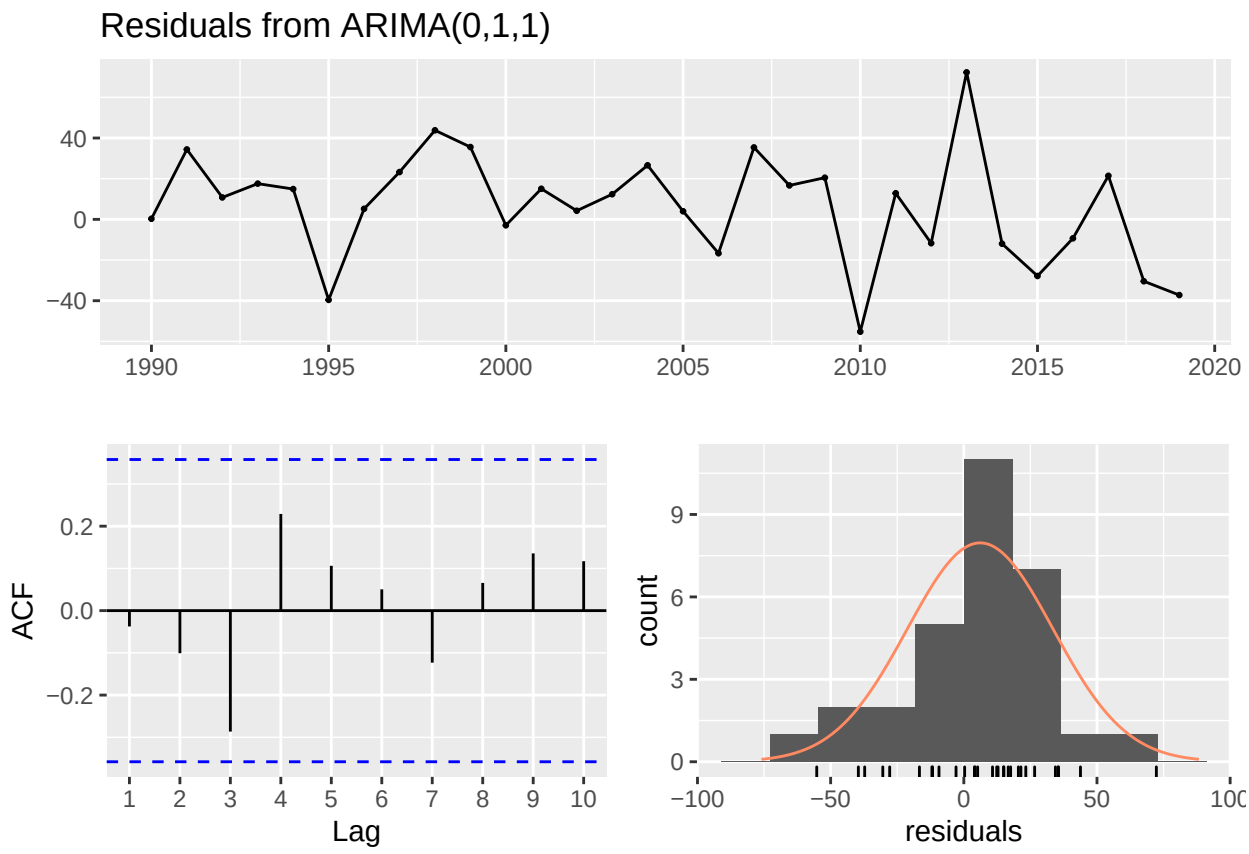


```
##
##  Ljung-Box test
##
## data:  Residuals from ARIMA(0,1,1)
## Q* = 5.7823, df = 5, p-value = 0.328
##
## Model df: 1.   Total lags used: 6
```

Northern Pintail AHM - Latitude Forecast: Spring 2020

G. Scott Boomer

Branch of Assessment and Decision Support
Division of Migratory Bird Management
U.S. Fish and Wildlife Service
scott_boomer@fws.gov

20 August 2020

Abstract

Due to the COVID-19 pandemic, waterfowl breeding populations were not directly observed in the spring of 2020. As a result, waterfowl harvest regulations will have to be informed with information based on predictions of breeding population sizes and habitat conditions. We developed an estimation and forecasting framework to predict the distribution (weighted latitude) of the pintail (*Anas acuta*) breeding population in the spring of 2020 based on historical breeding distribution information from 1980–2019. We used an autoregressive integrated moving average (ARIMA) estimation framework to develop a model to forecast the breeding distribution of pintails in 2020. A 1st order autoregressive model [ARIMA (1,0,0)] was best supported by the data. Based on our selected model, the forecast of the latitude of the 2020 pintail breeding population is 55.16 degrees (95% PI = 51.78 − 58.55).

Contents

List of Tables

List of Figures

Background

Due to the COVID-19 pandemic, the United States Fish and Wildlife Service (USFWS) and its partners were unable to conduct the Waterfowl Breeding Population and Habitat Survey (WBPHS) to estimate the 2020 waterfowl breeding populations as well as evaluate breeding habitat conditions. As a result, the promulgation of waterfowl harvest regulations in 2020 will require some modifications to the decision protocols that typically govern the regulatory process. In the absence of this information, the USFWS proposes to base 2020 regulatory decisions on predictions of breeding population sizes and habitat conditions. Current system models for which we have AHM decision frameworks will be used to predict 2020 population sizes based on the breeding population sizes, habitat conditions, harvest, and harvest rates observed in 2019. However, several harvest strategies such as pintail AHM rely on other forms of information (e.g., breeding distribution) to establish decision thresholds. As a result, we developed an estimation framework to forecast the latitude of the 2020 pintail breeding population distribution.

Latitude Time Series Analysis

Data

```
nopi_dat<-getBPOP.fn(1430,"MAS",1980:2019,1e6)
# bind data into a time series object for convenience
lat_ts<-ts(nopi_dat$lat,frequency=1,start=1980,end=2019)
```

We are interested in predicting the 2020 pintail breeding distribution (weighted latitude) from the historical time series of breeding population estimates. We summarized breeding ground distribution information in the form of a BPOP weighted average of the latitude of the centroid of each strata in the traditional survey area of the Waterfowl Breeding Population and Habitat Survey (U.S. Fish and Wildlife Service 2019). Based on previous analyses that documented a temporal shift in the distribution of breeding pintails (Runge and Boomer 2005, M. C. Runge USGS, *personal communication*), we restricted our analyses to information from 1980–2019 (Figure 1).

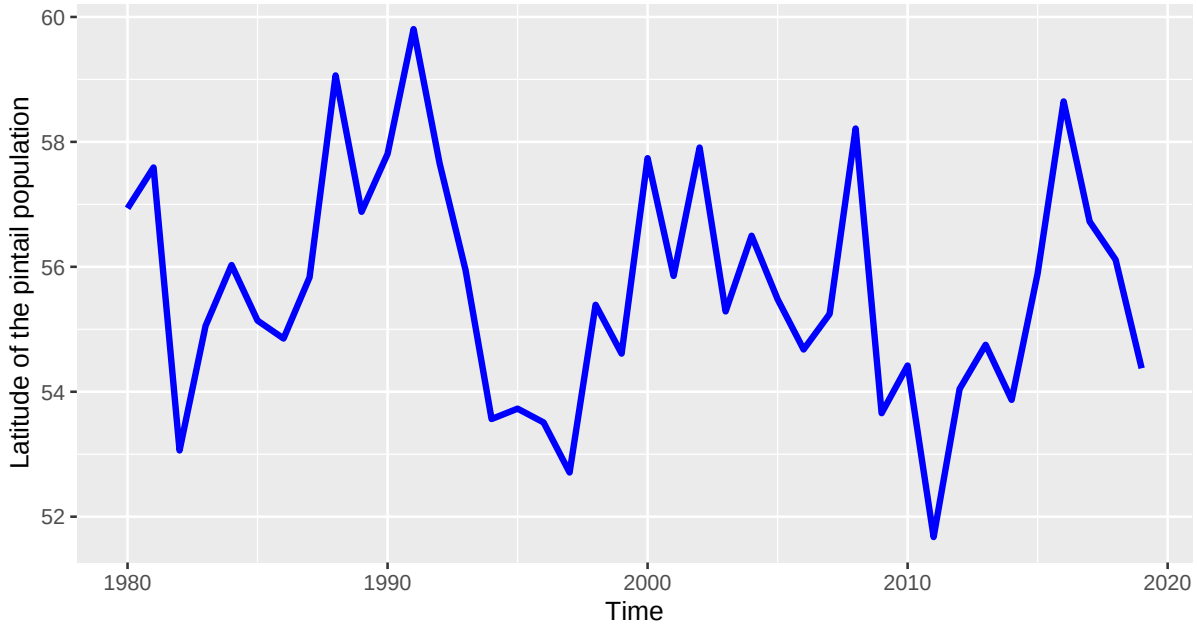

Figure 1: The observed latitude of the pintail breeding population distribution from 1980–2019.

We analysed the raw time series information for stationarity with unit root tests from the R tseries package (Trapletti and Hornik 2019). We started with an augmented Dicky-Fuller test limiting the number of lags to an AR(1) process to test the null hypothesis that the population time series is non-stationary. These test results provide strong evidence that the data are stationary.

```
#ggAcf(lat_ts)
adf.test(lat_ts, k = 0)
```

```
##
##  Augmented Dickey-Fuller Test
##
## data:  lat_ts
## Dickey-Fuller = -4.0426, Lag order = 0, p-value = 0.01812
## alternative hypothesis: stationary
```

To confirm this result, we used a KPSS test with a null hypothesis that the time series is stationary. These test results provide little evidence to conclude that the data are not stationary.

```
kpss.test(lat_ts,null="Level")
```

```
## Warning in kpss.test(lat_ts, null = "Level"): p-value greater than printed p-
## value

##
##  KPSS Test for Level Stationarity
##
## data:  lat_ts
## KPSS Level = 0.1211, Truncation lag parameter = 3, p-value = 0.1
```

We analysed the historical information with an autoregressive integrated moving average (ARIMA) estimation framework, using the auto.arima function from the Forecast R package (Hyndman et al. 2020, Hyndman and Khandakar 2008) to determine the appropriate number of lags and differencing (Hyndman and Athanasopoulos 2018) for the final specification of our ARIMA model.

```
  fit_lat<-auto.arima(lat_ts,stepwise=FALSE,approximation=FALSE,trace=TRUE)
```

```
##
##  ARIMA(0,0,0) with zero mean     : 437.1984
##  ARIMA(0,0,0) with non-zero mean : 165.9492
##  ARIMA(0,0,1) with zero mean     : Inf
##  ARIMA(0,0,1) with non-zero mean : 163.692
##  ARIMA(0,0,2) with zero mean     : Inf
##  ARIMA(0,0,2) with non-zero mean : 163.2817
##  ARIMA(0,0,3) with zero mean     : Inf
##  ARIMA(0,0,3) with non-zero mean : 165.7076
##  ARIMA(0,0,4) with zero mean     : Inf
##  ARIMA(0,0,4) with non-zero mean : 165.9126
##  ARIMA(0,0,5) with zero mean     : Inf
##  ARIMA(0,0,5) with non-zero mean : 168.7623
##  ARIMA(1,0,0) with zero mean     : Inf
##  ARIMA(1,0,0) with non-zero mean : 161.9086
##  ARIMA(1,0,1) with zero mean     : Inf
##  ARIMA(1,0,1) with non-zero mean : 164.2008
##  ARIMA(1,0,2) with zero mean     : Inf
##  ARIMA(1,0,2) with non-zero mean : 165.6069
##  ARIMA(1,0,3) with zero mean     : Inf
##  ARIMA(1,0,3) with non-zero mean : 169.0239
##  ARIMA(1,0,4) with zero mean     : Inf
##  ARIMA(1,0,4) with non-zero mean : 168.8571
##  ARIMA(2,0,0) with zero mean     : Inf
##  ARIMA(2,0,0) with non-zero mean : 164.0091
##  ARIMA(2,0,1) with zero mean     : Inf
##  ARIMA(2,0,1) with non-zero mean : 165.1546
##  ARIMA(2,0,2) with zero mean     : Inf
##  ARIMA(2,0,2) with non-zero mean : 167.9224
##  ARIMA(2,0,3) with zero mean     : Inf
##  ARIMA(2,0,3) with non-zero mean : Inf
##  ARIMA(3,0,0) with zero mean     : Inf
##  ARIMA(3,0,0) with non-zero mean : 165.1493
##  ARIMA(3,0,1) with zero mean     : Inf
##  ARIMA(3,0,1) with non-zero mean : 165.0755
##  ARIMA(3,0,2) with zero mean     : Inf
##  ARIMA(3,0,2) with non-zero mean : Inf
##  ARIMA(4,0,0) with zero mean     : Inf
##  ARIMA(4,0,0) with non-zero mean : 167.4134
##  ARIMA(4,0,1) with zero mean     : Inf
##  ARIMA(4,0,1) with non-zero mean : 167.8004
##  ARIMA(5,0,0) with zero mean     : Inf
##  ARIMA(5,0,0) with non-zero mean : 166.1395
```

```
##
##
##
##  Best model: ARIMA(1,0,0) with non-zero mean
```

```
  summary(fit_lat)
```

```
## Series: lat_ts
## ARIMA(1,0,0) with non-zero mean
##
## Coefficients:
##          ar1     mean
##       0.3836  55.6559
## s.e.  0.1450   0.4248
##
## sigma^2 estimated as 2.976:  log likelihood=-77.62
## AIC=161.24   AICc=161.91   BIC=166.31
##
## Training set error measures:
##                       ME     RMSE      MAE        MPE     MAPE      MASE
## Training set -0.01472947 1.681347 1.312912 -0.1177028 2.357408 0.7654633
##                      ACF1
## Training set -0.03108714
```

```
  print(fit_lat)
```

```
## Series: lat_ts
## ARIMA(1,0,0) with non-zero mean
##
## Coefficients:
##          ar1     mean
##       0.3836  55.6559
## s.e.  0.1450   0.4248
##
## sigma^2 estimated as 2.976:  log likelihood=-77.62
## AIC=161.24   AICc=161.91   BIC=166.31
```

```
  #checkresiduals(fit_lat)
```

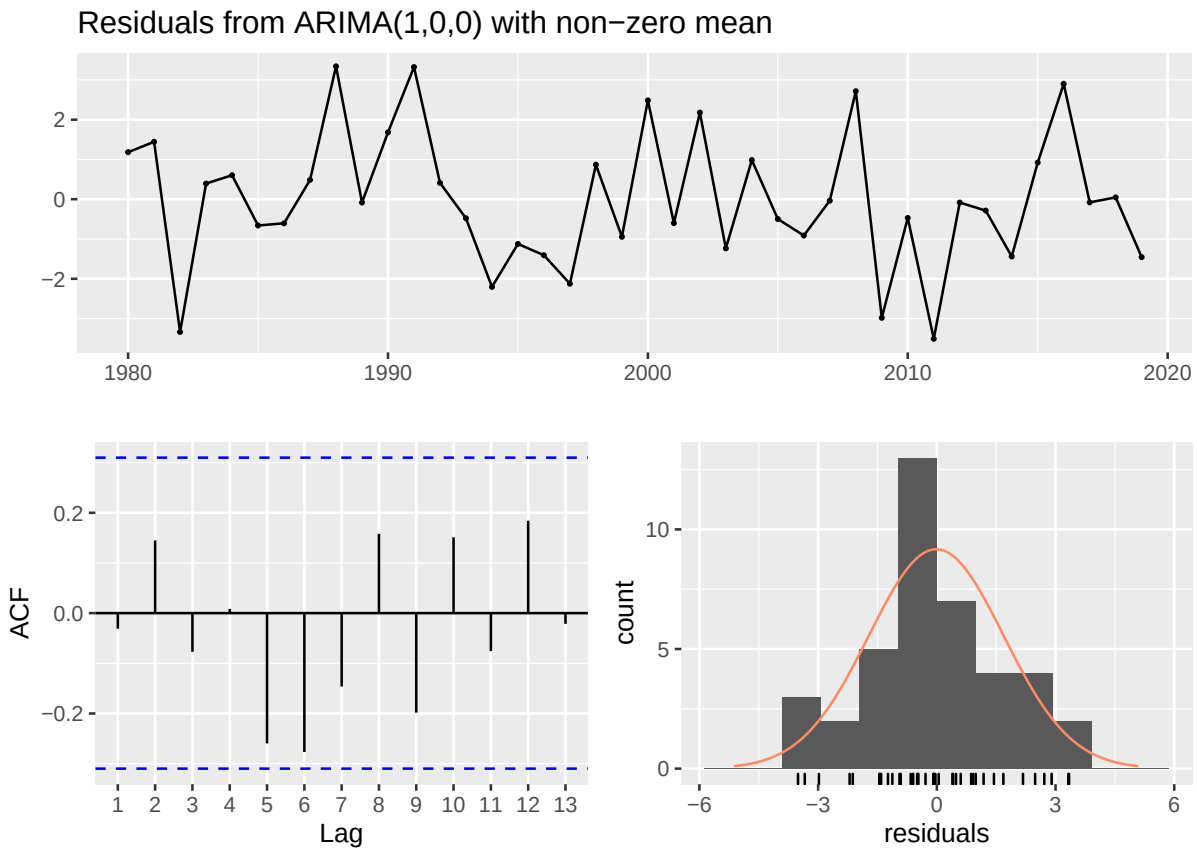

Figure 2: Residual diagnostics from the selected model [ARIMA (1,0,0)].

```
##
##  Ljung-Box test
##
## data:  Residuals from ARIMA(1,0,0) with non-zero mean
## Q* = 10.665, df = 6, p-value = 0.09931
##
## Model df: 2.   Total lags used: 8
```

2020 Pintail Latitude Forecast

The model selection results suggest that a 1st order autoregressive model [ARIMA (1,0,0)] is best supported by the data. Model diagnostics indicate that the residuals are uncorrelated and the selected model does not show a lack of fit (Figure 2). We can use these model results to forecast the distribution of the pintail breeding population in 2020.

```
lat_2020 <- forecast(fit_lat,h=1)
summary(lat_2020)
```

```
##
## Forecast method: ARIMA(1,0,0) with non-zero mean
##
## Model Information:
## Series: lat_ts
```

```
## ARIMA(1,0,0) with non-zero mean
##
## Coefficients:
##          ar1     mean
##       0.3836  55.6559
## s.e.  0.1450   0.4248
##
## sigma^2 estimated as 2.976:  log likelihood=-77.62
## AIC=161.24   AICc=161.91   BIC=166.31
##
## Error measures:
##                       ME     RMSE      MAE        MPE     MAPE      MASE
## Training set -0.01472947 1.681347 1.312912 -0.1177028 2.357408 0.7654633
##                      ACF1
## Training set -0.03108714
##
## Forecasts:
##      Point Forecast    Lo 80    Hi 80    Lo 95    Hi 95
## 2020       55.16463 52.95392 57.37534 51.78364 58.54562
```

```
autoplot(lat_2020) + xlab("Year") +  ylab("Latitude (degrees)") +ggtitle("")
```

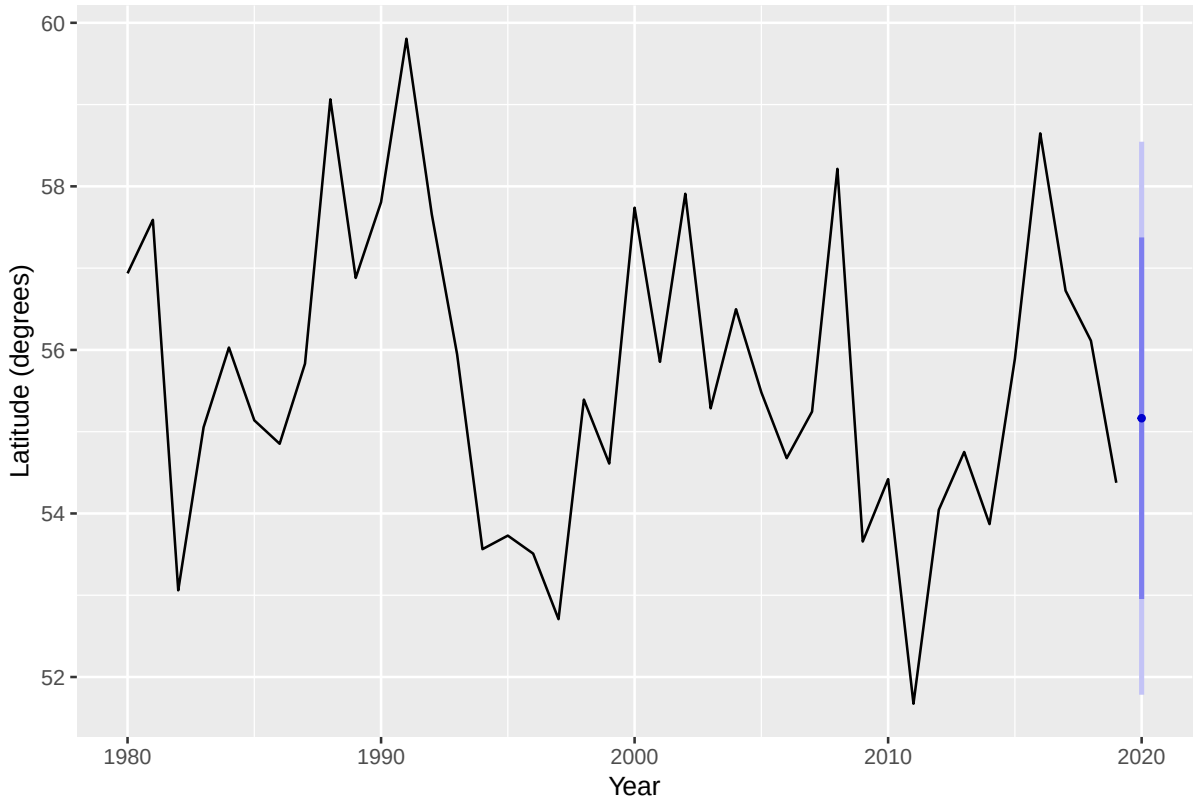

Figure 3: The 2020 forecast of the latitude of the pintail breeding population distribution.

```
  lat_2020_sd<-(lat_2020$upper[,1] - lat_2020$lower[,1]) /
    (2 * qnorm(.5 + lat_2020$level[1] / 200))
  mean_abs <- format(round(as.numeric(lat_2020$mean),2),nsmall=2)
  upper_abs<-format(round(lat_2020$upper[2],2),nsmall=2)
  lower_abs<-format(round(lat_2020$lower[2],2),nsmall=2)
  print(paste("SD =",round(lat_2020_sd,3),sep=""))
```

```
## [1] "SD =1.725"
```

Based on the selected model, the forecast for the latitude of the 2020 pintail breeding population is 55.16 degrees with a 95% prediction interval ranging from 51.78 to 58.55 (Figure 3).

References

Hyndman, R., and G. Athanasopoulos. 2018. Forecasting: principles and practice, 2nd edition. OTexts: Melbourne, Melbourne, Australia.

Hyndman, R., G. Athanasopoulos, C. Bergmeir, G. Caceres, L. Chhay, M. O'Hara-Wild, F. Petropoulos, S. Razbash, E. Wang, and F. Yasmeen. 2020. forecast: Forecasting functions for time series and linear models. R package version 8.12. URL http://pkg.robjhyndman.com/forecast.

Hyndman, R. J., and Y. Khandakar. 2008. Automatic time series forecasting: the forecast package for R. Journal of Statistical Software 26:1–22. URL http://www.jstatsoft.org/article/view/v027i03.

Runge, M. C., and G. S. Boomer, 2005. Population dynamics and harvest management of the continental northern pintail population. Unpublished Report. U.S. Geological Survey, Patuxent Wildlife Research Center, Laurel, MD. 42pp.

Trapletti, A., and K. Hornik. 2019. tseries: Time Series Analysis and Computational Finance. R package version 0.10-47. URL https://CRAN.R-project.org/package=tseries.

U.S. Fish and Wildlife Service, 2019. Waterfowl population status, 2019. U.S. Department of Interior, Washington, D.C., URL https://www.fws.gov/migratorybirds/pdf/surveys-and-data/Population-status/Waterfowl/WaterfowlPopulationStatusReport19.pdf.

Appendix H Mid-Continent Mallard Models

In 1995, we developed population models to predict changes in mid-continent mallards based on the traditional survey area which includes individuals from Alaska (Johnson et al. 1997). In 1997, we added mallards from the Great Lakes region (Michigan, Minnesota, and Wisconsin) to the mid-continent mallard stock, assuming their population dynamics were equivalent. In 2002, we made extensive revisions to the set of alternative models describing the population dynamics of mid-continent mallards (Runge et al. 2002, U.S. Fish and Wildlife Service 2002). In 2008, we redefined the population of mid-continent mallards Table H.1 to account for the removal of Alaskan birds (WBPHS strata 1–12) that are now considered to be in the western mallard stock and have subsequently rescaled the model set accordingly.

Table H.1 – Estimates (N) and associated standard errors (SE) of mid-continent mallards (in millions) observed in the WBPHS (strata 13–18, 20–50, and 75–77) and the Great Lakes region (Michigan, Minnesota, and Wisconsin) from 1992 to 2019. The waterfowl breeding population surveys were not conducted in 2020 due to the COVID-19 pandemic; 2020 numbers are based on model predictions.

	WBPHS area		Great Lakes region		Total	
Year	N	SE	N	SE	N	SE
1992	5.6304	0.2379	0.9964	0.1178	6.6267	0.2654
1993	5.4253	0.2068	0.9176	0.0827	6.3429	0.2227
1994	6.6292	0.2803	1.1304	0.1153	7.7596	0.3031
1995	7.7452	0.2793	1.0857	0.1323	8.8309	0.3090
1996	7.4193	0.2593	1.0074	0.0991	8.4267	0.2776
1997	9.3554	0.3041	1.0777	0.1140	10.4332	0.3248
1998	8.8041	0.2940	1.0783	0.1172	9.8825	0.3165
1999	10.0926	0.3374	1.0309	0.1282	11.1236	0.3610
2000	8.6999	0.2855	1.1993	0.1221	9.8992	0.3105
2001	7.1857	0.2204	0.8282	0.0718	8.0139	0.2318
2002	6.8364	0.2412	1.0684	0.0883	7.9047	0.2569
2003	7.1062	0.2589	0.8407	0.0647	7.9470	0.2668
2004	6.6142	0.2746	0.9465	0.0915	7.5607	0.2895
2005	6.0521	0.2754	0.8138	0.0677	6.8660	0.2836
2006	6.7607	0.2187	0.6249	0.0577	7.3856	0.2262
2007	7.7258	0.2805	0.7904	0.0752	8.5162	0.2904
2008	7.1914	0.2525	0.6865	0.0550	7.8779	0.2584
2009	8.0094	0.2442	0.6958	0.0625	8.7052	0.2521
2010	7.8246	0.2799	0.7793	0.0714	8.6039	0.2889
2011	8.7668	0.2650	0.7298	0.0720	9.4965	0.2746
2012	10.0959	0.3199	0.8612	0.1769	10.9571	0.3655
2013	10.0335	0.3586	0.7628	0.0744	10.7963	0.3662
2014	10.3989	0.3429	0.6459	0.0681	11.0448	0.3496
2015	11.1724	0.3582	0.6202	0.0514	11.7926	0.3619
2016	11.2083	0.3615	0.6925	0.0707	11.9008	0.3684
2017	9.9500	0.3298	0.6927	0.0523	10.6427	0.3339
2018	8.8044	0.2955	0.7634	0.0702	9.5678	0.3037
2019	9.0624	0.2823	0.6698	0.0679	9.7322	0.2903
2020	8.3372	1.4270	0.7310	0.1178	9.0681	1.4318

Model Structure

Collectively, the models express uncertainty (or disagreement) about whether harvest is an additive or compensatory form of mortality (Burnham et al. 1984), and whether the reproductive process is weakly or strongly density-dependent (i.e., the degree to which reproductive rates decline with increasing population size).

All population models for mid-continent mallards share a common "balance equation" to predict changes in breeding-population size as a function of annual survival and reproductive rates:

$$N_{t+1} = N_t \left(mS_{t,AM} + (1-m)(S_{t,AF} + R_t(S_{t,JF} + S_{t,JM}\phi_F^{sum}/\phi_M^{sum}))\right)$$

where:

N=breeding population size,

m = proportion of males in the breeding population,

S_{AM}, S_{AF}, S_{JF}, and S_{JM} = survival rates of adult males, adult females, young females, and young males, respectively,

R = reproductive rate, defined as the fall age ratio of females,

$\phi_F^{sum}/\phi_M^{sum}$= the ratio of female ($F$) to male ($M$) summer survival, and t = year.

We assumed that m and $\phi_F^{sum}/\phi_M^{sum}$ are fixed and known. We also assumed, based in part on information provided by Blohm et al. (1987), the ratio of female to male summer survival was equivalent to the ratio of annual survival rates in the absence of harvest. Based on this assumption, we estimated $\phi_F^{sum}/\phi_M^{sum} = 0.897$. To estimate m we expressed the balance equation in matrix form:

$$\begin{bmatrix} N_{t+1,AM} \\ N_{t+1,AF} \end{bmatrix} = \begin{bmatrix} S_{AM} & RS_{JM}\phi_F^{sum}/\phi_M^{sum} \\ 0 & S_{AF} + RS_{JF} \end{bmatrix} \begin{bmatrix} N_{t,AM} \\ N_{t,AF} \end{bmatrix}$$

and substituted the constant ratio of summer survival and means of estimated survival and reproductive rates. The right eigenvector of the transition matrix is the stable sex structure that the breeding population eventually would attain with these constant demographic rates. This eigenvector yielded an estimate of $m = 0.5246$.

Using estimates of annual survival and reproductive rates, the balance equation for mid-continent mallards over-predicted observed population sizes by 11.0% on average. The source of the bias is unknown, so we modified the balance equation to eliminate the bias by adjusting both survival and reproductive rates:

$$N_{t+1} = \gamma_S N_t \left(mS_{t,am} + (1-m)\left(S_{t,AF} + \gamma_R R_t \left(S_{t,JF} + S_{t,JM}\phi_F^{sum}/\phi_M^{sum}\right)\right)\right)$$

where γ denotes the bias-correction factors for survival (S), and reproduction (R). We used a least squares approach to estimate $\gamma_S = 0.9407$ and $\gamma_R = 0.8647$.

Survival Process

We considered two alternative hypotheses for the relationship between annual survival and harvest rates. For both models, we assumed that survival in the absence of harvest was the same for adults and young of the same sex. In the model where harvest mortality is additive to natural mortality:

$$S_{t,sex,age} = S^A_{0,sex}(1 - K_{t,sex,age})$$

and in the model where changes in natural mortality compensate for harvest losses (up to some threshold):

$$S_{t,sex,age} = \begin{cases} s^C_{0,sex} & if\ K_{t,sex,age} \leq 1 - s^C_{0,sex} \\ 1 - K_{t,sex,age} & if\ K_{t,sex,age} > 1 - s^C_{0,sex} \end{cases}$$

where s_0 = survival in the absence of harvest under the additive (A) or compensatory (C) model, and K = harvest rate adjusted for crippling loss (20%, Anderson and Burnham 1976). We averaged estimates of s_0 across banding reference areas by weighting by breeding-population size. For the additive model, $s_0 = 0.7896$ and 0.6886 for males and females, respectively. For the compensatory model, $s_0 = 0.6467$ and 0.5965 for males and females, respectively. These estimates may seem counterintuitive because survival in the absence of harvest should be the same for both models. However, estimating a common (but still sex-specific) s_0 for both models leads to alternative models that do not fit available band-recovery data equally well. More importantly, it suggests that the greatest uncertainty about survival rates is when harvest rate is within the realm of experience. By allowing s_0 to differ between additive and compensatory models, we acknowledge that the greatest uncertainty about survival rate is its value in the absence of harvest (i.e., where we have no experience).

Reproductive Process

Annual reproductive rates were estimated from age ratios in the harvest of females, corrected using a constant estimate of differential vulnerability. Predictor variables were the number of ponds in May in Prairie Canada (P, in millions) and the size of the breeding population (N, in millions). We estimated the best-fitting linear model, and then calculated the 80% confidence ellipsoid for all model parameters. We chose the two points on this ellipsoid with the largest and smallest values for the effect of breeding-population size, and generated a weakly density-dependent model:

$$R_t = 0.7166 + 0.1083P_t - 0.0373N_t$$

and a strongly density-dependent model:

$$R_t = 1.1390 + 0.1376P_t - 0.1131N_t$$

Predicted recruitment was then rescaled to reflect the current definition of mid-continent mallards which now excludes birds from Alaska but includes mallards observed in the Great Lakes region.

Pond Dynamics

We modeled annual variation in Canadian pond numbers as a first-order autoregressive process. The estimated model was:

$$P_{t+1} = 2.2127 + 0.3420P_t + \varepsilon_t$$

where ponds are in millions and ε_t is normally distributed with mean = 0 and variance = 1.2567.

Variance of Prediction Errors

Using the balance equation and sub-models described above, predictions of breeding-population size in year *t+1* depend only on specification of population size, pond numbers, and harvest rate in year *t*. For the period in which comparisons were possible, we compared these predictions with observed population sizes.

We estimated the prediction-error variance by setting:

$$
\begin{aligned}
e_t &= \ln\left(N_t^{obs}\right) - \ln\left(N_t^{pre}\right) \\
e_t &\sim N\left(0, \sigma^2\right) \\
\hat{\sigma^2} &= \textstyle\sum_t \left[\ln\left(N_t^{obs}\right) - \ln\left(N_t^{pre}\right)\right]^2 / (n-1)
\end{aligned}
$$

where N^{obs} and N^{pre} are observed and predicted population sizes (in millions), respectively, and n = the number of years being compared. We were concerned about a variance estimate that was too small, either by chance or because the number of years in which comparisons were possible was small. Therefore, we calculated the upper 80% confidence limit for σ^2 based on a Chi-squared distribution for each combination of the alternative survival and reproductive sub-models, and then averaged them. The final estimate of σ^2 was 0.0280, equivalent to a coefficient of variation of about 16.85%.

Model Implications

The population model with additive hunting mortality and weakly density-dependent recruitment (SaRw) leads to the most conservative harvest strategy, whereas the model with compensatory hunting mortality and strongly density-dependent recruitment (ScRs) leads to the most liberal strategy. The other two models (SaRs and ScRw) lead to strategies that are intermediate between these extremes. Under the models with compensatory hunting mortality (ScRs and ScRw), the optimal strategy is to have a liberal regulation regardless of population size or number of ponds because at harvest rates achieved under the liberal alternative, harvest has no effect on population size. Under the strongly density-dependent model (ScRs), the density dependence regulates the population and keeps it within narrow bounds. Under the weakly density dependent model (ScRw), the density-dependence does not exert as strong a regulatory effect, and the population size fluctuates more.

Model Weights

Model weights are calculated as Bayesian probabilities, reflecting the relative ability of the individual alternative models to predict observed changes in population size. The Bayesian probability for each model is a function of the model's previous (or prior) weight and the likelihood of the observed population size under that model. We used Bayes' theorem to calculate model weights from a comparison of predicted and observed population sizes for the years 1996–2019, starting with equal model weights in 1995.

Appendix I Western Mallard Models

In contrast to mid-continent, we did not model changes in population size for both the Alaska and southern Pacific Flyway (California, Oregon, Washington, and British Columbia combined) substocks of western mallards (Table I.1) as an explicit function of survival and reproductive rate estimates (which in turn may be functions of harvest and environmental covariates). We believed this so-called "balance-equation approach" was not viable for western mallards because of insufficient banding in Alaska to estimate survival rates, and because of the difficulty in estimating substock-specific fall age ratios from a sample of wings derived from a mix of breeding stocks.

Table I.1 – Estimates (N) and associated standard errors (SE) of western mallards (in millions) observed in Alaska (WBPHS strata 1–12) and the southern Pacific Flyway (California, Oregon, Washington, and British Columbia combined) from 1990 to 2019. The waterfowl breeding population surveys were not conducted in 2020 due to the COVID-19 pandemic; 2020 numbers are based on model predictions.

	Alaska		CA-OR[a]		WA-BC		SO–PF[b] Total		Total	
Year	N	SE	N	SE	N	SE	N	SE	N	SE
1990	0.3669	0.0370	NA	NA	NA	NA	NA	NA	NA	NA
1991	0.3853	0.0363	NA	NA	NA	NA	NA	NA	NA	NA
1992	0.3457	0.0387	NA	NA	NA	NA	NA	NA	NA	NA
1993	0.2830	0.0295	NA	NA	NA	NA	NA	NA	NA	NA
1994	0.3509	0.0371	0.4281	0.0425	NA	NA	NA	NA	NA	NA
1995	0.5242	0.0680	0.4460	0.0427	NA	NA	NA	NA	NA	NA
1996	0.5220	0.0436	0.6389	0.0802	NA	NA	NA	NA	NA	NA
1997	0.5842	0.0520	0.6325	0.1043	NA	NA	NA	NA	NA	NA
1998	0.8362	0.0673	0.4788	0.0489	NA	NA	NA	NA	NA	NA
1999	0.7131	0.0696	0.6857	0.1066	NA	NA	NA	NA	NA	NA
2000	0.7703	0.0522	0.4584	0.0532	NA	NA	NA	NA	NA	NA
2001	0.7183	0.0541	NA	NA	NA	NA	NA	NA	NA	NA
2002	0.6673	0.0507	0.3698	0.0327	NA	NA	NA	NA	NA	NA
2003	0.8435	0.0668	0.4261	0.0501	NA	NA	NA	NA	NA	NA
2004	0.8111	0.0639	0.3449	0.0352	NA	NA	NA	NA	NA	NA
2005	0.7031	0.0547	0.3920	0.0474	NA	NA	NA	NA	NA	NA
2006	0.5158	0.0469	0.4805	0.0576	NA	NA	NA	NA	NA	NA
2007	0.5815	0.0551	0.4808	0.0546	NA	NA	NA	NA	NA	NA
2008	0.5324	0.0468	0.3725	0.0478	NA	NA	NA	NA	NA	NA
2009	0.5030	0.0449	0.3746	0.0639	NA	NA	NA	NA	NA	NA
2010	0.6056	0.0531	0.4347	0.0557	0.1740	0.0132	0.6087	0.0572	1.2143	0.0781
2011	0.4158	0.0388	0.3763	0.0452	0.1411	0.0117	0.5174	0.0467	0.9332	0.0607
2012	0.5056	0.0511	0.4759	0.0550	0.1650	0.0117	0.6409	0.0563	1.1465	0.0760
2013	0.3384	0.0382	0.3830	0.0527	0.1573	0.0117	0.5403	0.0540	0.8787	0.0661
2014	0.5009	0.0574	0.3239	0.0553	0.1690	0.0123	0.4929	0.0566	0.9938	0.0806
2015	0.4709	0.0509	0.2612	0.0295	0.1678	0.0114	0.4290	0.0316	0.8999	0.0599
2016	0.5842	0.0654	0.3511	0.0365	0.1339	0.0078	0.4850	0.0373	1.0692	0.0753
2017	0.5385	0.0519	0.2701	0.0324	0.1743	0.0120	0.4444	0.0346	0.9828	0.0624
2018	0.4508	0.0451	0.3700	0.0436	0.2042	0.0115	0.5743	0.0451	1.0250	0.0637
2019	0.3611	0.0353	0.3237	0.0330	0.2008	0.0142	0.5245	0.0359	0.8855	0.0504
2020	0.4086	0.0731	NA	NA	NA	NA	0.5325	0.0559	0.9411	0.0920

[a] Available California survey estimates begin in 1992; Oregon surveys estimates begin in 1994 and were unavailable in 2001.

[b] Southern Pacific Flyway includes California, Oregon, Washington, and British Columbia observations.

Model Structure

To evaluate western mallard population dynamics, we used a discrete logistic model (Schaefer 1954), which combines reproduction and natural mortality into a single parameter r, the intrinsic rate of growth. The model assumes density-dependent growth, which is regulated by the ratio of population size, N, to the carrying capacity of the environment, K (i.e., equilibrium population size in the absence of harvest). In the traditional formulation, harvest mortality is additive to other sources of mortality, but compensation for hunting losses can occur through subsequent increases in production. However, we parameterized the model in a way that also allows for compensation of harvest mortality between the hunting and breeding seasons. It is important to note that compensation modeled in this way is purely phenomenological, in the sense that there is no explicit ecological mechanism for compensation (e.g., density-dependent mortality after the hunting season). The basic model for both the Alaska and southern Pacific Flyway substocks has the form:

$$N_{t+1} = \left[N_t + N_t r\left(1 - \frac{N_t}{K}\right)\right](1 - \alpha_t)$$

where,

$$\alpha_t = dh_t^{AM}$$

and where t = year, h^{AM} = the harvest rate of adult males, and d = a scaling factor. The scaling factor is used to account for a combination of unobservable effects, including un-retrieved harvest (i.e., crippling loss), differential harvest mortality of cohorts other than adult males, and for the possibility that some harvest mortality may not affect subsequent breeding-population size (i.e., the compensatory mortality hypothesis).

Estimation Framework

We used Bayesian estimation methods in combination with a state-space model that accounts explicitly for both process and observation error in breeding population size. This combination of methods is becoming widely used in natural resource modeling, in part because it facilitates the fitting of non-linear models that may have non-normal errors (Meyer and Millar 1999). The Bayesian approach also provides a natural and intuitive way to portray uncertainty, allows one to incorporate prior information about model parameters, and permits the updating of parameter estimates as further information becomes available. Breeding population data are available for California and Oregon from 1994–2019 (except for 2001), British Columbia from 2006–2019, and Washington from 2010–2019 (see Table I.1). We attempted to use correlations with adjacent states to impute data back to 1992 for WA and BC, but could not find a reasonable correlation between those surveys and other regions (potentially due to a short time series). Therefore, we imputed population estimates for BC and WA by sampling values from the mean and variance within the MCMC framework. Specifically, we calculated the total mean and variance of breeding population sizes based on observed data (2006–2019 for British Columbia, and 2010–2019 for Washington), and then used those means and variances to sample a population size for the missing years (1992–2005 for British Columbia; and 1992–2009 for Washington) during each iteration of MCMC sampling. Although this approach imputes values based on a random draw, it does acknowledge added uncertainty in those estimates compared to the years with observed data. Further, given the low annual variability and lack of trend, we have no evidence that the recent survey estimates used to generate the mean and variance are not a reasonable approximation of historical breeding population sizes.

We first scaled N by K as recommended by Meyer and Millar (1999), and assumed that process errors were lognormally distributed with mean 0 and variance σ^2. Thus, the process model had the form:

$$\begin{aligned} P_t &= N_t/K \\ \log(P_t) &= \log\left(\left[P_{t-1} + P_{t-1} r\left(1 - P_{t-1}\right)\right]\left(1 - dh_{t-1}^{AM}\right)\right) + e_t \end{aligned}$$

where,

$$e_t \sim N(0, \sigma^2)$$

The observation model related the unknown population sizes ($P_t K$) to the population sizes (N_t) estimated from the breeding-population surveys in Alaska and southern Pacific Flyway. We assumed that the observation process yielded additive, normally distributed errors, which were represented by:

$$N_t = P_t K + \varepsilon_t^{BPOP},$$

where,

$$\varepsilon_t^{BPOP} \sim N(0, \sigma^2_{BPOP}).$$

permitting us to estimate the process error, which reflects the inability of the model to completely describe changes in population size. The process error reflects the combined effect of misspecification of an appropriate model form, as well as any un-modeled environmental drivers. We initially examined a number of possible environmental covariates, including the Palmer Drought Index in California and Oregon, spring temperature in Alaska, and the El Niño Southern Oscillation Index (http://www.cdc.noaa.gov/people/klaus.wolter/MEI/mei.html). While the estimated effects of these covariates on r or K were generally what one would expect, they were never of sufficient magnitude to have a meaningful effect on optimal harvest strategies. We therefore chose not to further pursue an investigation of environmental covariates, and posited that the process error was a sufficient surrogate for these un-modeled effects. Parameterization of the models also required measures of harvest rate. Beginning in 2002, harvest rates of adult males were estimated directly from the recovery of reward bands. Prior to 1993, we used direct recoveries of standard bands, corrected for band-reporting rates provided by Nichols et al. (1995*b*). We also used the band-reporting rates provided by Nichols et al. (1995*b*) for estimating harvest rates in 1994 and 1995, except that we inflated the reporting rates of full-address and toll-free bands based on an unpublished analysis by Clint Moore and Jim Nichols (Patuxent Wildlife Research Center). We were unwilling to estimate harvest rates for the years 1996–2001 because of suspected, but unknown, increases in the reporting rates of all bands. For simplicity, harvest rate estimates were treated as known values in our analysis, although future analyses might benefit from an appropriate observation model for these data.

In a Bayesian analysis, one is interested in making probabilistic statements about the model parameters (θ), conditioned on the observed data. Thus, we are interested in evaluating $P(\theta|data)$, which requires the specification of prior distributions for all model parameters and unobserved system states (θ) and the sampling distribution (likelihood) of the observed data $P(data|\theta)$. Using Bayes theorem, we can represent the posterior probability distribution of model parameters, conditioned on the data, as:

$$P(\theta|data) \propto P(\theta) \times P(data|\theta)$$

Accordingly, we specified prior distributions for model parameters *r, K, d,* and P_0, which is the initial population size relative to carrying capacity. For both substocks, we specified the following prior distributions for *r, d,* and σ^2:

$$\begin{aligned} r &\sim Lognormal(-1.0397, 0.69315) \\ d &\sim Uniform(0, 2) \\ \sigma^2 &\sim Inverse-gamma(0.001, 0.001) \end{aligned}$$

The prior distribution for r is centered at 0.35, which we believe to be a reasonable value for mallards based on life-history characteristics and estimates for other avian species. Yet the distribution also admits considerable uncertainty as to the value of r within what we believe to be realistic biological bounds. As for the harvest-rate scalar, we would expect $d \geq 1$ under the additive hypothesis and $d < 1$ under the compensatory hypothesis. As we had no data to specify an informative prior distribution, we specified a vague prior in which d could take on a wide range of values with equal probability. We used a traditional, uninformative prior distribution for σ^2. Prior distributions for K and P_0 were substock-specific and are described in the following sections.

We used the public-domain software JAGS (Plummer (2003); https://sourceforge.net/projects/mcmc-jags) to derive samples from the joint posterior distribution of model parameters via MCMC simulations. We obtained 800,000 samples from the joint posterior distribution, discarded the first 700,000, and then thinned the remainder by 50, resulting in a sample of 2,000 for each of 5 chains, or 10,000 total samples.

Alaska mallards

Data selection—Breeding population estimates of mallards in Alaska (and the Old Crow Flats in Yukon) are available since 1955 in WBPHS strata 1–12 (Smith 1995). However, a change in survey aircraft in 1977 instantaneously increased the detectability of waterfowl, and thus population estimates (Hodges et al. 1996). Moreover, there was a rapid increase in average annual temperature in Alaska at the same time, apparently tied to changes in the frequency and intensity of El Niño events (http://www.cdc.noaa.gov/people/klaus.wolter/MEI/mei.html). This confounding of changes in climate and survey methods led us to truncate the years 1955–1977 from the time series of population estimates.

Modeling of the Alaska substock also depended on the availability of harvest-rate estimates derived from band-recovery data. Unfortunately, sufficient numbers of mallards were not banded in Alaska prior to 1990. A search for covariates that would have allowed us to make harvest-rate predictions for years in which band-recovery data were not available was not fruitful, and we were thus forced to further restrict the time series to 1990 and later. Even so, harvest rate estimates were not available for the years 1996–2001, and 2014 because of unknown changes in band-reporting rates or lack of banding data. Because available estimates of harvest rate showed no apparent variation over time, we simply used the mean and standard deviation of the available estimates and generated independent samples of predictions for the missing years based on a logit transformation and an assumption of normality:

$$ln\left(\frac{h_t}{1-h_t}\right) \sim Normal(-2.4209, 0.0659) \quad \text{for } t = 1996\text{–}2001, \text{ and } 2014.$$

Prior distributions for K and P_0—We believed that sufficient information was available to use mildly informative priors for K and P_0. During the development of this framework, the Alaska substock had approximately 0.8 million mallards. If harvest rates have been comparable to that necessary to achieve maximum sustained yield (MSY) under the logistic model (i.e., $r/2$), then we would expect $K \approx 1.6$ million. On the other hand, if harvest rates have been less than those associated with MSY, then we would expect $K < 1.6$ million. Because we believed it was not likely that harvest rates were $> r/2$, we believed the likely range of K to be 0.8–1.6 million. We therefore specified a prior distribution that had a mean of 1.4 million, but had a sufficiently large variance to admit a wide range of possible values:

$$K \sim Lognormal(0.13035, 0.41224)$$

Extending this line of reasoning, we specified a prior distribution that assumed the estimated population size of approximately 0.4 million at the start of the time series (i.e., 1990) was 20–60% of K. Thus on a log scale:

$$P_o \sim Uniform(-1.6094, -0.5108)$$

Parameter estimates—The logistic model and associated posterior parameter estimates provided a reasonable fit to the observed time series of population estimates. The posterior means of K and r were similar to their priors, although their variances were considerably smaller (Table I.2). However, the posterior distribution of d was essentially the same as its prior, reflecting the absence of information in the data necessary to reliably estimate this parameter.

Table I.2 – Estimates of model parameters resulting from fitting a discrete logistic model to a time series of estimated population sizes and harvest rates of mallards breeding in Alaska from 1990 to 2019.

Parameter	Mean	SD	2.5% CI[a]	Median	97.5% CI
K	1.090	0.321	0.658	1.019	1.878
d	1.286	0.484	0.240	1.354	1.969
r	0.283	0.113	0.089	0.275	0.527
σ^2	0.024	0.010	0.010	0.022	0.050

[a] CI = credible interval.

Southern Pacific Flyway (CA-OR-WA-BC) mallards

Data selection—Breeding-population estimates of mallards in California are available starting in 1992, but not until 1994 in Oregon. Also, Oregon did not conduct a survey in 2001. To avoid truncating the time series, we used the admittedly weak relationship ($P = 0.02$) between California-Oregon population estimates to predict population sizes in Oregon in 1992, 1993, and 2001. The fitted linear model was:

$$N_t^{OR} = 60196 + 0.0911(N_t^{CA})$$

To derive realistic standard errors, we assumed that the predictions had the same mean coefficient of variation as the years when surveys were conducted ($n = 24$, CV = 0.089). The estimated sizes and variances of the southern Pacific Flyway substock were calculated by simply summing the state-specific estimates.

We pooled band-recovery data for the southern Pacific Flyway substock and estimated harvest rates in the same manner as that for Alaska mallards. Although banded sample sizes were sufficient in all years, harvest rates could not be estimated for the years 1996–2001 because of unknown changes in band-reporting rates. As with Alaska, available estimates of harvest rate showed no apparent trend over time, and we simply used the mean and standard deviation of the available estimates and generated independent samples of predictions for the missing years based on a logit transformation and an assumption of normality:

$$ln\left(\frac{h_t}{1-h_t}\right) \sim Normal(-1.8615, 0.0267) \quad \text{for } t = 1996\text{–}2001$$

Prior distributions for K and P_0—Unlike the Alaska substock, the California-Oregon population had been relatively stable with a mean of 0.48 million mallards while developing western mallard AHM. We believed K should be in the range 0.48–0.96 million, assuming the logistic model and that harvest rates were $\leq r/2$. The addition of Washington and British Columbia mallards to the southern Pacific Flyway substock did not result in substantive changes to historically stable population dynamics, but increased the overall size of the southern Pacific Flyway population by approximately 30%. Therefore, we scaled the prior to increase the expected carrying capacity by 30%. We therefore specified a prior distribution on K that had a mean of 0.8 million, but with a variance sufficiently large to admit a wide range of possible values:

$$K \sim Lognormal(-0.2262, 0.2638)$$

The estimated size of the California-Oregon substock was 0.47 million at the start of the time series (i.e., California plus the imputed Oregon estimate in 1992). We used a similar line of reasoning as that for Alaska for specifying a prior distribution P_0, positing that initial population size was 40-100% of K. Thus on a log scale:

$$P_o \sim Uniform(-0.9163, 0.0)$$

Parameter estimates—The logistic model and associated posterior parameter estimates provided a reasonable fit to the observed time series of population estimates. The posterior means of K and r were similar to their priors, although the variances were considerably smaller (Table I.3). Interestingly, the posterior mean of d was < 1, suggestive of a compensatory response to harvest; however the standard deviation of the estimate was large, with the upper 95% credibility limit > 1.

Table I.3 – Estimates of model parameters resulting from fitting a discrete logistic model to a time series of estimated population sizes and harvest rates of mallards breeding in the southern Pacific Flyway (California, Oregon, Washington, and British Columbia combined) from 1992 to 2019.

Parameter	Mean	SD	2.5% CI[a]	Median	97.5% CI
K	0.843	0.194	0.598	0.795	1.345
d	0.534	0.358	0.046	0.461	1.407
r	0.285	0.167	0.066	0.250	0.703
σ^2	0.008	0.005	0.002	0.007	0.019

[a] CI = credible interval.

For each western mallard substock, we further summarized the simulation results for r, K, and the scaling factor d to admit parametric uncertainty with a formal correlation structure within the optimization procedure used to calculate the harvest strategy. We first defined a joint distribution for 3 discrete outcomes for each of the 3 population parameters. We used the 30 and 70 percent quantiles for each parameter as the cut points to define three bins for which to discretize 3 values of each posterior distribution. We then determined the frequency of occurrence of each of the 27 possible combinations of each parameter value falling within the 3 bins from the MCMC simulation results. These frequencies were then assigned parameter values based on the midpoint of bin ranges (15, 50, 85 percent quantiles) to specify the joint distribution of the population parameter values used in the optimization.

Appendix J Atlantic Flyway Multi-stock Models

Similar to western mallards we did not have adequate data to model changes in breeding population size of the species included in the multi-stock framework (Table J.1) to use the balance-equation approach. Therefore, we used discrete logistic models similar to those used to model western mallard population dynamics. We initially intended to use the same model structure for all four species in the strategy, but because of the lack of preseason banding data for ring-necked ducks and goldeneyes, we implemented two different forms of the discrete logistic model.

Table J.1 – Estimates (N) and associated standard errors (SE) of American green-winged teal (AGWT), wood ducks (WODU), ring-necked ducks (RNDU), and goldeneyes (GOLD) (in millions) observed in eastern Canada (WBPHS strata 51–53, 56, 62–72) and U.S. (Atlantic Flyway states) from 1998 to 2019. The waterfowl breeding population surveys were not conducted in 2020 due to the COVID-19 pandemic; 2020 numbers are based on model predictions.

	AGWT[a]		WODU[b]		RNDU[a]		GOLD[a]	
Year	N	SE	N	SE	N	SE	N	SE
1998	0.3003	0.0700	0.9588	0.1171	0.5858	0.1274	0.5505	0.1452
1999	0.3887	0.0769	0.9737	0.1191	0.6948	0.1539	0.6599	0.1378
2000	0.3567	0.0637	0.9342	0.1119	0.9210	0.3552	0.6425	0.1703
2001	0.2985	0.0578	0.9238	0.1106	0.6584	0.1235	0.7462	0.1836
2002	0.4056	0.0736	0.9563	0.1143	0.6697	0.1128	0.8526	0.2170
2003	0.3930	0.0843	0.9185	0.1118	0.6701	0.0987	0.6448	0.1899
2004	0.4635	0.0974	0.9383	0.1267	0.7375	0.1486	0.5925	0.1385
2005	0.3404	0.0746	0.9206	0.1112	0.6225	0.0900	0.5170	0.1070
2006	0.3332	0.0699	0.9526	0.1145	0.6542	0.1048	0.4740	0.1005
2007	0.4406	0.1338	0.9570	0.1157	0.8330	0.1195	0.6613	0.1549
2008	0.4063	0.0936	0.9235	0.1132	0.6713	0.1238	0.6268	0.1571
2009	0.4290	0.1047	0.9423	0.1143	0.6839	0.1349	0.5419	0.1265
2010	0.4171	0.1069	0.9351	0.1125	0.6759	0.1173	0.5348	0.1322
2011	0.4023	0.1057	0.9461	0.1141	0.6093	0.0961	0.5459	0.1215
2012	0.3647	0.0878	0.9786	0.1192	0.6331	0.1180	0.5747	0.1696
2013	0.4001	0.2186	0.9874	0.1250	0.7832	0.4361	0.6203	NA[c]
2014	0.3058	0.0719	0.9962	0.1211	0.5968	0.0999	0.5800	0.2081
2015	0.3126	0.0751	0.9870	0.1211	0.7132	0.1947	0.4390	0.1024
2016	0.3194	0.0802	1.0022	0.1242	0.7326	0.1389	0.5034	0.1404
2017	0.3447	0.0695	1.0365	0.1486	0.6119	0.1282	0.5616	0.1570
2018	0.3395	0.0749	0.9901	0.1243	0.6275	0.1289	0.4891	0.1291
2019	0.3028	0.0634	1.0189	0.1215	0.6935	0.1513	0.5159	0.1489
2020	0.3502	0.0377	0.9409	0.0727	0.7026	0.0695	0.5761	0.0996

[a] Breeding population size estimates from eastern survey area (WBPHS strata 51–53, 56, 62–72)

[b] Breeding population size estimates from Atlantic Flyway states (Florida north to Maine)

[c] The SE of the goldeneyes estimate for 2013 is not reported due to insufficient counts.

Model Structures

We had sufficient preseason bandings for American green-winged teal and wood ducks to estimate harvest rates directly from band recovery analysis, so we used a similar model to western mallards:

$$N_{t+1} = \left[N_t + N_t r\left(1 - \frac{N_t}{K}\right)\right](1 - h_t),$$

where N = breeding population size, r = the maximum intrinsic growth rate, K = carrying capacity, and h = harvest rate estimated from banding data. The model does not have age or sex structure and banding summaries indicated reasonable sample sizes for adults and juveniles of both sexes, so we pooled all banding data when estimating an overall population harvest rate. This form of the discrete logistic model assumes that density dependent growth (or declines) are instantaneous and loss to harvest occurs following the instantaneous growth [i.e., next year's population is based on the current year population, density dependent growth, and surviving the hunting season at a rate equal to $(1 - h)$]. This model assumes that harvest is additive and r and K provide a measure of the harvest potential for these species.

Because we did not have sufficient data to estimate harvest rates for ring-necked ducks and goldeneyes, we used a slightly modified version of the above model that includes total harvest rather than harvest rate:

$$N_{t+1} = \left[N_t + N_t r\left(1 - \frac{N_t}{K}\right)\right] - dH_t,$$

where H = total harvest in number of birds, and d = a scaling parameter to account for incomplete overlap between the spatial scale for which H and N are calculated (i.e., breeding population surveys are limited to a discrete region in eastern U.S. and Canada, whereas the harvest data can be collected from birds that breed outside of the survey region).

Estimation Framework

We used Bayesian estimation methods with a state-space model (Meyer and Millar 1999) to estimate the parameters of the discrete logistic model for all four species in the multi-stock framework. This modeling approach allows us to explicitly model the process (i.e., the unobservable true underlying dynamics of the population) and observation (sampling a portion of the population) components that generated the observed data. As recommended by Meyer and Millar (1999), we scaled N by K to help improve convergence and assumed that the process error was lognormally distributed. Therefore, the process model for American green-winged teal and wood ducks was:

$$\log(P_t) = \log\left(\left[P_{t-1} + P_{t-1} r\left(1 - P_{t-1}\right)\right](1 - h_{t-1})\right) + e_t,$$

whereas the process model for ring-necked ducks and goldeneyes was:

$$\log(P_t) = \log\left(\left[P_{t-1} + P_{t-1} r\left(1 - P_{t-1}\right)\right] - d\frac{H_{t-1}}{K}\right) + e_t,$$

with

$$P_t = N_t/K, and$$

$$e_t \sim N(0, \sigma^2)$$

for both model structures. The process error (e_t) represents the inability of the discrete logistic model to accurately characterize population changes. We assumed that the standard errors for the breeding population size estimates were normally distributed and linked the process model to the observed data as:

$$N_t = P_t K + \varepsilon_t^{BPOP},$$

where

$$\varepsilon_t^{BPOP} \sim N(0, \sigma^2_{BPOP}).$$

The posterior estimates for the discrete logistic parameters for each species are listed in Table J.2.

Table J.2 – Estimates of model parameters resulting from fitting a discrete logistic model to a time series of estimated population sizes and harvest rates of American green-winged teal (AGWT), wood ducks (WODU), ring-necked ducks (RNDU), and goldeneyes (GOLD) breeding in eastern Canada and U.S. from 1998 to 2019.

Parameter	Species	Mean	SD	2.5% CI[a]	Median	97.5% CI
K	AGWT	0.5398	0.0708	0.4158	0.5291	0.6863
K	WODU	1.5919	0.2014	1.2617	1.5632	2.0229
K	RNDU	0.9024	0.1641	0.6490	0.8745	1.2395
K	GOLD	0.7332	0.1292	0.5239	0.7077	1.0132
P_0	AGWT	0.5993	0.0773	0.4405	0.6050	0.7336
P_0	WODU	0.5769	0.0753	0.4309	0.5804	0.7060
P_0	RNDU	0.6287	0.0710	0.4740	0.6372	0.7531
P_0	GOLD	0.6637	0.0964	0.4588	0.6662	0.8512
d	AGWT	NA	NA	NA	NA	NA
d	WODU	NA	NA	NA	NA	NA
d	RNDU	0.5376	0.2753	0.0669	0.5577	0.9983
d	GOLD	0.5887	0.2814	0.0848	0.6296	1.0000
r	AGWT	0.4424	0.1071	0.2587	0.4287	0.6579
r	WODU	0.4001	0.0838	0.2630	0.3875	0.5669
r	RNDU	0.4153	0.1086	0.2278	0.4008	0.6329
r	GOLD	0.2332	0.0528	0.1374	0.2271	0.3381
σ^2	AGWT	0.0052	0.0061	0.0002	0.0032	0.0165
σ^2	WODU	0.0023	0.0020	0.0002	0.0017	0.0061
σ^2	RNDU	0.0038	0.0044	0.0002	0.0023	0.0118
σ^2	GOLD	0.0140	0.0139	0.0002	0.0099	0.0402

[a] CI = credible interval.

Data—The USFWS and Atlantic Flyway agreed to use breeding population size data from the largest area possible for the multi-stock AHM framework. The complete eastern Canada and Maine area has been surveyed since 1998 and is the largest area representing breeding population sizes of American green-winged teal, ring-necked ducks, and goldeneyes that are harvested in the Atlantic Flyway. The BBS survey (1966–current) and AFBWS (1993–current) data that are used to estimate wood duck breeding population size provide a longer time series for that species in the Atlantic Flyway. However, changes in band inscriptions and the lack of an appropriate reporting rate for adjusting harvest rate for that species during the mid-1990s precluded us from estimating reliable harvest rates that were needed for the discrete logistic model. Therefore, we limited the data for all species to 1998–current for the Atlantic Flyway multi-stock AHM framework (see Table J.1).

Prior distributions —Inferences from Bayesian analyses are derived from posterior distributions that are proportional to the likelihood of the data given model parameters multiplied by the prior probabilities of those parameters. We used two different approaches for estimating prior distributions for K and r. For K, we used a uniform prior because we had no *a priori* information that could allow us to put more weight on a specific K for each species. However, we felt we could identify endpoints for the uniform distribution as the

mean observed population size (i.e., current harvest levels are completely compensatory) and double the mean observed population size (i.e., populations are currently being harvested at maximum sustainable yield [MSY] and are at $\frac{1}{2}K$). We extended the uniform prior 20% less and 20% greater than these end points to account for uncertainty in observational data. These prior values were based on observed breeding population sizes from 1998 to 2015, which represented the extent of the time series when the development of the multi-stock framework first began. We felt that we had a more justifiable theoretical basis to estimate a non-uniform prior for r based on previous research. For each species, we used the demographic invariant method (Niel and Lebreton 2005) with survival rate estimates based on an allometric relationship between species mass and survival in captive birds (Johnson et al. 2012) to develop informed lognormal priors (Table J.3). We used a non-informative inverse gamma prior for estimating process variation.

Table J.3 – Lognormal mean and standard deviations (SD) used to describe the prior distributions for maximum intrinsic growth rate (r) for American green-winged teal (AGWT), wood ducks (WODU), ring-necked ducks (RNDU), and goldeneyes (GOLD) in eastern Canada and U.S.

Species	Mean	SD
AGWT	−0.80396	0.23495
WODU	−0.89116	0.24417
RNDU	−0.90198	0.24294
GOLD	−1.42346	0.20831

Appendix K Modeling Waterfowl Harvest Rates

Mid-continent Mallards

We modeled harvest rates of mid-continent mallards within a Bayesian hierarchical framework. We developed a set of models to predict harvest rates under each regulatory alternative as a function of the harvest rates observed under the liberal alternative, using historical information. We modeled the probability of regulation-specific harvest rates (h) based on normal distributions with the following parameterizations:

$$\begin{aligned}
&\text{Closed:} && p(h_C) \sim N(\mu_C, \nu_C^2) \\
&\text{Restrictive:} && p(h_R) \sim N(\mu_R, \nu_R^2) \\
&\text{Moderate:} && p(h_M) \sim N(\mu_M, \nu_M^2) \\
&\text{Liberal:} && p(h_L) \sim N(\mu_L, \nu_L^2)
\end{aligned}$$

For the restrictive and moderate alternatives we introduced the parameter γ to represent the relative difference between the harvest rate observed under the liberal alternative and the moderate or restrictive alternatives. Based on this parameterization, we are making use of the information that has been gained (under the liberal alternative) and are modeling harvest rates for the restrictive and moderate alternatives as a function of the mean harvest rate observed under the liberal alternative. For the harvest-rate distributions assumed under the restrictive and moderate regulatory alternatives, we specified that γ_R and γ_M are equal to the prior estimates of the predicted mean harvest rates under the restrictive and moderate alternatives divided by the prior estimates of the predicted mean harvest rates observed under the liberal alternative. Thus, these parameters act to scale the mean of the restrictive and moderate distributions in relation to the mean harvest rate observed under the liberal regulatory alternative. We also considered the marginal effect of framework-date extensions under the moderate and liberal alternatives by including the parameter δ_f.

To update the probability distributions of harvest rates realized under each regulatory alternative, we first needed to specify a prior probability distribution for each of the model parameters. These distributions represent prior beliefs regarding the relationship between each regulatory alternative and the expected harvest rates. We used a normal distribution to represent the mean and a scaled inverse-chi-square distribution to represent the variance of the normal distribution of the likelihood. For the mean (μ) of each harvest-rate distribution associated with each regulatory alternative, we use the predicted mean harvest rates provided in (U.S. Fish and Wildlife Service 2000, 13–14), assuming uniformity of regulatory prescriptions across Flyways. We set prior values of each standard deviation (ν) equal to 20% of the mean (CV = 0.2) based on an analysis by Johnson et al. (1997). We then specified the following prior distributions and parameter values under each regulatory package:

Closed (in U.S. only):

$$p(\mu_C) \sim N\left(0.0088, \tfrac{0.0018^2}{6}\right)$$

$$p(\nu_C^2) \sim Scaled\ Inv - \chi^2(6, 0.0018^2)$$

These closed-season parameter values are based on observed harvest rates in Canada during the 1988–93 seasons, which was a period of restrictive regulations in both Canada and the United States.

For the restrictive and moderate alternatives, we specified that the standard error of the normal distribution of the scaling parameter is based on a coefficient of variation for the mean equal to 0.3. The scale parameter of the inverse-chi-square distribution was set equal to the standard deviation of the harvest rate mean under the restrictive and moderate regulation alternatives (i.e., CV = 0.2).

Restrictive:

$p(\gamma_R) \sim N\left(0.51, \frac{0.15^2}{6}\right)$

$p(\nu_R^2) \sim Scaled\,Inv - \chi^2(6, 0.0133^2)$

Moderate:

$p(\gamma_M) \sim N\left(0.85, \frac{0.26^2}{6}\right)$

$p(\nu_r^2) \sim Scaled\,Inv - \chi^2(6, 0.0223^2)$

Liberal:

$p(\mu_L) \sim N\left(0.1305, \frac{0.0261^2}{6}\right)$

$p(\nu_R^2) \sim Scaled\,Inv - \chi^2(6, 0.0261^2)$

The prior distribution for the marginal effect of the framework-date extension was specified as:

$$p(\delta_f) \sim N\left(0.02, 0.01^2\right)$$

The prior distributions were multiplied by the likelihood functions based on the last 22 years of data under liberal regulations, and the resulting posterior distributions were evaluated with Markov chain Monte Carlo simulation. Posterior estimates of model parameters and of annual harvest rates are provided in Table K.1.

Western Mallards

We modeled harvest rates of western mallards using a similar parameterization as that used for mid-continent mallards. However, we did not explicitly model the effect of the framework date extension because we did not use data observed prior to when framework date extensions were available. In the western mallard parameterization, the effect of the framework date extensions are implicit in the expected mean harvest rate expected under the liberal regulatory option.

Closed:	$p(h_C) \sim N(\mu_C, \nu_C^2)$
Restrictive:	$p(h_R) \sim N(\gamma_R \mu_L, \nu_R^2)$
Moderate:	$p(h_M) \sim N(\gamma_M \mu_L, \nu_M^2)$
Liberal:	$p(h_L) \sim N(\mu_L, \nu_L^2)$

We set prior values of each standard deviation (ν) equal to 30% of the mean (CV = 0.3) to account for additional variation due to changes in regulations in the other Flyways and their unpredictable effects on the harvest rates of western mallards. We then specified the following prior distribution and parameter values for the liberal regulatory alternative:

Table K.1 – Parameter estimates for predicting mid-continent mallard harvest rates resulting from a hierarchical, Bayesian analysis of mid-continent mallard band-recovery information from 1998 to 2019.

Parameter	Estimate	SD	Parameter	Estimate	SD
μ_C	0.0088	0.0021	h_{1998}	0.1019	0.0068
ν_C	0.0019	0.0005	h_{1999}	0.0983	0.0070
γ_R	0.5097	0.0617	h_{2000}	0.1233	0.0082
ν_R	0.0129	0.0033	h_{2001}	0.0927	0.0084
γ_M	0.8484	0.1059	h_{2002}	0.1211	0.0042
ν_M	0.0214	0.0054	h_{2003}	0.1102	0.0041
μ_L	0.1071	0.0059	h_{2004}	0.1297	0.0047
ν_L	0.0167	0.0023	h_{2005}	0.1139	0.0053
δ_f	0.0035	0.0062	h_{2006}	0.1027	0.0043
			h_{2007}	0.1125	0.0040
			h_{2008}	0.1179	0.0045
			h_{2009}	0.1012	0.0035
			h_{2010}	0.1108	0.0049
			h_{2011}	0.0965	0.0058
			h_{2012}	0.1023	0.0048
			h_{2013}	0.1045	0.0051
			h_{2014}	0.1097	0.0061
			h_{2015}	0.1005	0.0065
			h_{2016}	0.1122	0.0067
			h_{2017}	0.1053	0.0045
			h_{2018}	0.0984	0.0044
			h_{2019}	0.0952	0.0049

Table K.2 – Parameter estimates for predicting western mallard harvest rates resulting from a hierarchical, Bayesian analysis of western mallard band-recovery information from 2008 to 2019.

Parameter	Estimate	SD	Parameter	Estimate	SD
μ_C	0.0090	0.0186	h_{2008}	0.1484	0.0065
ν_C	0.0182	0.0046	h_{2009}	0.1360	0.0058
γ_R	0.5083	0.0607	h_{2010}	0.1385	0.0062
ν_R	0.0173	0.0044	h_{2011}	0.1256	0.0055
γ_M	0.8550	0.1028	h_{2012}	0.1326	0.0055
ν_M	0.0289	0.0073	h_{2013}	0.0940	0.0047
μ_L	0.1347	0.0072	h_{2014}	0.1606	0.0072
ν_L	0.0270	0.0045	h_{2015}	0.1551	0.0069
			h_{2016}	0.1588	0.0079
			h_{2017}	0.1565	0.0078
			h_{2018}	0.1247	0.0060
			h_{2019}	0.1298	0.0061

Closed (in US only):

$p(\mu_C) \sim N\left(0.0088, \frac{0.00264^2}{6}\right)$

$p(\nu_C^2) \sim Scaled\,Inv - \chi^2(6, 0.00264^2)$

Restrictive:

$p(\gamma_R) \sim N\left(0.51, \frac{0.153^2}{6}\right)$

$p(\nu_R^2) \sim Scaled\,Inv - \chi^2(6, 0.01867^2)$

Moderate:

$p(\gamma_M) \sim N\left(0.85, \frac{0.255^2}{6}\right)$

$p(\nu_R^2) \sim Scaled\,Inv - \chi^2(6, 0, 0.03112^2)$

Liberal:

$p(\mu_L) \sim N\left(0.1220, \frac{0.03661^2}{6}\right)$

$p(\nu_R^2) \sim Scaled\,Inv - \chi^2(6, 0.03661^2)$

The prior distributions were multiplied by the likelihood functions based on the last 12 years of data under liberal regulations, and the resulting posterior distributions were evaluated with Markov chain Monte Carlo simulation. Posterior estimates of model parameters and of annual harvest rates are provided Table K.2.

Eastern Waterfowl Stocks

We estimated expected harvest rates and associated variances for American green-winged teal and wood ducks as a function of the Atlantic Flyway's liberal regulatory alternative using birds banded in eastern Canada and

the Atlantic Flyway during 1998–2014 (banding reference areas 8, 15, 16; the states of North Carolina, South Carolina, Georgia, and Florida; the provinces of New Brunswick, Nova Scotia, Newfoundland and Labrador, Prince Edward Island, and eastern Quebec). We used these bands and their direct recoveries in binomial models to estimate direct recovery probabilities and then adjusted those recovery probabilities with regional reporting rates (birds banded in these areas were recovered in eastern Canada, the Atlantic Flyway, and Mississippi Flyway; Boomer et al. 2013) to estimate harvest rates (U.S. Fish and Wildlife Service 2017). We pooled age and sex classes for this estimation because the discrete logistic model used for this assessment does not incorporate age and sex structure. We used Bayesian methods and Markov chain Monte Carlo (MCMC) methods to estimate annual recovery probabilities and adjusted the recovery probabilities within the MCMC to obtain variances and incorporate uncertainty in the estimates of reporting rates (Padding et al. 2018).

Banding and recovery data were insufficient for estimating the expected ring-necked duck and goldeneye harvest rates, so we used annual estimates of harvest (H) from the Harvest Information Program and the fall population size to make inferences about harvest rate (Runge et al. 2004). We estimated the annual fall population size (NF) from the discrete logistic model, and then estimated the expected harvest rate as H/NF (Runge et al. 2004). Therefore, the estimates of harvest rate for ring-necked ducks and goldeneyes were both calculated as derived parameters in the discrete logistic model used to estimate r and K for the population. We used Bayesian methods and a state-space model to fit the discrete logistic models and calculate derived estimates of harvest rate for these species (Appendix J). Breeding population estimates for ring-necked ducks and goldeneyes in eastern North America were available beginning in 1998, therefore we estimated the expected harvest rate for both species based on 1998–2014 harvest and population estimates.

Table K.3 – Annual harvest rate estimates (h) and associated standard errors (SE) for American green-winged teal (AGWT), wood ducks (WODU), ring-necked ducks (RNDU), and goldeneyes (GOLD) in eastern Canada (WBPHS strata 51–53, 56, 62–72) and U.S. (Atlantic Flyway states) from 1998 to 2019.

	AGWT[a]		WODU[a]		RNDU[b]		GOLD[b]	
Year	h	SE	h	SE	h	SE	h	SE
1998	0.179	0.0254	0.1095	0.0077	0.2381	0.0217	0.039	0.0044
1999	0.1334	0.0096	0.1264	0.0083	0.1786	0.0183	0.0372	0.0043
2000	0.135	0.0093	0.1206	0.0078	0.1264	0.0147	0.0354	0.0042
2001	0.1104	0.0088	0.1393	0.0086	0.1136	0.0132	0.0179	0.0022
2002	0.1025	0.0085	0.1258	0.0074	0.1145	0.0129	0.0247	0.0202
2003	0.1254	0.009	0.1172	0.008	0.1221	0.0135	0.0321	0.006
2004	0.1032	0.0097	0.1094	0.0074	0.0903	0.0103	0.0344	0.0043
2005	0.099	0.0089	0.1136	0.0071	0.1248	0.0129	0.0366	0.0049
2006	0.1041	0.0094	0.1085	0.0065	0.1505	0.0154	0.0285	0.004
2007	0.1043	0.008	0.1077	0.0067	0.1216	0.0131	0.0297	0.0041
2008	0.1112	0.0084	0.1193	0.0072	0.1347	0.0143	0.0348	0.0048
2009	0.1043	0.0092	0.1123	0.0065	0.124	0.0135	0.0277	0.0039
2010	0.1155	0.0088	0.1467	0.0084	0.1	0.0109	0.0242	0.0035
2011	0.1098	0.0082	0.1291	0.0074	0.1566	0.0163	0.0277	0.0041
2012	0.115	0.0094	0.1473	0.0085	0.1929	0.0209	0.0304	0.0048
2013	0.1186	0.0099	0.1217	0.0073	0.1497	0.0187	0.0311	0.0053
2014	0.1072	0.0093	0.1602	0.0093	0.1264	0.0159	0.018	0.0031
2015	0.139	0.0132	0.1328	0.0079	0.1289	0.0161	0.0132	0.0022
2016	0.1183	0.0115	0.1372	0.0083	0.1352	0.0167	0.0185	0.003
2017	0.1222	0.0114	0.175	0.0101	0.1097	0.0136	0.0205	0.0033
2018	0.1114	0.01	0.1334	0.0078	0.1226	0.0147	0.0177	0.0028
2019	0.1178	0.0108	0.1309	0.0075	0.0773	0.0094	0.0189	0.003

[a] Estimated from band recovery data.

[b] Estimated from a fall flight and total harvest.

Table K.4 – Parameter estimates for predicting American green-winged teal (AGWT), wood duck (WODU), ring-necked duck (RNDU), and goldeneye (GOLD) expected harvest rates for season lengths < 60 days and bag limits < 6 birds.

Parameter	AGWT	WODU	RNDU	GOLD
γ_C	0.1413	0.0484	0.1904	0.1848
γ_R	0.4872	0.6048	0.4427	0.2759
γ_M	0.7607	0.7339	0.7405	0.5172

The Atlantic Flyway has not experienced more restrictive duck hunting regulations (e.g., 30-day season and a 3-bird limit) since the early 1990s. Furthermore, preseason duck banding efforts in eastern North America were limited until the 1990s. Therefore, we relied on data collected through the annual USFWS's Parts Collection Survey (PCS) to estimate expected harvest rates during seasons < 60 days and/or bag limits < 6 birds as a proportion of the liberal package (see Padding et al. 2018 for details). We used daily bag composition data from the PCS to estimate the proportional reduction in harvest of each species that was expected to result from smaller bag limits under the moderate and restrictive regulatory alternatives (bag limit effect), following methods described by Martin and Carney (1977) and Balkcom et al. (2010). For each of the four species, we then summed the expected Flyway-wide reductions due to reduced season lengths and the expected reduction due to a smaller bag limits to estimate total expected reductions as proportions of the harvest under the liberal regulatory alternative (i.e., we estimated a γ_M, γ_R, γ_C for each species). Therefore, we estimated the expected harvest rate under the closed, moderate, and restrictive alternatives as

$$h_i = h_L \times \gamma_i,$$

where i indexes moderate, restrictive, or closed seasons in the U. S.

To estimate the expected effect of a January 31 ending framework date for the liberal and moderate alternatives, we relied on the observed effect of a 16-day framework date extension implemented in 2002 that increased the mallard harvest rate by 0.0052 (U.S. Fish and Wildlife Service 2017, Appendix G). We estimated a mean additional extension of 3 days for the January 31 fixed ending date, and assumed that the effect per day would be the same as the observed per day effect of the previous extension. The resulting predicted increase in harvest rate ($3/16 \times 0.0052 = 0.000975$) was added to the expected harvest rate estimates for the liberal and moderate alternatives.

Appendix L Northern Pintail Models

The Flyway Councils have long identified the northern pintail as a high-priority species for inclusion in the AHM process. In 2010, the USFWS and Flyway Councils adopted an adaptive management framework to inform northern pintail harvest management. A detailed progress report that describes the evolution of the pintail harvest strategy is available online (http://www.fws.gov/migratorybirds/NewsPublicationsReports.html). The northern pintail adaptive harvest management protocol considers two population models that represent alternative hypotheses about the effect of harvest on population dynamics: one in which harvest is additive to natural mortality, and another in which harvest is compensatory to natural mortality. We describe the technical details of the northern pintail model set below.

Latitude Bias Correction Model

Northern pintails tend to settle on breeding territories farther north during years when the prairies are dry and farther south during wet years. When pintails settle farther north, a smaller proportion are counted during the Waterfowl Breeding Population and Habitat Survey (WBPHS strata: 1–18, 20–50, 75–77), thus the population estimate is biased low in comparison to years when the birds settle farther south. This phenomenon may be a result of decreased detectability of pintails during surveys in northern latitudes compared to southern latitudes or because birds settle in regions not covered by the survey. Runge and Boomer (2005) developed an empirical relationship to correct the observed breeding population estimates for this bias. Based on this approach, the latitude-adjusted breeding population size ($cBPOP_t$) in year t, can be calculated with

$$cBPOP_t = e^{ln(oBPOP_t) + 0.741(mLAT_t - 51.68)}$$

where $oBPOP_t$ is the observed breeding population size in year t and $mLAT_t$ is the mean latitude of the observed breeding population in year t. The mean latitude of the pintail breeding population distribution is based on the geographical centroid of each stratum in the traditional survey area (WBPHS strata: 1–18, 20–50, 75–77). In year t, we calculate a mean latitude ($mLAT_t$) weighted by the population estimates from each strata with

$$mLAT_t = \sum_j [Lat_j(oBPOP_{t,j}/oBPOP_t)]$$

where Lat_j is the latitude of survey stratum j.

Population Models

Two population models are considered: one in which harvest is additive to natural mortality, and another in which harvest is compensatory to natural mortality. The models differ in how they handle the winter survival rate. In the additive model, winter survival rate is a constant, whereas winter survival is density-dependent in the compensatory model.

For the additive harvest mortality model, the latitude-adjusted population size ($cBPOP$) in year $t+1$, is calculated with

$$cBPOP_{t+1} = \left(cBPOP_t s_s \left(1 + \gamma_R \hat{R}_t\right) - \frac{\hat{H}_t}{(1-c)} \right) s_w$$

where $cBPOP_t$ is the latitude-adjusted breeding population size in year t, s_s and s_w are the summer and winter survival rates, respectively, γ_R is a bias-correction constant for the age-ratio, c is the crippling loss rate, $\hat{R}_t$ is the predicted age-ratio, and $\hat{H}_t$ is the predicted continental harvest. The model uses the following constants: $s_s = 0.70$, $s_w = 0.93$, $\gamma_R = 0.8$, and $c = 0.20$.

The compensatory harvest mortality model serves as a hypothesis that stands in contrast to the additive harvest mortality model, positing a strong but realistic degree of compensation. The compensatory model assumes that the mechanism for compensation is density-dependent post-harvest (winter) survival (Runge 2007). The form is a logistic relationship between winter survival and post-harvest population size, with the relationship anchored around the historic mean values for each variable. For the compensatory model, predicted winter survival rate in year t (s_t) is calculated as

$$s_t = s_0 + (s_1 - s_0)\left[1 + e^{-(a + b(P_t - \bar{P}))}\right]^{-1},$$

where s_1 (upper asymptote) is 1.0, s_0 (lower asymptote) is 0.7, b (slope term) is -1.0, P_t is the post-harvest population size in year t (expressed in millions), $\bar{P}$ is the mean post-harvest population size (4.295 million from 1974 through 2005), and

$$a = \text{logit}\left(\frac{\bar{s} - s_0}{s_1 - s_0}\right)$$

or

$$a = \log\left(\frac{\bar{s} - s_0}{s_1 - s_0}\right) - \log\left\{1 - \left(\frac{\bar{s} - s_0}{s_1 - s_0}\right)\right\},$$

where $\bar{s}$ is 0.93 (mean winter survival rate).

Age Ratio Submodel

Recruitment ($\hat{R}$) in year t is measured by the vulnerability-adjusted, female age-ratio in the fall population and is predicted as

$$\hat{R}_t = e^{(7.6048 - 0.13183 mLAT_t - 0.09212 cBPOP_t)}$$

where $mLAT_t$ is the mean latitude of the observed breeding population in year t and $cBPOP_t$ is the latitude-adjusted breeding population in year t (expressed in millions).

Harvest Submodel

Predicted continental harvest ($\hat{H}$) in year t is calculated with

$$\hat{H}_t = H_{PF} + H_{CF} + H_{MF} + H_{AF} + H_{AKCan}$$

where H_{PF}, H_{CF}, H_{MF}, and H_{AF} are the predicted harvest in the Pacific, Central, Mississippi, and Atlantic Flyways, respectively. The expected harvest from Alaska and Canada H_{AKCan} is assumed fixed and equal to 67,000 birds. Flyway specific harvest predictions are calculated with

Table L.1 – Total pintail harvest expected from the set of regulatory alternatives specified for each Flyway under the northern pintail adaptive harvest management protocol.

Pacific Atlantic	**Central Mississippi**	**Total Harvest**
Closed	Closed	67,000
Liberal 1	Closed	278,000
Liberal 1	Restrictive 3	410,000
Liberal 1	Moderate 3	523,000
Liberal 1	Liberal 1	569,000
Liberal 2	Closed	357,000
Liberal 2	Restrictive 3	490,000
Liberal 2	Moderate 3	603,000
Liberal 2	Liberal 2	672,000

$$H_{PF} = -12051.41 + 1160.960days + 73911.49bag$$

$$H_{CF} = -95245.20 + 2946.285days + 15228.03bag + 23136.04sis$$

$$H_{MF} = -59083.66 + 3413.49days + 7911.95bag + 59510.10sis$$

$$H_{PF} = -2403.06 + 360.950days + 5494.00bag$$

where *days* is the season length, *bag* is the daily bag limit, and *sis* is an indicator variable with value equal to 0 (full season equal to length from general duck season) or 1 (restrictive season within the liberal or moderate regulatory alternative for general duck season, i.e., partial season). Each regulatory combination of bag limit and season length has an associated predicted pintail harvest (Table L.1).

Model Weights

The relative degree of confidence that we have in the additive or compensatory mortality hypothesis can be represented with model weights that are updated annually from a comparison of model specific predictions and observed population sizes. For the period 1974–2018, the subsequent year's breeding population size (on the latitude-adjusted scale) was predicted with both the additive and compensatory models, and compared to the observed breeding population size (on the latitude-adjusted scale). The mean-squared error of the predictions from the additive model (MSE_{add}) was calculated as:

$$MSE_{add} = \frac{1}{(t-1975)+1} \sum_{t=1975}^{t} \left(cBPOP_t - cBPOP_t^{add} \right)^2,$$

and the mean-squared error of the predictions from the compensatory model were calculated in a similar manner.

We calculated model weights for the additive and compensatory model as a function of their relative mean-squared errors. The model weight for the additive model (W_{add}) was determined by

$$W_{add} = \frac{\frac{1}{MSE_{add}}}{\frac{1}{MSE_{add}} + \frac{1}{MSE_{comp}}}$$

The model weight for the compensatory model was found in a corresponding manner, or by subtracting the additive model weight from 1.0. As of 2019, the compensatory model did not fit the historic data as well as the additive model; the model weights were 0.573 for the additive model and 0.427 for the compensatory model.

Equilibrium Conditions

Equilibrium analyses of the additive model suggest a carrying capacity of 7.33 million (on the latitude-adjusted scale), maximum sustained yield (MSY) of 446,000 at an equilibrium population size of 3.30 million, and harvest rate of 10.9% (Runge and Boomer 2005). The yield curve resulting from the compensatory model is significantly skewed compared to the additive model (Figure L.1). Compared to the additive model, the compensatory model results in a lower carrying capacity (4.67 million), a higher MSY (561 thousand) at a lower equilibrium population size (2.99 million), and a higher maximum harvest rate (14.9%).

The average model, based on 2019 model weights, produces a yield curve that is intermediate between the additive and compensatory models. An equilibrium analysis of the weighted model results in carrying capacity, MSY, equilibrium population size at MSY, and maximum harvest rate that are intermediate between the additive and compensatory model results (5.45 million, 492 thousand, 3.11 million, and 12.6% respectively).

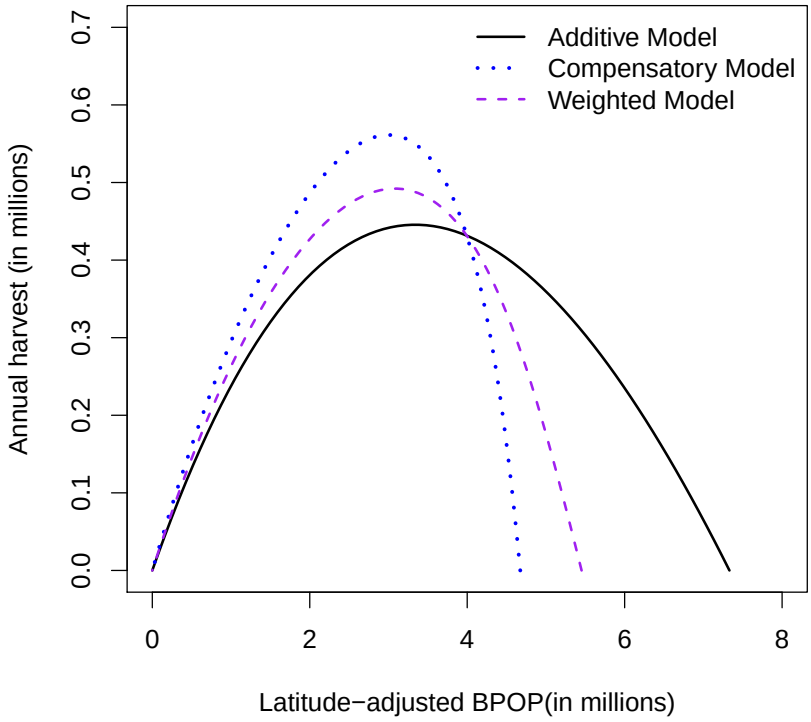

Figure L.1 – Harvest yield curves resulting from an equilibrium analysis of the northern pintail model set based on 2019 model weights.

Appendix M Scaup Model

We use a state-space formulation of scaup population and harvest dynamics within a Bayesian estimation framework (Meyer and Millar 1999, Millar and Meyer 2000). This analytical framework allows us to represent uncertainty associated with the monitoring programs (observation error) and the ability of our model formulation to predict actual changes in the system (process error).

Process Model

Given a logistic growth population model that includes harvest (Schaefer 1954), scaup population and harvest dynamics are calculated as a function of the intrinsic rate of increase (r), carrying capacity (K), and harvest (H_t). Following Meyer and Millar (1999), we scaled population sizes by K (i.e., $P_t = N_t/K$) and assumed that process errors (ϵ_t) are lognormally distributed with a mean of 0 and variance $\sigma^2_{process}$. The state dynamics can be expressed as

$$P_{1974} = P_0 e^{\varepsilon_{1974}}$$

$$P_t = \left(P_{t-1} + rP_{t-1}\left(1 - P_{t-1}\right) - H_{t-1}/K\right) e^{\varepsilon_t}, \quad t = 1975, \ldots, 2019,$$

where P_0 is the initial ratio of population size to carrying capacity. To predict total scaup harvest levels, we modeled scaup harvest rates (h_t) as a function of the pooled direct recovery rate (f_t) observed each year with

$$h_t = f_t/\lambda_t.$$

We specified reporting rate (λ_t) distributions based on estimates for mallards (*Anas platyrhynchos*) from large scale historical and existing reward banding studies (Henny and Burnham 1976, Nichols et al. 1995*b*, P. Garrettson unpublished data). We accounted for increases in reporting rate believed to be associated with changes in band type (e.g., from AVISE and new address bands to 1-800 toll free bands) by specifying year specific reporting rates according to

$$\begin{aligned} \lambda_t &\sim Normal(0.38, 0.04), \quad t = 1974, \ldots, 1996 \\ \lambda_t &\sim Normal(0.70, 0.04), \quad t = 1997, \ldots, 2019. \end{aligned}$$

We then predicted total scaup harvest (H_t) with

$$H_t = h_t \left[P_t + rP_t\left(1 - P_t\right)\right] K, \quad t = 1974, \ldots, 2019.$$

Observation Model

We compared our predictions of population and harvest numbers from our process model to the observations collected by the Waterfowl and Breeding Habitat Survey (WBPHS) and the Harvest Survey programs with the following relationships, assuming that the population and harvest observation errors were additive and normally distributed. May breeding population estimates were related to model predictions by

$$N_t^{Observed} - P_t K = \varepsilon_t^{BPOP},$$

where

$$\varepsilon_t^{BPOP} \sim N(0, \sigma^2_{t,BPOP}), \quad t = 1974, \ldots, 2019,$$

where $\sigma^2_{t,BPOP}$ is specified each year with the BPOP variance estimates from the WBPHS.

We adjusted our harvest predictions to the observed harvest data estimates with a scaling parameter (q) according to

$$H_t^{Observed} - \left(h_t \left[P_t + rP_t \left(1 - P_t\right)\right] K\right)/q = \varepsilon_t^H, \quad t = 1974, \ldots, 2019,$$

where,

$$\varepsilon_t^H \sim N(0, \sigma^2_{t,Harvest}).$$

We assumed that appropriate measures of the harvest observation error $\sigma^2_{t,Harvest}$ could be approximated by assuming a coefficient of variation for each annual harvest estimate equal to 0.15 (Paul Padding pers. comm.). The final component of the likelihood included the year specific direct recovery rates that were represented by the rate parameter (f_t) of a Binomial distribution indexed by the total number of birds banded preseason and estimated with,

$$f_t = m_t/M_t,$$
$$m_t \sim Binomial(M_t, f_t)$$

where m_t is the total number of scaup banded preseason in year t and recovered during the hunting season in year t and M_t is the total number of scaup banded preseason in year t.

Bayesian Analysis

Following Meyer and Millar (1999), we developed a fully conditional joint probability model, by first proposing prior distributions for all model parameters and unobserved system states and secondly by developing a fully conditional likelihood for each sampling distribution.

Prior Distributions

For this analysis, a joint prior distribution is required because the unknown system states P are assumed to be conditionally independent (Meyer and Millar 1999). This leads to the following joint prior distribution for the model parameters and unobserved system states

$$\begin{aligned} P(r, K, q, f_t, \lambda_t, \sigma^2_{Process}, P_0, P_{1,\ldots,T}) = \\ p(r)p(K)p(q)p(f_t)p(\lambda_t)p(\sigma^2_{Process})p(P_0)p(P_1|P_0, \sigma^2_{Process}) \\ \times \prod_{t=2}^{n} p(P_t|P_{t-1}, r, K, f_{t-1}, \lambda_{t-1}, \sigma^2_{Process}) \end{aligned}$$

In general, we chose non-informative priors to represent the uncertainty we have in specifying the value of the parameters used in our assessment. However, we were required to use existing information to specify

informative priors for the initial ratio of population size to carrying capacity (P_0) as well as the reporting rate values (λ_t) specified above that were used to adjust the direct recovery rate estimates to harvest rates.

We specified that the value of P_0, ranged from the population size at maximum sustained yield ($P_0 = N_{MSY}/K = (K/2)/K = 0.5$) to the carrying capacity ($P_0 = N/K = 1$), using a uniform distribution on the log scale to represent this range of values. We assumed that the exploitation experienced at this population state was somewhere on the right-hand shoulder of a sustained yield curve (i.e., between MSY and K). Given that we have very little evidence to suggest that historical scaup harvest levels were limiting scaup population growth, this seems like a reasonable prior distribution.

We used non-informative prior distributions to represent the variance and scaling terms, while the priors for the population parameters r and K were chosen to be vague but within biological bounds. These distributions were specified according to

$$\begin{aligned}
P_0 &\sim Uniform(ln(0.5), 0), \\
K &\sim Lognormal(2.17, 0.667), \\
r &\sim Uniform(0.00001, 2), \\
f_t &\sim Beta(0.5, 0.5), \\
q &\sim Uniform(0.0, 2), \\
\sigma^2_{Process} &\sim Inverse\ Gamma(0.001, 0.001).
\end{aligned}$$

Likelihood

We related the observed population, total harvest estimates, and observed direct recoveries to the model parameters and unobserved system states with the following likelihood function:

$$\begin{aligned}
&P(N_{1,\ldots,T}, H_{1,\ldots,T}, m_{1,\ldots,T} M_{1,\ldots,T} | r, K, f_t, \lambda_t, q, \sigma^2_{Process}, \sigma^2_{Harvest}, P_{1,\ldots,T}) = \\
&\quad \times \prod_{t=1}^{T} p(N_t | P_t, K, \sigma^2_{BPOP}) \times \prod_{t=1}^{T} p(H_t | P_t, r, K, q, f_t, \lambda_t, \sigma^2_{Harvest}) \\
&\quad \times \prod_{t=1}^{T} p(m_t | M_t, f_t)
\end{aligned}$$

Posterior Evaluation

Using Bayes theorem we then specified a posterior distribution for the fully conditional joint probability distribution of the parameters given the observed information according to

$$\begin{aligned}
&P(r, K, q, f_t, \lambda_t, \sigma^2_{Process}, P_0, P_{1,\ldots,T} | N_{1,\ldots,T}, H_{1,\ldots,T}, m_{1,\ldots,T}, M_{1,\ldots,T}) \propto \\
&\quad p(r)p(K)p(q)p(f_t)p(\lambda_t)p(\sigma^2_{Process})p(P_0)p(P_1 | P_0, \sigma^2_{Process}) \\
&\quad \times \prod_{t=2}^{n} p(P_t | P_{t-1}, r, K, f_{t-1}, \lambda_{t-1}, \sigma^2_{Process}) \times \prod_{t=1}^{T} p(N_t | P_t, K, \sigma^2_{BPOP}) \\
&\quad \times \prod_{t=1}^{T} p(H_t | P_t, r, K, q, f_t, \lambda_t, \sigma^2_{Harvest}) \times \prod_{t=1}^{T} p(m_t | M_t, f_t)
\end{aligned}$$

Table M.1 – Model parameter estimates resulting from a Bayesian analysis of scaup breeding population, harvest, and banding information from 1974 to 2019.

Parameter	Mean	SD	2.5% CI	Median	97.5% CI
r	0.1342	0.0451	0.0634	0.1277	0.2409
K	8.7645	1.6932	6.2250	8.5055	12.5000
σ^2	0.0078	0.0031	0.0034	0.0072	0.0151
q	0.7550	0.0402	0.6806	0.7536	0.8397

We used MCMC methods to evaluate the posterior distribution using WinBUGS (Spiegelhalter et al. 2003). We randomly generated initial values and simulated 5 independent chains each with 1,000,000 iterations. We discarded the first half of the simulation and thinned each chain by 250, yielding a sample of 10,000 points. We calculated Gelman-Rubin statistics (Brooks and Gelman 1998) to monitor for lack of convergence. The state-space formulation and Bayesian analysis framework provided reasonable fits to the observed breeding population and total harvest estimates with realistic measures of variation. The 2019 posterior estimates of model parameters based on data from 1974 to 2019 are provided in Table M.1.

We further summarized the simulation results for r, K, and the scaling parameter q to admit parametric uncertainty with a formal correlation structure within the optimization procedure used to calculate the harvest strategy. We first defined a joint distribution for 3 discrete outcomes for each of the 3 population parameters. We used the 30 and 70 percent quantiles for each parameter as the cut points to define three bins for which to discretize 3 values of each posterior distribution. We then determined the frequency of occurrence of each of the 27 possible combinations of each parameter value falling within the 3 bins from the MCMC simulation results. These frequencies were then assigned parameter values based on the midpoint of the bin ranges (15, 50, 85 percent quantiles) to specify the joint distribution of the population parameter values used in the optimization.